AFRL-HE-WP-TR-1998-0045

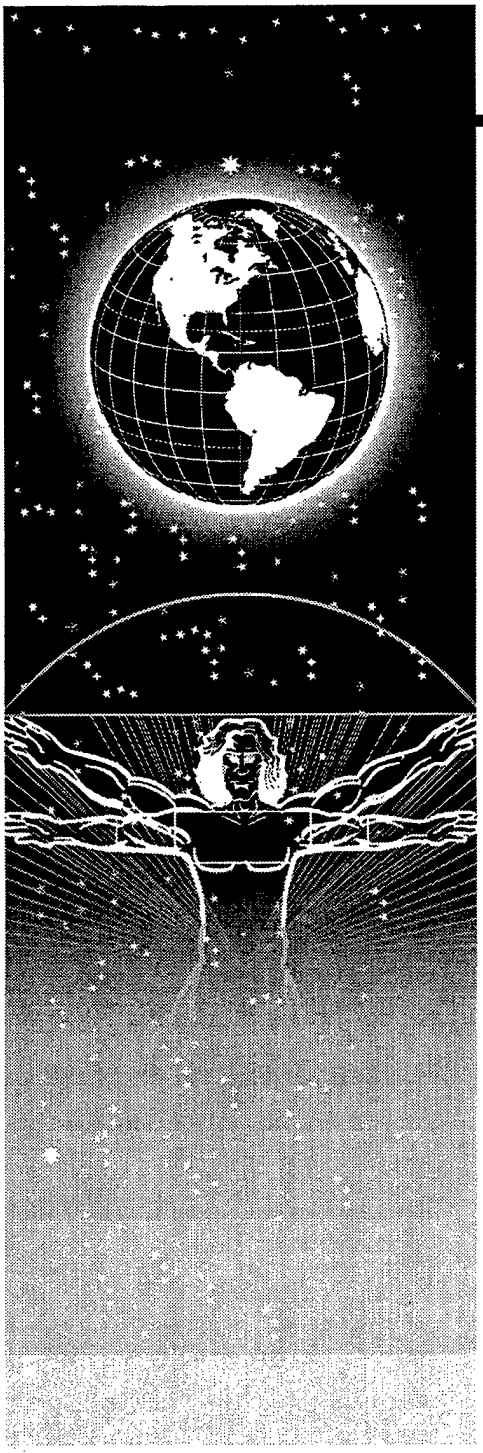

UNITED STATES AIR FORCE RESEARCH LABORATORY

DARPA

DISPLAY RUGGEDIZATION FOR MILITARY APPLICATIONS USING AUTOMOTIVE-GRADE ACTIVE MATRIX LIQUID CRYSTAL DISPLAYS

James B. Armstrong
Sonia R. Dodd

HONEYWELL TECHNOLOGY CENTER
HONEYWELL, INC.
21111 N. 9TH AVE.
MS: 2G29E1
PHOENIX AZ 85027-2708

James M. Henz

DEFENSE AVIONICS SYSTEMS
HONEYWELL, INC.
9201 SAN MATEO BLVD.
MS C-14
ALBUQUERQUE NM 87113-2227

MAY 1998

FINAL REPORT FOR THE PERIOD AUGUST 1996 TO OCTOBER 1997

Human Effectiveness Directorate
Crew System Interface Division
2255 H Street
Wright-Patterson AFB, OH 45433-7022

NOTICES

When US Government drawings, specifications, or other data are used for any purpose other than a definitely related Government procurement operation, the Government thereby incurs no responsibility nor any obligation whatsoever, and the fact that the Government may have formulated, furnished, or in any way supplied the said drawings, specifications, or other data, is not to be regarded by implication or otherwise, as in any manner licensing the holder or any other person or corporation, or conveying any rights or permission to manufacture, use, or sell any patented invention that may in any way be related thereto.

Please do not request copies of this report from the Air Force Research Laboratory. Additional copies may be purchased from:

National Technical Information Service
5285 Port Royal Road
Springfield, Virginia 22161

Federal Government agencies registered with the Defense Technical Information Center should direct requests for copies of this report to:

Defense Technical Information Center
8725 John J. Kingman Road, Suite 0944
Ft. Belvoir, Virginia 22060-6218

DISCLAIMER

This Technical Report is published as received and has not been edited by the Air Force Research Laboratory, Human Effectiveness Directorate.

TECHNICAL REVIEW AND APPROVAL

AFRL-HE-WP-TR-1998-0045

This report has been reviewed by the Office of Public Affairs (PA) and is releasable to the National Technical Information Service (NTIS). At NTIS, it will be available to the general public, including foreign nations.

This technical report has been reviewed and is approved for publication.

FOR THE COMMANDER

JOHN F. KENT, COL, USAF, BSC
Deputy Chief, Crew System Interface Division
Air Force Research Laboratory

REPORT DOCUMENTATION PAGE

Form Approved
OMB No. 0704-0188

1. AGENCY USE ONLY *(Leave blank)*	2. REPORT DATE	3. REPORT TYPE AND DATES COVERED
	May 1998	Final Report, August 1996 - October 1997

4. TITLE AND SUBTITLE
Display Ruggedization For Military Applications
Using Automotive-Grade Active Matrix Liquid Crystal Displays

5. FUNDING NUMBERS
C: F33615-96-C-1943
PE: 62708E
PR: ARPA
TA: AA
WU: 11

6. AUTHOR(S)
* James B. Armstrong * Sonia R. Dodd
** James M. Henz

7. PERFORMING ORGANIZATION NAME(S) AND ADDRESS(ES)
* Honeywell Technology Center, Honeywell Inc.
21111 N. 19th Ave., MS: 2G29E1, Phoenix AZ 85027-2708
** Defense Avionics Systems, Honeywell Inc.
9201 San Mateo Blvd. NE, MS C-14, Albuquerque NM 87113-2227

8. PERFORMING ORGANIZATION REPORT NUMBER

9. SPONSORING / MONITORING AGENCY NAME(S) AND ADDRESS(ES)
Air Force Research Laboratory (AFRL)
Human Effectiveness Directorate
Crew System Interface Division
Air Force Materiel Command
Wright-Patterson AFB OH 45433-7022

10. SPONSORING / MONITORING AGENCY REPORT NUMBER
AFRL-HE-WP-TR-1998-0045

11. SUPPLEMENTARY NOTES

12a. DISTRIBUTION / AVAILABILITY STATEMENT
Approved for public release: distribution unlimited

12b. DISTRIBUTION CODE

13. ABSTRACT *(Maximum 200 words)*

This report discusses the results of a Honeywell Technology Center program focused on developing thermal management methodologies and flip-chip-on-glass (FCOG) driver bonding techniques which are key to ruggedizing automotive-grade commercial off-the-shelf (COTS) active matrix liquid crystal displays (AMLCD) for use in military applications like the F-16 high-performance fighter environment. Through extensive thermal modeling, several techniques were identified to facilitate heat flow away from the temperature-sensitive liquid crystal material, keeping the core temperature within acceptable operating limits (below +85C) in worse case conditions (200 fL with +50C ambient and 883Watts/m^2 solar load in a closed cockpit) without the use of forced air cooling for display sizes up to 5x5-inch. Environmental testing on eight modified Sharp displays verified modeling results. The FCOG bonding has many inherent advantages over traditional tape automated bonding (TAB) techniques, one of which is 75% reduction in off-glass interconnect density, making them much less susceptible to vibration failure. Several FCOG bonding materials (e.g., anisotropic conductive films) have been explored and tested using various test vehicles and subjected to F-16 environmental conditions for temperature shock, temperature cycling, vibration, and humidity.

14. SUBJECT TERMS
ruggedized displays, active matrix liquid crystal displays, AMLCD, flip chip on glass driver, FCOG, display thermal management, flat panel displays, military displays, cockpit displays, commercial off-the-shelf displays, COTS

15. NUMBER OF PAGES
119

16. PRICE CODE

17. SECURITY CLASSIFICATION OF REPORT	18. SECURITY CLASSIFICATION OF THIS PAGE	19. SECURITY CLASSIFICATION OF ABSTRACT	20. LIMITATION OF ABSTRACT
Unclassified	Unclassified	Unclassified	Unlimited

This Page Intentionally Left Blank

TABLE OF CONTENTS

LIST OF FIGURES

LIST OF TABLES

LIST OF ACRONYMS

ACA	Anisotropic Conductive Adhesive
ACF	Anisotropic Conductive Film
AMLCD	Active Matrix Liquid Crystal Display
AR	Anti-Reflection
COTS	Commercial off the Shelf
C-SAM	C-mode Scanning Acoustic Microscopy
DGA	Display Glass Assembly
ESC™	Electronic System Cooling (trademark of SDRC)
FCOG	Flip-Chip-On-Glass
FEA	Finite Element Analysis
FEM	Finite Element Model
fL	foot-Lambert
IC	Integrated Circuit
IMI	International Micro Industries, Inc.
I/O	Input/Output
ITO	Indium-Tin Oxide
LCD	Liquid Crystal Display
LSI	Large Scale Integrated Circuit
NRE	Non-Recurring Expense
PDLC	Polymer Dispersed Liquid Crystal
PIDS	Prime Item Development Specification (F-16)
PWB	Printed Wiring Board
RTV	Room Temperature Vulcanizing (Silicone Rubber)
SDRC™	Structural Dynamics Research Corporation
SEM	Scanning Electron Microscope
STN	Super-Twisted Nematic (LCD)
TAB	Tape-Automated Bonding
TC	Thermal Coupling
TC1, 2, 3, 4	Test Chip 1, 2, 3, 4 respectively
TEC	Thermoelectric Cooler
TN	Twisted Nematic (LCD)
UV	Ultra Violet

1. Introduction

One of the most tantalizing military display technology opportunities lies in the glaring cost differential between military and commercial industrial/automotive-grade liquid crystal displays (LCDs). Focusing on the lowest-level LCD glass assembly alone, the cost differences can be an order of magnitude or more. While the performance specifications differ significantly between the two classes, the cost difference still renders the commercial industrial/automotive-grade LCDs compellingly attractive. The program reported on herein addressed two particular pieces of the commercial technology application puzzle:

- Identification of a methodology for creating a thermal cocoon about a commercial display such that the LCD remains within its specified operating limits, and
- Identification of at least one material and process suitable for bonding/connecting flip-chip integrated circuit (IC) drivers onto LCD glass substrates, as well as in hostile military aircraft environments.

1.1 Executive Summary

The purchase price difference between commercial and militarized LCDs can be spectacular, in some cases more than an order of magnitude. For example, a laptop computer active-matrix LCD glass stack (with drivers) may cost on the order of $300-$1000 (in 1998-9, in large quantity), depending on size and resolution. By way of contrast, the cost of a DGA (LCD glass and drivers) of similar size, but custom designed for a tactical cockpit, may cost in the neighborhood of $10,000. Much of this cost is

driven by the need for custom components and materials, unique performance requirements, low production quantities, and small-volume manufacturing infrastucture and overhead costs. That cost differential shrinks substantially for corresponding higher-level assemblies, the result of a significant number of remanufacturing steps necessary to adapt the commercial LCDs for use. Despite that cost shrinkage, however, there remains enough cost differential at these higher assembly levels to still commend the use of commercial technology where the application can tolerate the residual performance disparities.

Until recently, the higher cost of these custom military displays has precluded the use of fully mil-qualifiable color active matrix color displays in many applications. But in the last couple of years, there have been several initiatives to use commercial LCDs (in some modified form) in military platforms (e.g., C-130J, T-38, Crusader Self-Propelled Howitzer).

In order to use commercial displays in these applications, several remanufacture steps are necessary (Figure 1-1). Commercial displays are usually provided as a ready-to-use, ready-to-mount module, with the display components mounted inside a steel protecting and supporting frame. The first step us usually to remove this frame to permit subsequent amendments of the LCD glass stack and peripheral components.

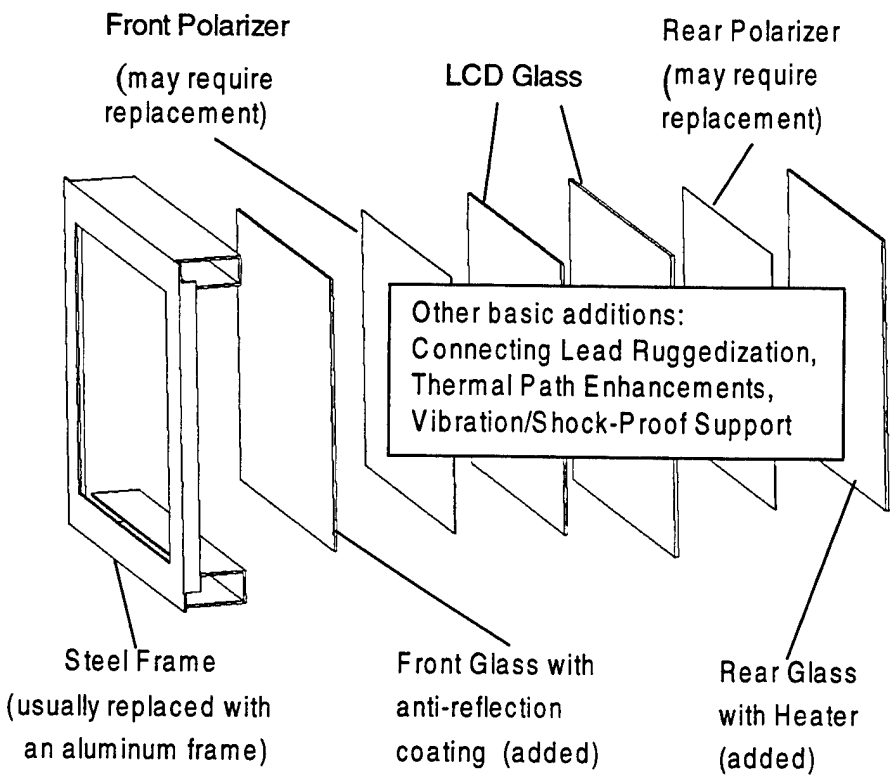

Figure 1-1 Usual Amendments to Commercial LCDs

Next, it may be necessary to remove and replace the polarizers if the commercial material has been found to be vulnerable to heat or humidity in environmental test. At this point, the modified commercial LCD glass corresponds approximately to the state of the militarized LCD glass in its simplest form. But, several steps remain for both types of displays. These subsequent steps add cost to both types of LCDs, but from a percentage standpoint, the net cost differential continues to diminish.

Additional specialized optical films may be incorporated into the LCD stack to alter the viewing properties of the display (e.g., viewing angle). A front anti-reflection coated glass is bonded to the front of the display to improve contrast and strengthen the LCD stack. A heater glass is bonded to the rear of the display to permit heating of the display

to operating condition from a cold state. Additional fabrication steps vibration-proof the lead structure. The edges of the laminated stack may be further encapsulated to protect the polarizers and other panel components against humidity. Finally, the display glass is installed in a new supporting/mounting frame.

At this stage, the LCD display element is a part of a higher-level subassembly. With the added labor, material, and process yield costs, the value embodied in the commercial display assembly has increased considerably, regardless of the militarized or commercial starting point. However, yields in the first few disassembly and cleaning steps (and associated yields) for the commercial panel add cost uniquely to those devices.

The ability to ruggedize a commercial panel (particularly the lead assemblies) against vibration, shock, and temperature environments is another critical gatekeeper for the application of commercial LCDs. While many of the ruggedization issues are being addressed in the programs previously identified, we asked two questions for which the answers appeared not to be generally available. One question was quite general, the other more specific:

1. Are there practical general ways to provide a thermal micro-climate in which an industrial-grade or automotive grade commercial display (with some modification) can operate and survive in the most demanding of military avionic display environments?

2. If special mil-qualifiable panel drivers are required, and if the use of flip-chip-on-glass drivers offers sufficient spatial, manufacturing, and/or reliability benefit, is there at least one chip bonding material and process that could be demonstrated to be mil-compatible. And can it also provide at least some measure of repairability to improve yield and cost?

To test the effectiveness of potential solutions identified, we applied the F-16 color flat-panel display design and test conditions. These requirements constitute a set of the most challenging current combinations of military avionic design and test conditions, including compact packaging of a high-luminance flat-panel display, high solar radiation power-loading on the screen, and absence of forced-air cooling. If a solution could be found for these difficult conditions, then most other aircraft environments would be found more hospitable, not less, to appropriately modified commercial displays. These test conditions were used as a guide for both design and validation testing.

1.1.1 Thermal Cocoon Results and Payoff

To the thermal cocoon question, we found the answer was "Yes" for small displays (up to 5x5-inch), and a conditional "Yes" for cockpit displays up to about 50 sq. in. active area, all under one of the most demanding sets of military avionic environmental and design requirements. The details of the investigation and results are reported in Section 2.

We addressed the thermal question by first selecting a representative baseline automotive-grade commercial Sharp LQ6RA52 display with a relatively high 85°C maximum operating temperature. This particular device (Figure 1-2, Figure 1-3, and Figure 1-4) was chosen because it was commercially available, and the manufacturer's temperature specifications were close to those required for the F-16 application.

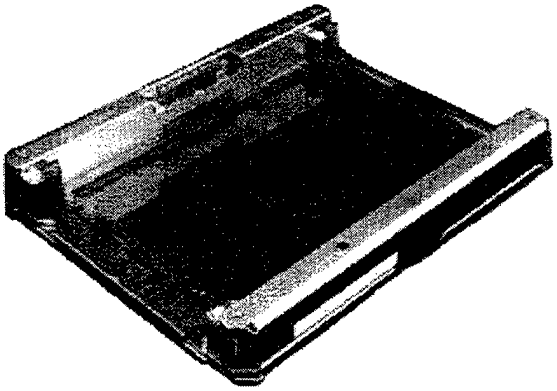

Figure 1-2 Rear View of Unmodified Sharp Display (with steel frame)

Figure 1-3 Automotive-grade Sharp LQ6RA52

A thermal model was then created of the display, and of a backlight capable of delivering the F-16 performance figures. The thermal model was used to develop improvements in the thermal environment of the display. The results of the modeling effort were then validated through the fabrication and test of display assemblies embodying various levels of improvement.

The keys to success in this task were the facilitation of heat flow out of the LCD stack (by several means as dictated by the particular display size), and use of active heat pumping with heat pipes and thermoelectric coolers for the larger display sizes.

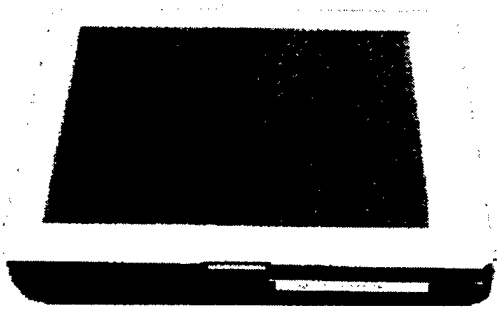

Figure 1-4 Front View of Unmodified Sharp Display

Payoff – We have identified generally useable design amendments that permit the use of commercial automotive/industrial-grade displays, even in the challenging F-16 cockpit environmental conditions. If the display is no more than 5x5-inch in active area, it can be used without cooling air and in the presence of significant solar loading. If larger, then tradeoffs among environmental specification, cooling resources, and design specifics may still allow them to be used in similar environments.

The work also focused attention on particular aspects of the typical design task which will improve control of the thermal environment of all flat panel displays, military-specific designs or otherwise. This in turn is reflected in improved reliability and/or reduced power dissipation.

Finally, the investigation into heat pipes as a means for extracting heat from the display stack revealed a significant reduction in the cost of the devices over the last two years. This in turn opened an opportunity to apply these useful devices more widely in the overall thermal design of display units, and in other avionic packages as well.

Finally, the lessons learned are applicable to a wide range of future display applications, both land and airborne.

1.1.2 Flip-Chip-on-Glass Results and Payoff

We also found the answer to be "Yes" to the flip-chip driver bonding/connection question. A Sony anisotropic conducting film (ACF) bonding material was found to have excellent bonding and electrical conductivity properties for the mil environment, and offered repairability during the manufacturing process. We also answered a collateral question, "Will the driver bonding/connecting method used in the baseline commercial display stand up under military temperature test conditions?" We also found that answer was "Yes" for the specific commercial automotive-grade Sharp display used and tested in the program. The details of the investigation and results are reported in Section 3.

In the flip-chip-on-glass (FCOG) bonding process research, we sought at least one chip-bonding material which was straightforward to use, produced low-resistance electrical connections, was stable over the mil-temperature range, was not susceptible to humidity, and offered at least some degree of repairability during the manufacturing process.

To evaluate materials and processes, we created two types of test articles, one for quick preliminary screening of prospects, and a second for more extensive humidity, temperature, and vibration testing. The latter test vehicle incorporated a large number of contacts per test article, allowing us to get statistically significant results, and get a good sense of the contacts' electrical performance over temperature. Many of the bonded

connections were also tested for shear strength, and imaged acoustically to evaluate the bond quality.

A Sony anisotropic conductive film bonding material was found to provide the desired performance, as well as permitting replacement of malfunctioning chips during the manufacturing process. The material is a heat-curable material loaded with gold microspheres. Under heat and compression, gold bumps (connecting points) on the driver chips compress the gold microspheres into electrical conducting contact with the LCD's connecting traces. Elsewhere, the spheres remain out of contact with one another and the material is insulating. The material can be partially cured and tested, allowing for easy removal of the chip if the device or its positioning is defective. If properly functional, the material may be fully heat-cured, giving it excellent environmental stability.

While other materials we investigated may have proved successful with additional supplier dialog, we found this particular material immediately satisfactory in our preliminary screenings, and it held up as well in subsequent more rigorous testing. With the Sony material, we were able to satisfy the program objective of verifying the existence of at least one material and process that is compatible with the mil environment.

Payoff – The identification of at least one reliable bonding material means that the option is open for considering use of flip-chip drivers with either commercial or custom LCD panels intended for use in the military environment. To do so as an after-market add-on, some additional design consideration must be given to the means by which the connector

pad pattern on the IC drivers is to be interconnected with the conductor runs on the commercial LC glass. That task may be accomplished by custom layout of the IC's connecting pads, or through an intermediate transition connection means.

In addition, the material and process identified may be suggested to a custom LCD manufacturer who wishes to use flip-chip drivers, and has the degree of freedom of specifically patterning the LCDs connecting electrodes to match the driver IC's pad layout. This option potentially benefits manufacturability and reliability through reduction in connections and connector densities.

The ability to repair a mislocated or malfunctioning driver chip is a powerful asset. This can significantly improve manufacturing yield, for either LCD manufacturer or after-market LCD modifier. Further, this material and process may also be suitable for bonding TAB or other types of interconnects, where repairability will have similar benefit.

Finally, since we found these particular Sharp drivers and bonding robust under the testing performed, there is the possibility of using at least some commercial LCDs as manufactured with chip-on-glass drivers. And if the bonding material proves vulnerable, the manufacturer may be directed to the material that we found suitable for military environments.

The details of the investigations and results are contained in the two sections following:

Section 2 – Thermal Modeling

Section 3 – Flip-Chip-on-Glass Driver Bonding

1.2. Acknowledgments

The success of this program derives from the combined efforts and interests of a number of people and organizations. The authors are particularly appreciative of contributions of the following:

Defense Advanced Research Projects Agency (DARPA): Dr. Mark Hartney and Dr. Bruce Gnade for the financial support of the program.

Air Force Research Laboratory (previously Wright Laboratory before October 1997):

- First Lieutenant Timothy W. Jackson for support, direction, and government program management, as well as thorough technical review and valuable contributions in the creation of the final report.

- Darrel Hopper for his concern for the topical issue, insights and support at program reviews, and general support of the program and its objectives.

- Captain Thomas Quast for his contributions in getting the program under contract, and providing program management during the first two months.

Honeywell, with particular recognition of the fine interdivisional collaboration:

Honeywell Technology Center (Phoenix AZ):

- Technicians Charles Chanley and Norma Chavez for device fabrication and analysis support

- Jerry Roush for electronics support.

Honeywell Defense Avionics Systems (Albuquerque NM):

- Jay Stanke for thermal analysis support

Quartus Engineering Inc. (San Diego CA):

- Mark Stabb for thermal analysis support.

2. Thermal Modeling Task

As a starting point, we baselined a specific Sharp industrial-grade display with an 85°C maximum temperature. We used thermal modeling as our basic research tool. The F-16 Color Multifunction Display performance requirements and thermal environment were imposed in our baseline conditions.[1] We studied both modifications to the LCD stack itself, and adaptations of the LCD installation. We further imposed the constraint that any redesign would not alter the design of any of the components of the as-supplied LCD glass stack without analysis or testing to identify any possible performance and production consequences (e.g., assuming thicker LCD substrate glass).

The program revealed that the specified incident solar loading dominated the thermal problem. Though backlight heating is always a concern, in this particular application, its heat contribution to the problem was less significant than the solar loading.

We found that mounting improvements and LCD stack improvement could allow commercial displays as large as 5x5-inch to function in the F-16 environment. In this size range, sufficient lateral heat flow could be created to allow the heat to be passively conducted to the relatively cool display housing. In the larger sizes, however, one or more transparent layers of relatively high thermal conductivity material were added to the stack to improve lateral heat flow.

LCD stack sizes greater than 5x5-inch require more aggressive active cooling (e.g., heat-pipes and thermoelectric cooling), or reductions in solar loading (less than the F-16 requirement) in order to prevent undesirable temperature buildup and gradients in the LCD. For sizes larger than 7x7-inch or 6x8-inch, even active edge cooling is insufficient, inducing high center glass temperatures and large temperature gradients in the glass. In order to use these larger displays, moving air must be available to facilitate heat removal from the face of the display.

The primary improvements revealed by the investigation involved techniques including:

- Improvement of the thermal path to the outer case of the display.
- Insertion of clear, thermally-conducting layer(s) into the LCD stack.
- Use of active heat pumping by means of thermoelectric coolers and heat pipes.

For displays greater than about 50-in.^{2} active display area, one or both of two other measures may eliminate active cooling:

- Reduction of solar loading to below that of the F-16's specification.
- Provide forced-air cooling.

This alters the baseline conditions of this study, but may permit the use of still larger commercial displays in this military avionic environment.

In the course of the investigation, we found that the temperature limits for the unmodified Sharp display appear to be only operational limits. Temperature excursions over the full

mil temperature range (and above) produced no apparent degradation of the display, and no destructive failure. Further, the measured LCD clearing temperatures exceeded the manufacturer's recommended maximum operating temperatures by as much as 9°C.

2.1 Introduction and Background

There are several considerations that must be addressed with the use of Active Matrix Liquid Crystal Display (AMLCD) technologies in military aircraft environments that typically are not associated with commercial applications of this same technology. These include high temperature environments, high solar radiation environments associated with the open canopy, high altitude operation, and absence of forced air or direct impingement-cooling techniques.

As an example, in the F-16 environment, in-flight steady-state conditions may require the display to simultaneously operate at a display luminance of 200 foot-Lamberts (fL), in ambient behind-the-instrument-panel temperatures of 50°C, under a solar flux of 883Watts/m^2, and without cooling air for the display. The high ambient temperature is a result of the high solar load on the open bubble canopy design found in fighter applications. The display is required to operate at 200 fL luminance in order to be readable (i.e., adequate contrast ratio) in the high ambient light level accompanying the high specified solar load.

The thermal concern is that commercial off-the-shelf (COTS) displays are typically only rated to operate at temperatures below 85°C on the display glass surface. This temperature is defined by the clearing point of the display (the upper temperature threshold at which the display no longer responds visually to its electrical signals). At temperatures above the clearing point, the liquid crystal material fails to behave as a crystalline structure, the molecular orientations becoming more random in nature. Once this occurs, the display loses its ability to control the passage of light and the display will clear. There is no permanent (irreversible) damage associated with operational temperature excursions and the display will perform correctly once it is returned to a temperature lower than its clearing point.

The basic structure of the LCD does not lend itself well to the task of transferring heat off of the display surface. The LCD "glass," as it is often referred to, is typified (Figure 2-1) by two parallel layers of Corning 7059™ glass that are sealed to each other at the periphery, enclosing a thin cavity filled with liquid crystal material. The inner surface of one layer (active glass) is coated with several thin patterned layers to create the matrix of thin-film transistors that control the optical orientation of the liquid crystal material.

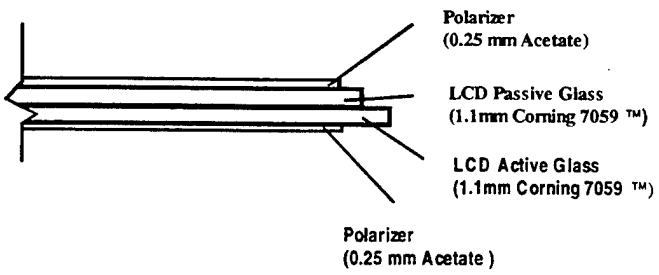

Figure 2-1 Typical Commercial AMLCD Laminate Structure

The second glass layer (passive glass) contains a portion of the transparent electrode structure that cooperates with the structures on the passive glass to define the electrically addressable display elements. A polarizing element is laminated on both outside surfaces of the glass assembly to complete the optical light valve. These polarizers may need to be replaced if the commercial polarizers supplied prove susceptible to test temperatures or humidity.

Each layer of glass is 1.1-mm thick and has a thermal conductivity of only 1.04W/m°K. Each polarizer is on the order of 0.25 mm thick and has a thermal conductivity of 0.25 W/m°K. Not only is the glass a poor thermal conductor, but the stack is also only 5% transmissive to the light it receives from both the backlight and the solar load. The absorbed incident light is converted directly to additional heat on the glass surface.

As a result, initial thermal analysis of an unmodified 3.6x4.6-inch (3.2x4.3-inch active area) display in the F-16 environment predicts a glass temperature of 96.4°C under full solar load and at the specified 200 fL display luminance. This substantially exceeds the typical upper operating temperature rating of commercial LCDs.

2.2 Approach

Environment – In order to evaluate the current cooling schemes, and to perform thermal analysis for alternate methods, the challenging F-16 cockpit environment was chosen for the test case. The F-16 environment combines high (883W/m^2) solar load on the display face, high operating ambient temperature (50°C), high luminance requirement (200 fL),

and cooling limited to free convection and radiation from the display housing and display face. Other fighter aircraft such as the F-15 and the F-18 have similar environmental requirements, but have cooling air available and do not pose as great a thermal challenge. Even though the F-16 environment is being studied as a worst case application, the lessons learned in this application are still applicable to other airframes in which solar load and high ambient temperatures are a concern (e.g., F-15, F-18, etc.).

An alternate set of operating conditions was examined for a single configuration of each size of display. In this case, the backlight power remained the same, but the solar load was reduced from 883W/m^2 to 667W/m^2 (75.6%), and the ambient air temperature was raised from 50°C to 55°C. For each of the six display sizes, the "best" configuration from the original boundary conditions was rerun using the new conditions. Minimum and maximum temperatures of the display glass, frame, and diffuser were predicted from the thermal model for each of the six sizes, reported in Appendix A.

Baseline commercial display selection – The existing display size in the F-16 is 4x4-inch. This is one reason for selecting a Sharp™ 3.6x4.6-inch automotive-grade display (16.5 in^2) for the baseline display. The Sharp LQ6RA52 also has design features and optical transmission typical of commercial displays. It has a laminate structure consisting of two layers of Corning 7059™ with two acetate polarizers, exhibits 48% transmission, and has an operating temperature range of -30°C to +85°C.[2] This Sharp display has been used in other COTS ruggedization studies due to its extended temperature range.[3] This particular panel is fabricated with flip-chip-on-glass (FCOG) drivers. In addition to

meeting the mechanical and performance guidelines typical of commercially available displays, it is readily available, relatively inexpensive (approximately $800 in small quantities), and is supplied with the circuitry necessary to operate with a RGB signal.

High-level breakdown – As illustrated in Figure 2-2, the structure of the LCD module breaks down into the LCD glass assembly itself, the additional LCD stack components adjacent to the front face of the LCD glass, and those adjacent to the rear, a backlight, and the display unit housing (ignoring for the moment the means by which these are interconnected). Our objective was to thermally "cocoon" the LCD, creating a mini-environment around the temperature-limited LCD glass component, such that the LCD could function properly in the aircraft environment.

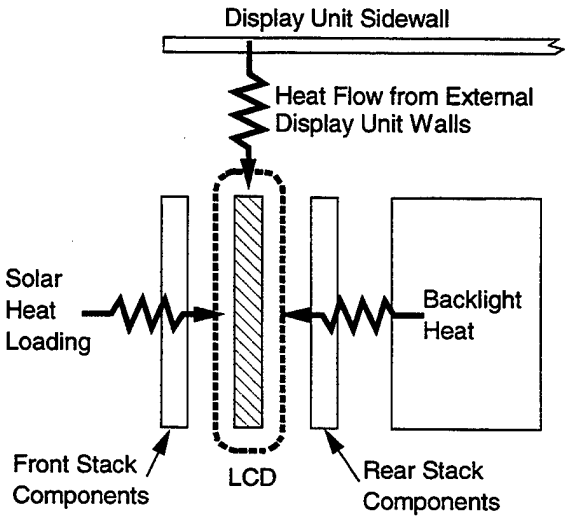

Figure 2-2 High-level Thermal Structure

In order to validate the thermal model program results, the principal beneficial design amendments developed in the program were incorporated into hardware models which, along with an unmodified baseline assembly, permitted both validation of the model and confirmation of the predicted benefits of the modifications.

The fundamental task was to minimize heat flow into the mini-environment, and facilitate heat flow out of the mini-environment.

Modeling detail – We initially identified some seven opportunity zones (Figure 2-3). Through symmetries and similarities, the opportunities consolidate in substance into three: (1) rejection and minimization of heat flow into the complete display stack, (2) minimization of heat flow into the commercial LCD stack itself, and (3) facilitation of heat flow out of the LCD stack. The backlight efficiency and heat rejection opportunity (opportunity 6 in Figure 2-3) was not specifically studied in this program whose focus was the LCD stack itself.

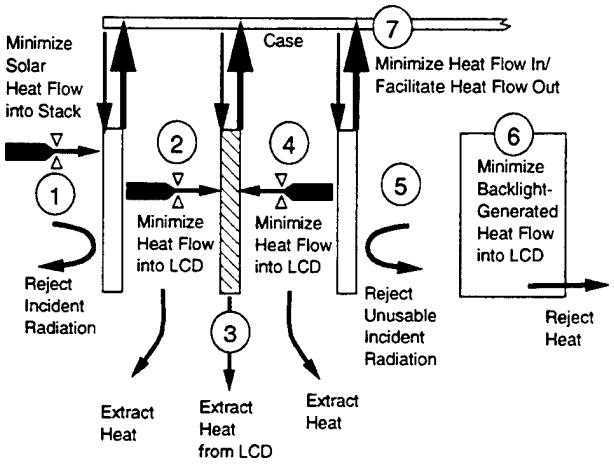

Figure 2-3 Thermal Opportunities

From the thermal modeling standpoint, the problem was analyzed in terms of basic heat transfer, free convection, radiation, and conduction (Figure 2-4). The main heat sources in this problem are the solar loading in the form of visible and infrared (IR) energy, and the backlight (also visible and IR). The visible energies from the sun and the backlight are converted to heat in the display as a function of the display's ability to transmit or absorb energy at these wavelengths. The main paths for power to leave the display are free convection off of the display surface to the surroundings, conduction from the sides of the display to the display housing, and radiation to the surroundings.

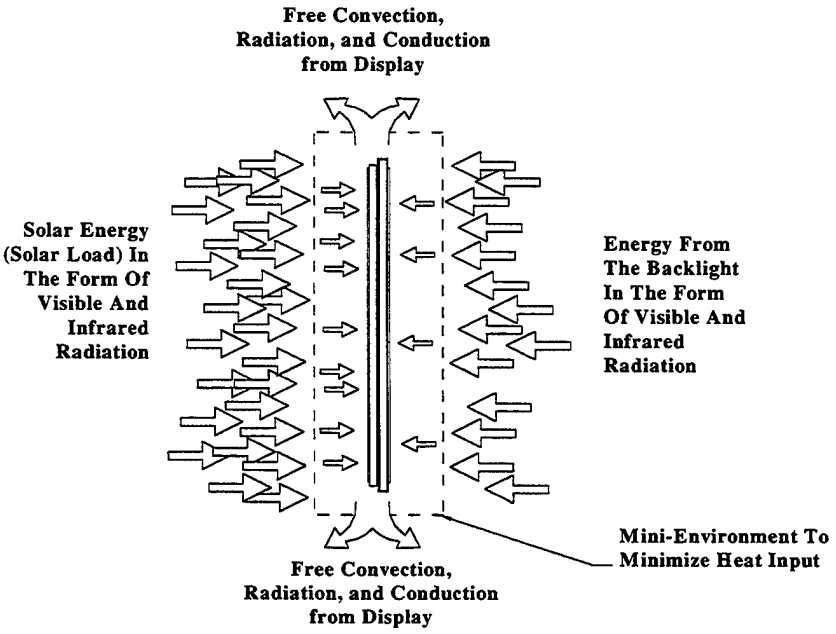

Figure 2-4 Energy and Heat Flow Paths in/out of LCD Stack

We focused on isolating the LCD glass from power influx from the external ambient and the rest of the display structure, removing the heat from the commercial LCD glass as efficiently as possible, and rejecting heat benignly into the ambient air and display housing. In this way, we sought to create the desired mini-climate for the display.

2.3 AMLCD Thermal Model Basics

Table 2-1 provides an overview of concepts considered as a means for improving the thermal environment of the LCD. Included is a brief description of the technique, a note as to whether or not it was chosen to be fully modeled, and an indication as to whether the technique proved beneficial. The table is broken into categories of heat removal, isolation, and heat rejection. Not all of the listed techniques were fully modeled but all of

them were evaluated for viability. For the sake of clarity and brevity only the final configurations that were found to be most effective and that have the potential to be economically implemented are presented in this report.

Table 2-1 Alternative LCD Temperature Reduction Techniques

TECHNIQUE	DESCRIPTION	MODELED?
Heat Removal		
Improved lateral heat flow	Ohara TR-5/TR-6 glass with an improved thermal conductivity of 1.4W/(m•K) that can be laminated on existing display to improve lateral heat conduction.	Modeled.
Improved heat flow via free air convection loop from back of display to ambient	The back of display could be allowed to freely exchange air from the cooler outside world, essentially providing another free convective surface in addition to the front surface.	Not modeled. Difficult to exclude/remove external light-absorbing contamination from the rear display surface.
Thermal enhancement of interface materials	Thermally conductive RTVs and pads to improve the heat transfer coefficient from the glass to the housing.	Modeled.
Liquid cooled display	Liquid could be pumped through display housing to improve its conduction coefficient.	Not modeled. No liquid cooling allowed by F-16 (and most others).
Active cooling	Thermoelectric coolers (TEC) to pump heat from display at housing interface to improve heat transfer.	Modeled.
Improved lateral heat flow	Diamond coatings sprayed on display surfaces to improve conduction.	Not modeled due to excessive process cost & coefficient of expansion problem.
Improved lateral heat flow	Sapphire glass with a thermal conductivity of 40W/(m•K) that can be laminated on existing display to improve conduction.	Modeled.
Active cooling	Heat pipes - 1/8-inch diameter copper tube filled with a liquid (e.g., alcohol) that operates through a phase change to "pump" heat from hot spots to cold spots along the pipes length. The pipe is approximately 60 times as conductive as copper.	Modeled.
Improved chassis thermal conductivity	High thermal conductivity carbon graphite composite chassis.	Not modeled. Typical aluminum chassis was a sufficiently good conductor in this case.

Table 2-1 (continued)

TECHNIQUE	DESCRIPTION	MODELED?
Improved chassis thermal conductivity	Copper CERMET™ coating sprayed onto interior of aluminum to improve thermal conductivity of display housing.	Not modeled. Typical aluminum chassis was a sufficient conductor in this application.
Isolation		
Air gaps in display stack	Air gaps could be built into display stack to limit the amount of heat introduction to display by convection from backlight.	Modeled.
Thermally enhancing interface materials	Insulating materials or buffers used to isolate the glass from the chassis.	Not modeled because in all cases the chassis was a resource, cooler than the display.
Heat Rejection		
Switchable radiation-reflecting film	For example 3M manufactures an electrically-switchable Privacy Film consisting of a polymer-dispersed liquid crystal (PDLC) material sandwiched between two layers of polyester. In the absence of an electric field, the material is a diffuse reflector. With a field applied, the film is transparent, but 70% transmissive.	Not modeled. These films exhibit low transmission when activated, increasing backlight power and heat. Many such materials are transparent to IR energy; long-term stability of organic components in solar-exposure ambient unknown.
Hot mirror	Thin-film spectrally selective filter to pass visible light and reflect infra-red from front of display.	Not modeled. No existing material with suitable properties. Development out of cost constraints of program. For sharp cutoff between IR and visible, cutoff wavelength varies strongly with angle. Some cutoff of red visible probable.

2.4 Conceptual Starting Point

The starting assumptions for the thermal model are listed below:

1. Ambient air is 50°C in accordance with F-16 specifications for high-temperature operating condition.
2. Solar radiation is 883W/m^2 in accordance with F-16 specifications.
3. Forced convection and cooling air are not available (F-16 constraint).
4. Verification of model predictions within ±5°C is adequate for validation, but a maximum 80°C LCD operating temperature to be sought, acknowledging the potential prediction error (Sharp specification is 85°C).
5. LCD glass and polarizer layers are modeled as manufactured by Sharp.
6. LCD glass/polarizer subassembly is mounted in lightweight aluminum frame, replacing the original steel frame.
7. Backlight (obtained from Korry Electronics) is not modified.
8. Thermal conduction to airframe and instrument panel is not considered (F-16 constraint).
9. An additional layer of glass (1.1 mm Corning 7059™), with an anti-reflection (AR) coating, is bonded to the front surface of the commercial LCD to protect the polarizer and minimize surface reflections.
10. An additional layer of glass (1.1 mm Corning 7059™), coated with a thin electrically-conductive layer of indium tin oxide (ITO), is bonded to the rear of the LCD stack for electric heating under cold ambient conditions to bring the LCD to operating temperatures (typically 20°C).

All configurations of the display have this basic laminate structure, but alternate materials were evaluated for the cover and heater glass in place of the typical Corning 7059.™ Figure 2-5 diagrams a cross section of this structure.

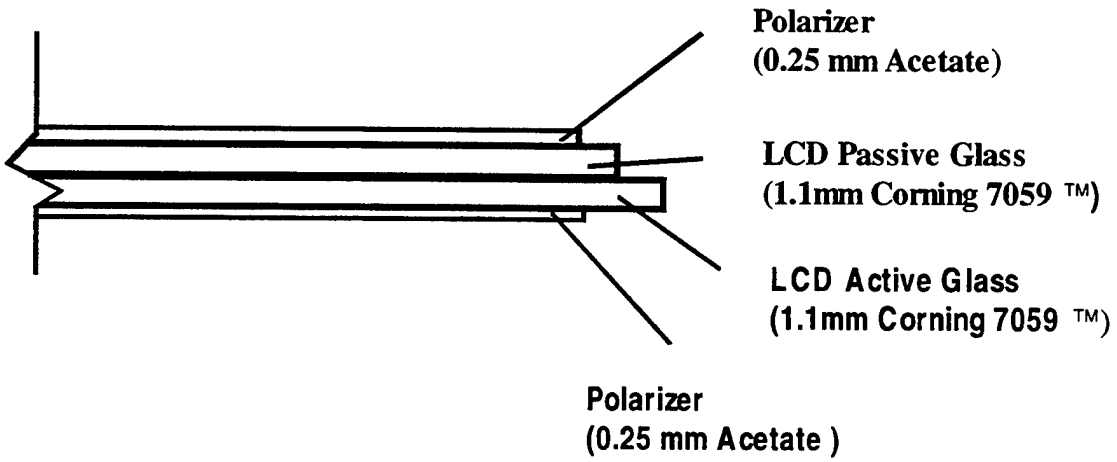

Figure 2-5 Cross Section of Typical Commercial AMLCD Laminate Structure

Estimates were also made regarding specifics of the thermal loads within the model, establish boundary conditions for the model. In order to obtain estimates for the fluorescent lamp power required to generate the 200 fL as specified in the F-16 requirements, several measurements were made of the lamp power and luminance, with and without the display. The results of these measurements are shown in Figure 2-6. From the data of Figure 2-6, it was determined that 7.3 Watts at the bulb would net 200 fL through the display. A lamp power of 8.0 Watts was the value used in the thermal model to allow for lamp efficiency degradation over time.

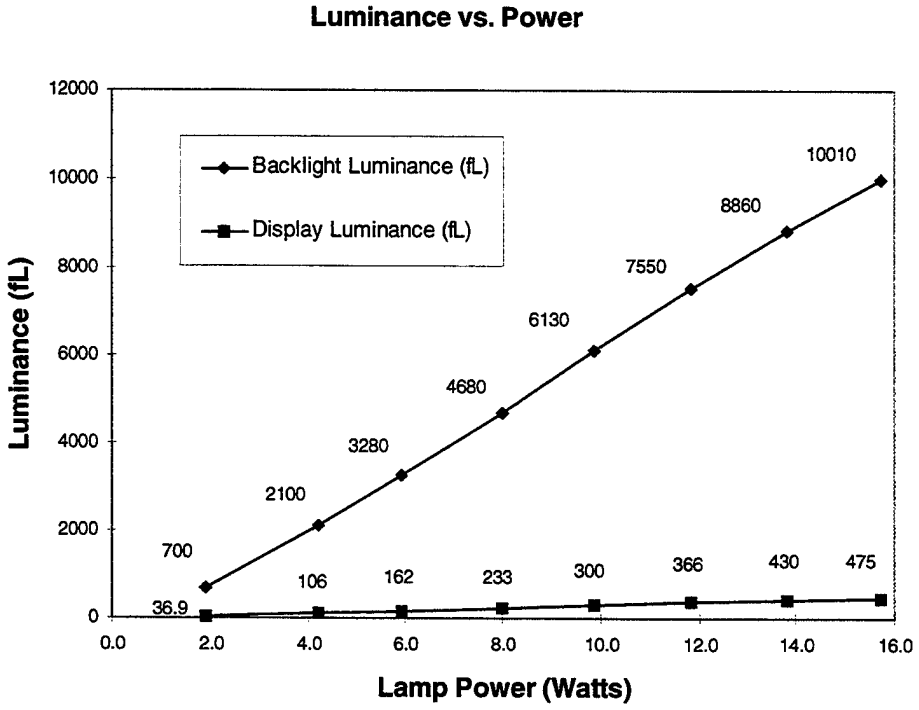

Figure 2-6 Backlight and Display Luminance as a Function of Lamp Power

The fluorescent lamp power is apportioned in Table 2-2 Fluorescent Lamp Power Distribution.[4]

Table 2-2 Fluorescent Lamp Power Distribution

Energy Type	Percent of Total Lamp Power	Power for 8.0 Watt Lamp
Emitted arc stream light (<800nm)	22%	1.76 watt
Emitted arc stream IR energy (>800nm)	36%	2.88 watt
Energy absorbed by lamp & reradiated as IR	42%	3.36 watt

The detailed energy absorption characteristics of the backlight are complex, and many specific material parameters are unavailable (not known, or proprietary to the backlight

supplier). Accordingly, the model was simplified by lumping some parameters, and making reasonable initial estimates of more critical parameters. As the validation models were constructed and tested, those parameters were further refined by comparing the predicted behavior with the actual behavior of the validation models.

It was assumed that all IR energy incident on the backlight cavity walls was absorbed.[5] (While some IR is reflected, most is absorbed again in its next contact with a surface). This energy was apportioned by approximating the view factors of each component relative to the bulb. For example, the cavity walls adjacent to the curved ends of the lamp see less of the light emitted by the lamp than do the other surfaces of the backlight cavity. It was assumed that the walls of the backlight cavity would reflect 100% of the visible light. Though not strictly true, the absorption was accounted for by lumping it in the 10% diffuser absorption for visible light. The LCD absorbs 95.2% of the light emerging from the diffuser.

The LCD absorbs most of the visible energy in the polarizers. However, to simplify the model's boundary conditions, all energy was absorbed in the active LCD glass. This is permissible because heat conduction through the thickness of the glass and acetate polarizers is very high compared to the in-plane conduction of the layers. The lamp heat energy convected and conducted away from the bulb was shared equally by the back wall (the thermal sink in the backlight), and the air near the sink. Table 2-3 Lamp Energy Allocation summarizes how the lamp energy was allocated among the thermal model components.

Table 2-3 Lamp Energy Allocation

Display Location	Energy Type	Percent of Total Lamp Energy
LCD	85% of the visible energy	18.7% total
Diffuser	25% of IR 10% of visible	11.2% total
Backlight side walls	30% of IR	10.8% total
Backlight rear wall (thermal sink)	45% of IR 50% of heat	37.2% total
Air near sink	50% of heat	21.0% total
Transmitted	5% of visible	1.1% total

For the solar loading, 50% of the solar energy was visible light and 50% was IR energy. Based on the Table 2-3 estimates, Table 2-4 Solar Energy Allocation summarizes the solar energy allocations for the ESC™ model components:

Table 2-4 Solar Energy Allocation

Display Location	Energy Type	Percent of Total Energy
LCD	90% of visible 60% of IR	75% total
Diffuser	30% of IR	15% total
Reflected	10% of visible 10% of IR	10% total

2.5 Creation of the Thermal Model

The baseline display stack elements are illustrated in Figure 2-7, Figure 2-8, and Figure 2-9. The display itself consists of two layers of 1.1-mm thick Corning 7059™ glass and two polarizers held in place with a lightweight stainless steel frame. As described previously, two additional layers of glass were laminated to the polarizers to protect them from scratches and humidity. The backlight consists of a serpentine fluorescent lamp enclosed in a lightweight steel case. This case has a substantial aluminum heatsink/reflector plate, and passes light through a polycarbonate diffuser stack to the LCD. The display and backlight are mechanically housed in a lightweight aluminum chassis that is 2.54-mm thick. The backlight used in the deliverable units was supplied by Korry Electronics Co. (Seattle, WA).

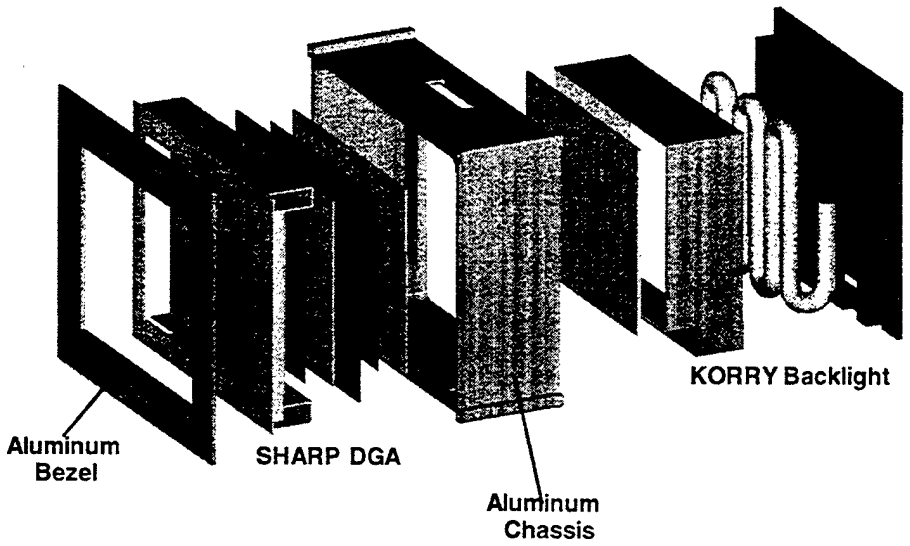

Figure 2-7 Exploded View of Display Stack Showing Major Components

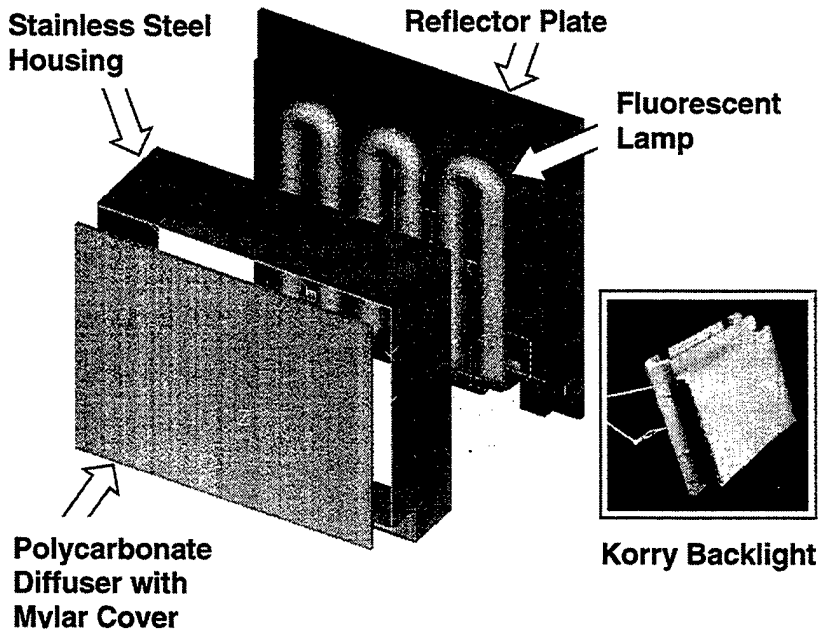

Figure 2-8 Exploded View of Backlight Components

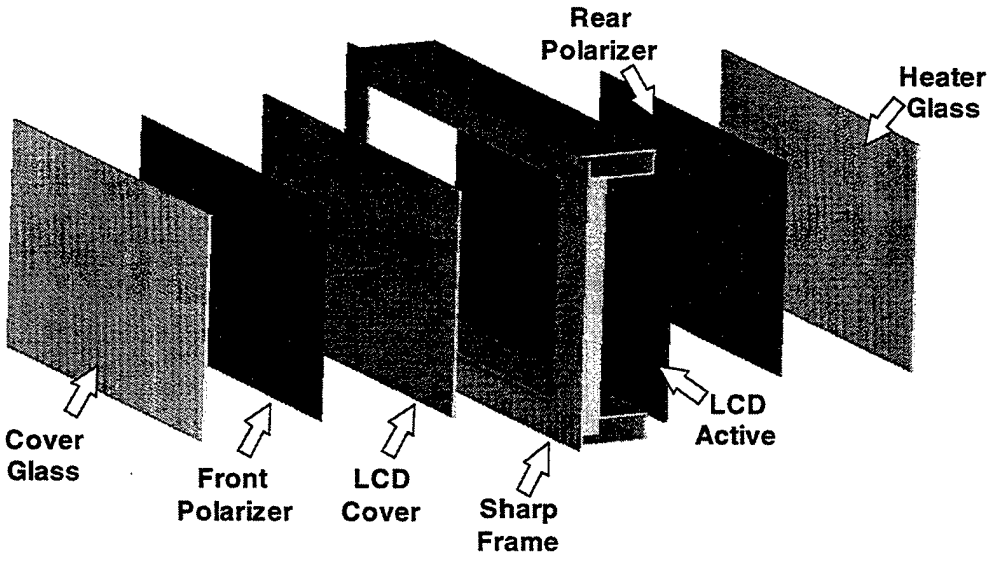

Figure 2-9 Exploded View of Backlight Components

Thermal Analysis Tool – The thermal analysis tool used for this analysis is Electronic System Cooling (ESC™) within Structural Dynamics Research Corporation (SDRC™) Master Series™ 5. This analysis software tool uses an iterative solution approach that couples a fluid solver to a conduction/radiation solver to provide a simultaneous solution of a fluid/solid mesh. This tool set made it possible to rapidly iterate "what-if?" analyses on a single model to efficiently evaluate the impact of changes in material properties such as thermal conductivity, and variations in physical properties such as thickness and surface roughness.

The basic process followed in the creation and solution of a thermal model is depicted in Figure 2-10. First the solid model is created in SDRC™ Master Modeler to provide the geometric relationships between the different components in the assembly. The next step is to apply finite element analysis (FEA) to the structure.

The FEA process permits the behavioral modeling of complex thermal structures such as the LCD assembly. At the atomic level, the structure consists of a huge number of molecules, interacting with each other in a still larger number of ways, an intractable computational problem. The FEA process divides the structure into a smaller number of chunks (nodes), with a finite number of connections to adjacent nodes, forming a mesh.

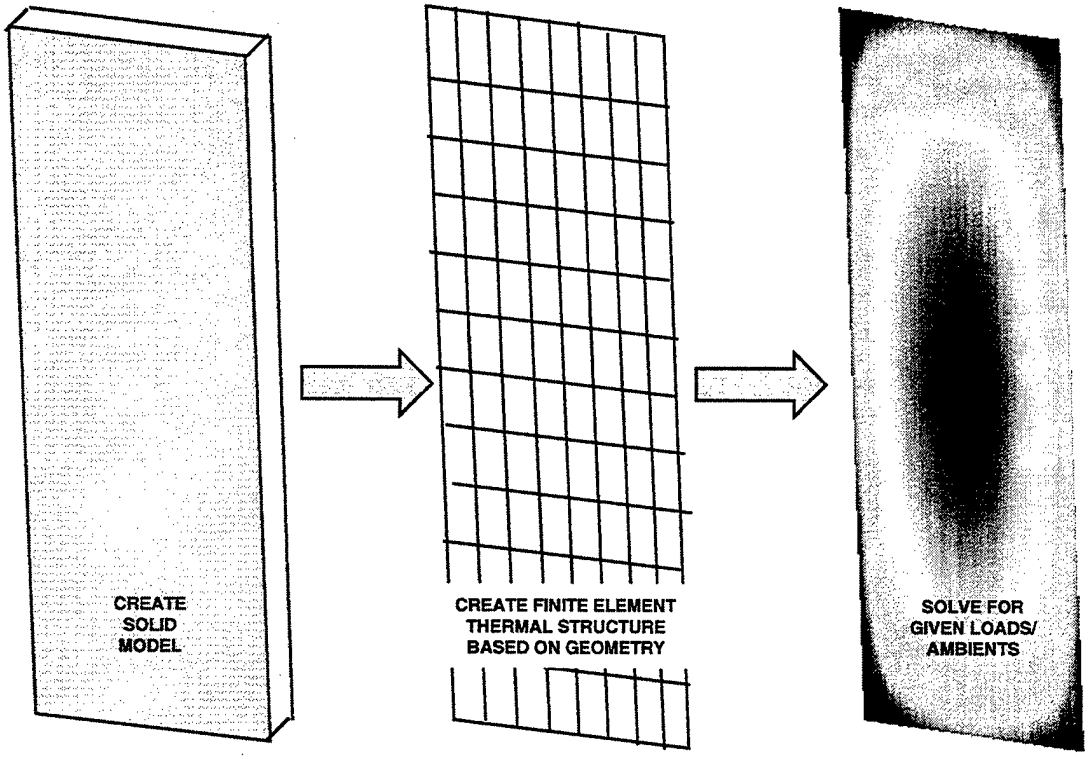

Figure 2-10 Simplified SDRC™ Thermal Design Sequence

The tractability of the computational problem is further improved by taking advantage of any boundary condition, structural consideration, or other condition, which permits local simplifying adjustments of node density and interconnection rules. Parameters such as solar load energy flow are imposed as boundary conditions. The balance to be struck is to have the node density made small enough that each node or interconnection's dynamic properties are linear (or at least analytic), while at the same time, keeping the total number of nodes and connections small enough for manageable computation. With the mesh properly defined, the dynamic behavior of the structure can be studied by examining the state (e.g., temperature) of specific nodes as time in advanced in small increments (with furious computation between time ticks).

After creation of the solid model, a meshing module is then used to create a Finite Element Model (FEM) of the solid with the correct physical and material properties, such as thermal conductivity, thickness, and emissivity. The ESC™ module is then used to define how the elements of each part within the assembly can receive or transfer heat (convection properties, radiation view factors, ambient temperature, contact coefficients, etc.).

The ESC™ model used in this analysis is constructed primarily of shell elements representing all the main surfaces of the frame, backlight, diffuser, and LCD panel. The LCD panel itself is modeled as a number of individual layers of shells, each connected to the adjacent layers through the use of ESC™ thermal couplings (TCs), also known as contact coefficients. The active LCD glass, the passive LCD glass, the front and rear polarizers, cover glass, and heater glass layers are modeled.

The edges of some of the LCD layers are lined with beams, as is the edge of the aluminum frame. Beams provide a means for terminating the mesh of a component, as well as a means for defining thermal contact coefficients for its connection(s) with adjacent elements. These beams allow the layers to be thermally connected using ESC™ TCs to account for the heat transfer between the LCD glass and the frame. The diffuser is modeled as two layers of shells, one representing the polycarbonate diffuser and the other representing a Mylar™ cover layer. These two layers are connected using an ESC™ TC

to represent the thermal resistance of the Mylar™ and a small air gap between it and the polycarbonate diffuser.

The air in the backlight is modeled with solid elements, and the natural convection within the backlight is automatically calculated in the ESC™ analyses based on surface finish values, temperature differentials within the cavity, obstructions, etc. Heat is assumed to convect to the air from the diffuser, sidewalls and sink in the backlight cavity.
In general, heat flows through the structure by direct conduction between the physical components, with the exceptions modeled using ESC™ thermal couplings. However, in two places the thermal heat transfer is more complicated. In the air gap between the backlight walls and the aluminum frame, it is assumed that heat is transferred via conduction through the air gap, and through radiation from one wall to the other. The situation is similar between the Mylar™ sheet of the diffuser assembly and the heater glass (or rear polarizer in the absence of the glass). The resulting mesh is illustrated in Figure 2-11. Any variation in mesh detail and density reflects dimensional and property variations in the different areas of the structure. [The LCD glass faces left, and the backlight is to the right in the figure].

Heat impinging on the model is rejected in three ways. All the outer surfaces of the structure dump heat to the surrounding by both convection and radiation. For some of the larger displays examined, active cooling in the form of heat pipes is used to extract heat from the frame and pass it to thermal electric cooling units (TECs).

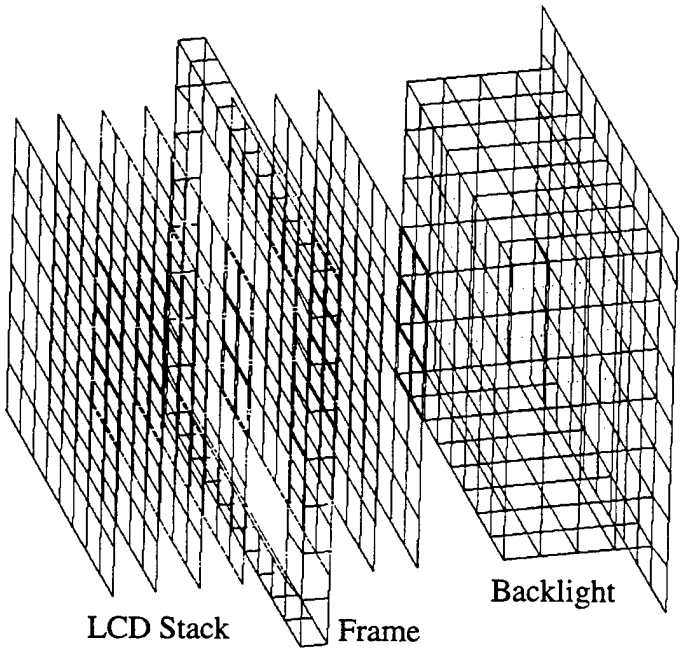

Figure 2-11 SDRC™ Finite Element Model of Display

The heat pipes were purchased from Noren Products, Menlo Park, CA, and consisted of a 10-inch length of 1/8-inch OD copper tubing whose inner surfaces are lined with a capillary wicking material. The sealed tubes also contain a vaporizable liquid.

When sufficient heat is applied to any site on the tube, the liquid in that locale vaporizes, extracting from the metal the latent heat of vaporization.[6] The vapor, with its higher kinetic energy, propagates quickly to a cooler portion of the tube, where it condenses and releases the heat of vaporization.

In this way, the heat is transported very rapidly from one part of the heat pipe to another. The condensed fluid is absorbed into the wicking material at the cool site. The capillary forces are strong enough to move the liquid back into the region where vaporization is occurring, so there is a continuous net liquid flow from cold to hot in the wicking material, completing the cycle. Manufacturers claim that heat pipes can have a thermal conductivity many thousands times that of copper. We modeled active heat removal from the heat pipes by means of thermoelectric cooling (TEC).

A number of iterations were carried out to fine tune the ESC™ model linkages and parameters to obtain better fidelity in predicting the results obtained from the verification test displays. Appendix C provides verification information for a number of ambient conditions and display configurations.

Figures 2-12, 2-13, and 2-14 show examples of the graphical SDRC™ output. Figure 2-12 shows a representation of temperature distribution in the LCD stack layers. The scale at the right (which may vary significantly from figure to figure!) shows the temperature range, in this case from 60°C to 97.4°C with red representing the hottest region. In this case, it may be clearly seen that the center of the layers is the hottest (on the order of 90°C), the result of relatively poor lateral heat flow in the glass and plastic layers. The third layer has blue edges (60°C). But, the temperature gradient is evidently quite high at the edge of this layer, indicating that heat is building up in the

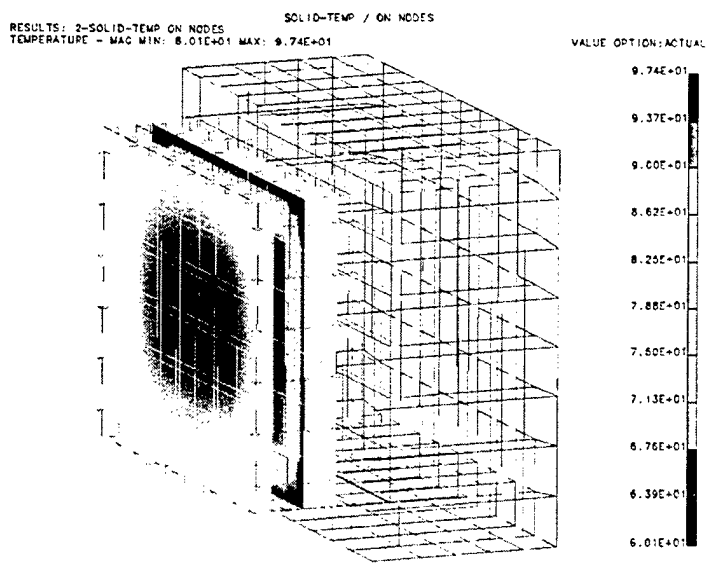

Figure 2-12 Sample Results - LCD Stack Temperature (°C)

See Appendix D for color version.

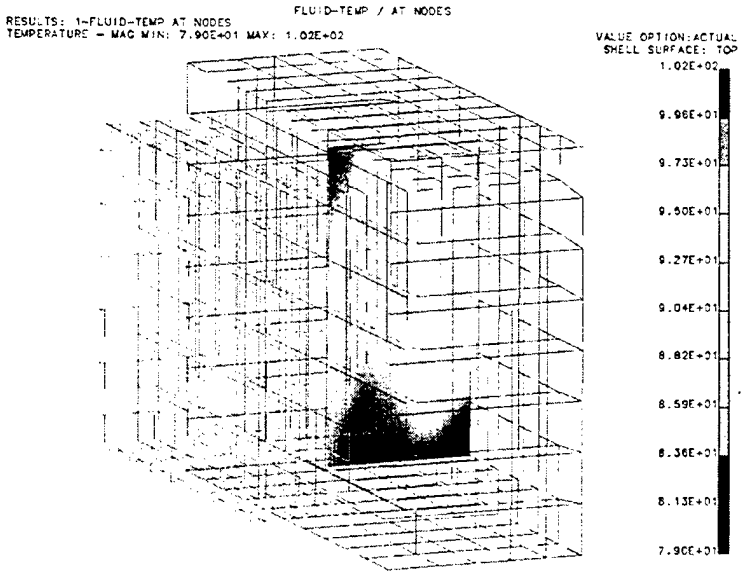

Figure 2-13 Sample Results - Air Slice Temperature (°C)

See Appendix D for color version.

layer in spite of aggressive extraction of heat from the layer at the edges. This is a situation similar to that found in larger displays with high solar loading where the power influx can overwhelm any practical means for extracting heat short of moving cooling air. It is also evident in the case shown that the other layers are not thermally well-coupled to the element edge-cooling the dark blue-edged third layer.

Figure 2-13 shows a front-to-back cross-section of the air temperature profile within the backlight cavity. The temperature scale is almost the same for this view. The rendering shows that the temperature is coolest at the bottom of the backlight, hottest at the top front edge, and that there is an apparent circulation of heat within the cavity. This circulation is clear in a different view, Figure 2-14, which indicates with arrows the convection flow pattern of the air within the backlight cavity.

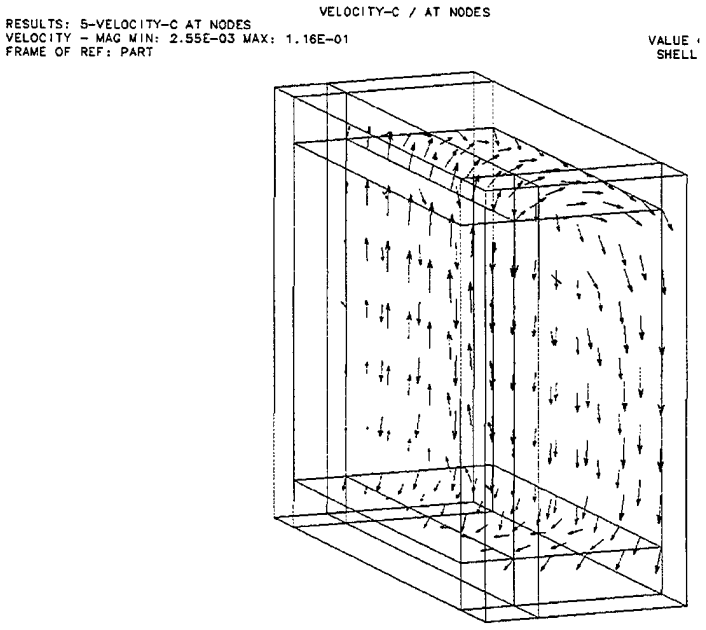

Figure 2-14 Sample Results - Air Cavity

2.6 Thermal Model Configurations

The 3.6x4.6-inch display was the baseline for both thermal modeling and for physical verification of the thermal model. The physical models (using the Sharp 3.6x4.6-inch LCD and adaptations) were created to validate the ESC™ thermal model for several power load conditions. The successful validation task provided the foundation for thermal modeling of displays in other sizes.

Displays up to 5x5-inch are typical for F-15, F-16, F-18 and similar fighter applications. However, larger displays may be required for F-22, C-17, C-130 and future advanced fighters. Consequently, several other sizes were modeled, including 4x4-inch, 5x5-inch, 6x6-inch, 6x8-inch, 7x7-inch, and 8x10-inch. Sensitivity studies evaluated the temperature rise from ambient due to solar heating, temperature gradient due to solar heating, efficiency of edge cooling, and effect of backlight power on the display temperature, all as a function of display size. Each size was evaluated with and without solar loading. Solar load was programmed in the model as a flux density so that the solar power also scaled with display size. Calculated backlight power was scaled with the display surface area to maintain a 200 foot-Lambert (fL) baseline.

[In some fighter applications, a luminance greater than 200 fL may be required to achieve the desired contrast ratio in high sunlight ambients, introducing additional heat into the display unit. Specular and diffuse reflectance, upon which contrast strongly depends, are

typically better in custom displays than in ruggedized industrial-grade displays. Consequently, the selection of a ruggedized industrial-grade display needs to be thoughtfully weighed against the potential for significant impacts on the overall display thermal design and display reliability.]

In each case, the basic structure modeled (and constructed, in the case of the verification models) was a modification of a typical as-manufactured LCD assembly. The LCD glass and polarizers (front and rear) were retained from the as-manufactured assembly. A front glass was bonded to the front polarizer. This glass usually is anti-reflection coated and provides physical protection for the front polarizer. A second glass layer was bonded to the rear polarizer. This rear glass usually has a transparent conductive coating used for cold-start warming of the LCD. The original steel frame for the LCD stack was replaced with a more thermally-conductive aluminum frame. Variations from this structure were incorporated in some of the modeled configurations.

Six basic configurations were evaluated. Four different configurations of the baseline 3.6x4.6-inch Sharp display were modeled (Configurations 1-4 respectively). Two other amendments, Configurations 5 and 6, were made for larger display areas that proved harder to cool.

Configuration 1 (Figure 2-15) – The passive LCD glass is in contact with the aluminum frame with a 30 psi dry contact interface. The cover and heater glasses are both 1.1mm Corning 7059™. The backlight is nominally spaced at 0.25 inches from the back of the LCD surface.

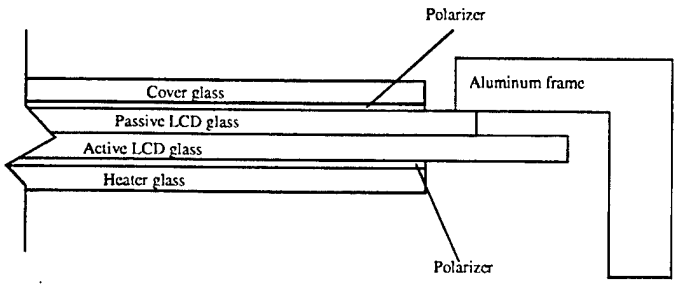

Figure 2-15 Configuration 1, Basic Amended LCD Structure

Configuration 2 (Figure 2-16) – A bead of thermally conductive RTV (room-temperature vulcanizing) silicone material was applied between the frame and the top LCD glass to improve thermal conductivity. The addition improved the joint coefficient of the top glass to the frame from 1.87 W/m°K to 13.8 W/m°K. It also created a 9.3 W/m°K joint coefficient from the bottom LCD glass to the frame, where there was previously no thermal connection.

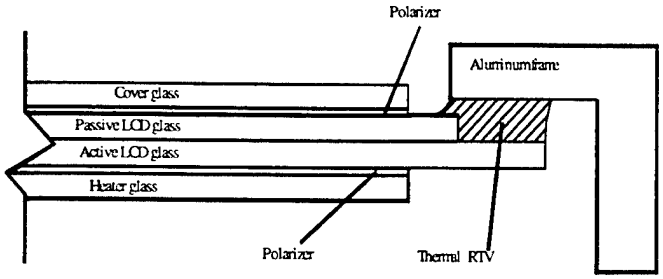

Figure 2-16 Configuration 2, with RTV

Configuration 3 (Figure 2-17) – The configuration is the nearly same as Configuration 2, except that the cover glass was replaced with sapphire to improve lateral heat flow.

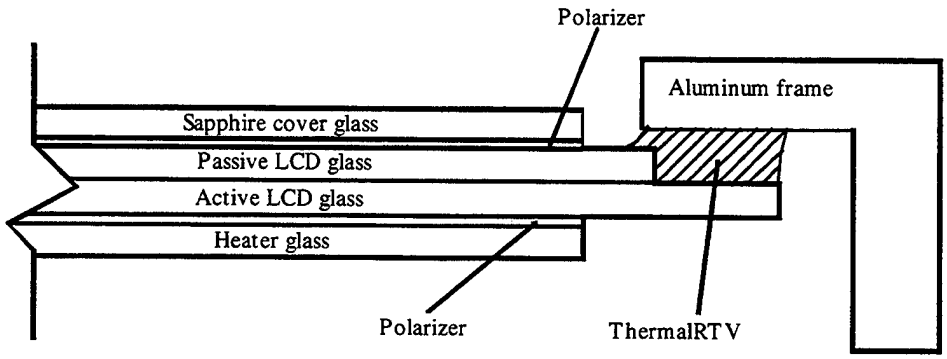

Figure 2-17 Configuration 3, Sapphire Layer Added

Configurations 4, 5, and 6 (Figure 2-18) – These structures are similar to Configuration 3. In Configuration 4, the bead of thermal RTV is extended to thermally connect the sapphire layer and the frame.

In addition, in Configuration 5 (used for modeling some of the larger display sizes), the rear heater glass layer is replaced by a second sapphire layer.

Finally, in Configuration 6, heat pipes are also added to Configuration 5. One end is

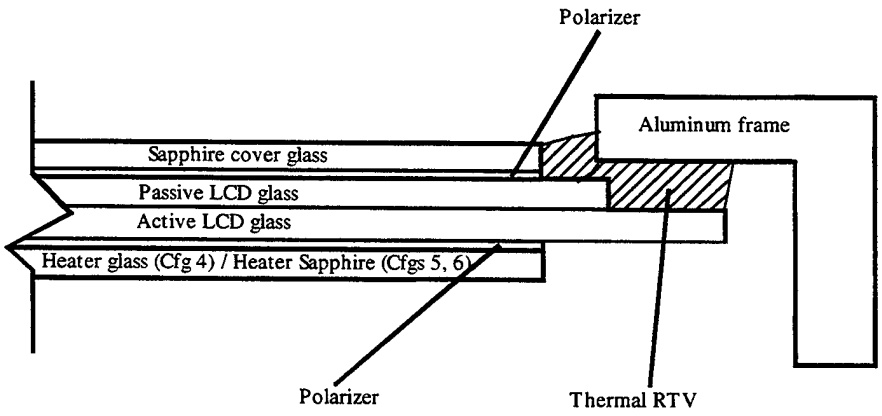

Figure 2-18 Configurations 4, 5, and 6

Finally, in Configuration 6, heat pipes are also added to Configuration 5. One end is thermally bonded to the aluminum frame, and the other is thermally terminated with a thermoelectric cooler (TEC) to actively extract heat from the heat pipes, frame, and LCD assembly. Figure 2-19 shows Configuration 6 with heatpipes incorporated into an aluminum chassis.

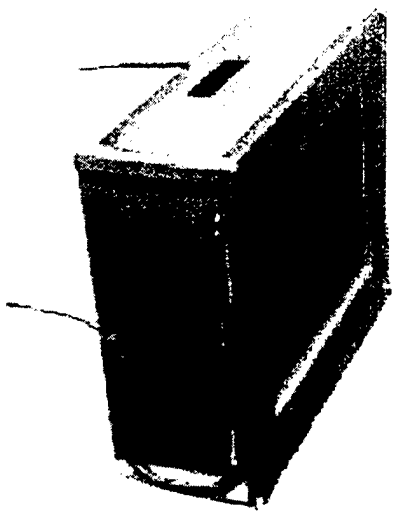

Figure 2-19 Verification Model Incorporating Heat Pipes

3.6x4.6-inch Display Results – The locations of some instructive thermal model temperature probe points for this display size and configuration are shown in Figure 2-20. This plot shows the temperatures at these points for Configurations 1-4, and was helpful in identifying what parts of the thermal path problem to focus on in subsequent work. In particular, it is evident that the focus of the effort needed to be on improving heat flow from the LCD to the frame. The frame at this stage of the development was already a thicker aluminum replacement for the less conductive steel frame supplied originally supplied with the LCD.

The plot of Figure 2-20 shows that Configurations 1-3 yield center temperatures in excess of the target 80°C limit. A large temperature differential also exists between the aluminum frame (the local cooling resource), and the glass center.

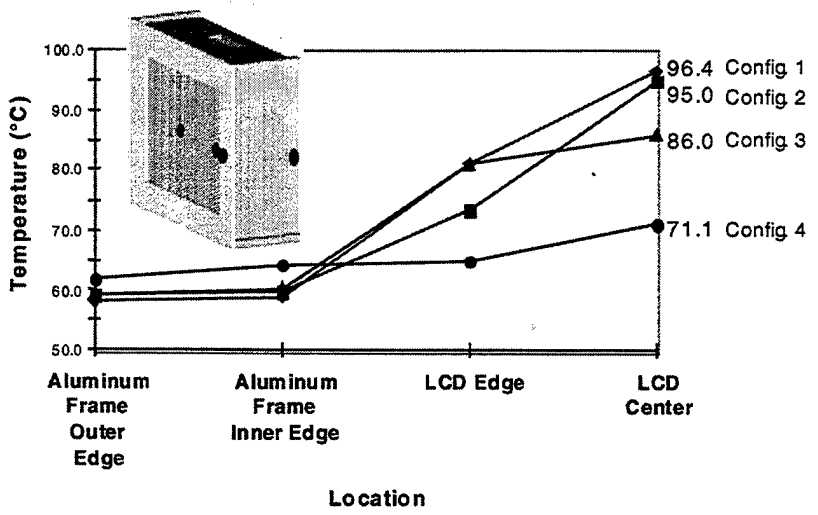

Figure 2-20 Thermal Model Temperature Probe Points

The addition of the sapphire layer in Configuration 3 helped drop the glass temperature by conveying more heat to the edge. However, in this particular configuration, the thermally-conductive RTV was not extended to make direct thermal connection with the sapphire layer.

When the RTV thermal connection was made between the aluminum frame and the sapphire layer (Configuration 4), the results were spectacular. Not only did the glass center temperature drop into the desired range, but also the temperature differentials dropped to about 11°C.

In subsequent modeling of larger display areas, additional modifications of the stack structures were required to keep the stack under the 80°C limit, techniques that were successful up to approximately 50 square inches of display area.

Two sets of results were obtained, corresponding to the conditions with and without the imposed solar load. In each case, the display unit ambient temperature was 50°C. A comparison of the two sets of results clearly shows the dominant effect of the solar loading on the overall thermal problem analyzed in this program.

In the no-solar-load case (Figure 2-21), all of the display sizes were shown to be capable of operation in an otherwise F-16 environment with no measures other than the baseline modifications (added glass layers and aluminum frame). Configurations 2, 3, and 4 (3.6x4.6-inch display) exhibit center-temperature reduction, but all of the configurations are well below the 80°C design objective. Interestingly enough, the larger displays also remained below the center-temperature design goal.

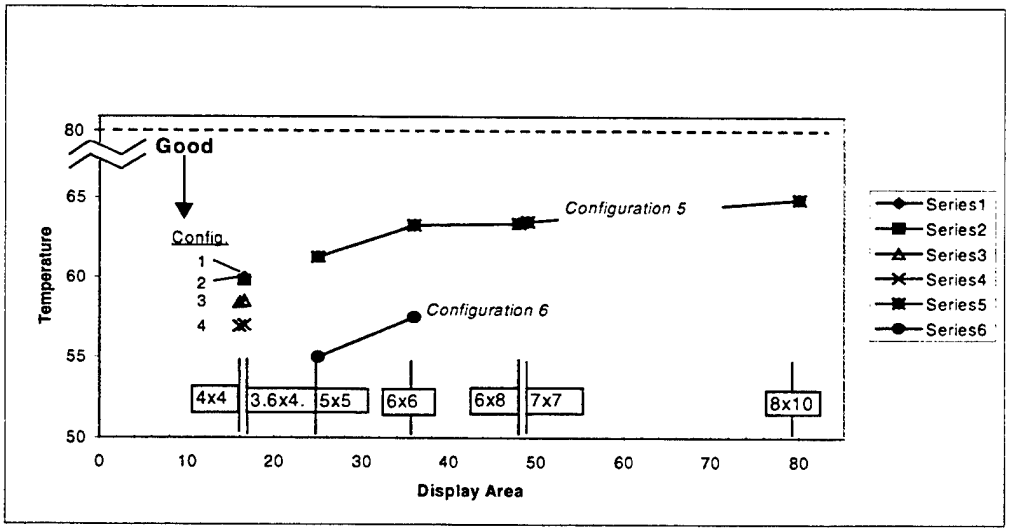

Figure 2-21 LCD Glass Center Temperature vs Display Size (No Solar Load)

It is a different story, however, with the solar load imposed (Figure 2-22). For the two small display sizes, only Configuration 4 was capable of keeping the LCD temperature below 80°C. For the larger 5x5-inch display, Configuration 5 yields marginal compliance. See Appendix D for tabular data for Figure 2-22.

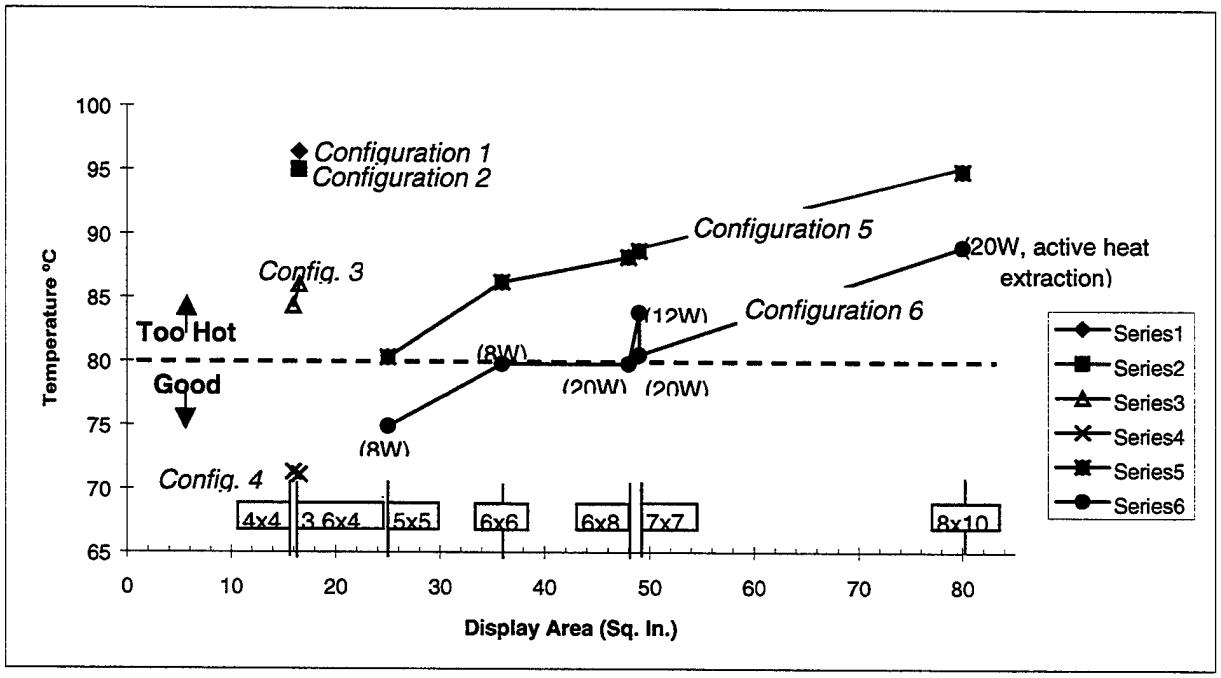

Figure 2-22 LCD Glass Center Temperature vs Display Size (Under Solar Load)

But, the same configuration does not work for still larger displays. For displays larger than 25 square inches, more aggressive cooling is required. Figure 2-22 shows that Configuration 6 can yield marginal compliance for displays as large as 48-49 square inches. Eight watts of active cooling are sufficient for a 6x6-inch display. Twenty watts are required for marginal compliance for 6x8-inch and 7x7-inch displays. It is also interesting to note the temperature difference between 12 Watt and 20 Watt cooling in the

case of the 7x7-inch display. Above that display size, the solar load essentially overwhelms reasonable levels of active cooling.

A different view of the results is given in Figure 2-23 showing the center-to-edge temperature differential in the glass as a function of display size. Configuration 1 exhibits about 15°C difference from center to edge of the glass. With the addition of the thermally-conductive RTV in Configuration 2, the difference goes up, but Figure 2-22 shows that the overall temperature has decreased. The increased differential in Configuration is due to the poor lateral conductivity of the glass. See Appendix D for tabular data for Figure 2-23.

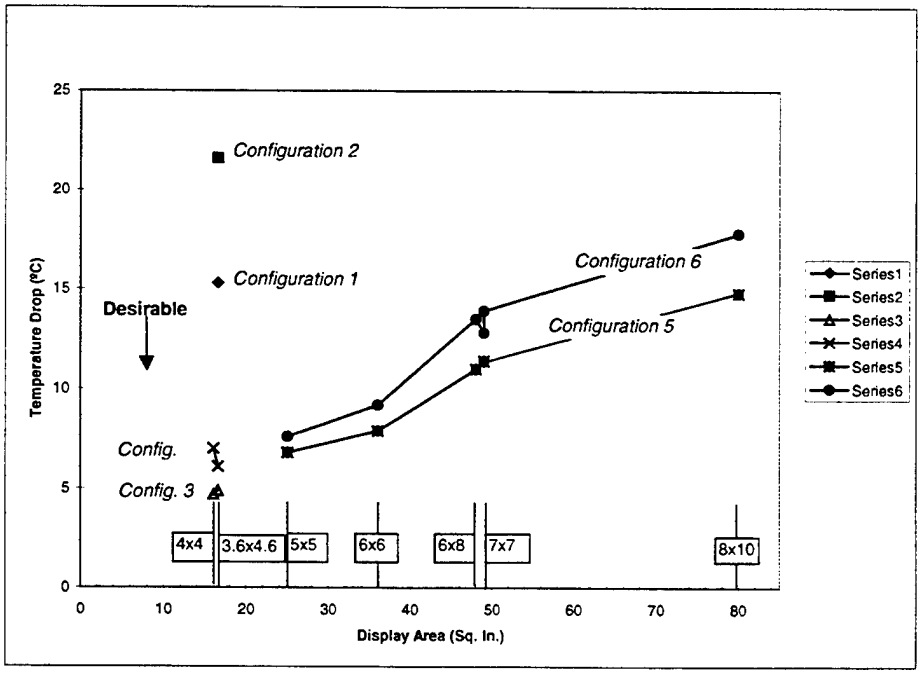

Figure 2-23 LCD Glass Center-to-Edge Temperature Difference (°C) with Solar Load

When the sapphire layer is introduced, both the temperature and differential decrease, and in Configuration 4, the display is cool enough to operate in the environment, and stress in the LCD glass is relatively small because the center-to-edge temperature differential is small.

As the display size increases, the differential also increases, despite the sapphire layer(s). The thermal path is longer, and the thickness of the layers has not changed, so the resistance to heat flow has increased over the distance. The temperature differential allowable is dependent upon the specifics of the display size and stack construction, but a 15°C differential is high, indicative of significant stress in the glass. Further, because the center is hotter than the edge of the glass, the glass periphery is in tension, the weakest condition for the glass. Accordingly, it is reasonable to conclude that it will be difficult to use commercial displays larger than about 49 square inches unless the solar loading is less than that of the F-16, and/or cooling air in some form is provided.

2.7 Testing of Deliverable Display Units

Thermal cycling testing in accordance with F-16 PIDS was performed on all eight ruggedized Sharp displays mounted into an aluminum chassis. The tests consisted of 10 cycles from -54°C to 55°C (stabilization periods required) at a rate of no less than 5°C/minute (Figure 2-24). The purpose of this test is to reveal potential flaws such as congealing of liquid, cracking or rupture of materials, deformation of components, and

fatigue of adhesives (e.g., polarizers, anisotropic conductive films or adhesives) in equipment that will experience these conditions.

Temperature shock testing per the F-16 PIDS (Figure 2-24) was performed on all eight ruggedized Sharp displays mounted in aluminum chassis. The tests consisted of 25 cycles from -54°C to +85°C (stabilization period required) at a rate of no less than 30°C/minute. The purpose of this test is to reveal any of the same set of failures previously described.

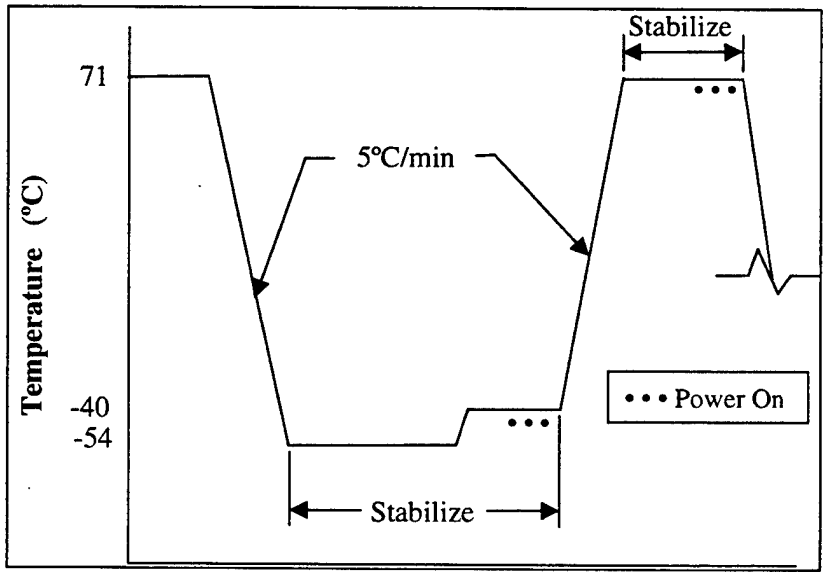

Figure 2-24 Thermal Cycling Test Profile

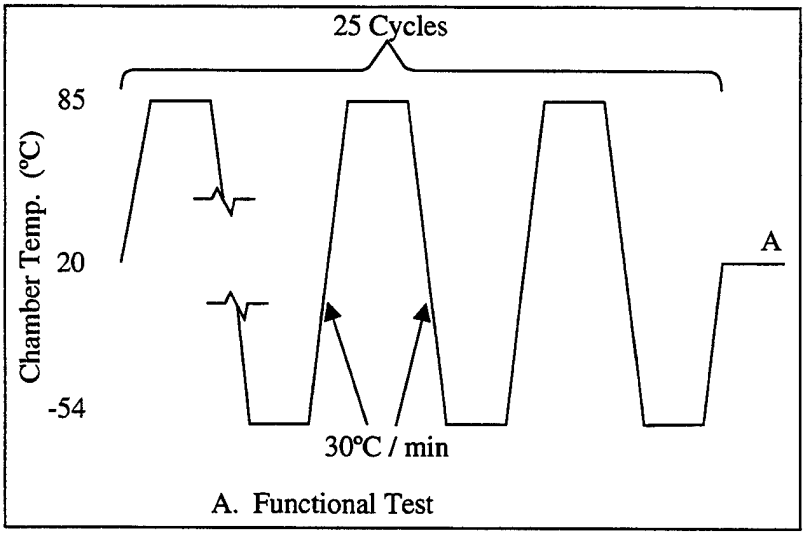

Figure 2-25 Thermal Shock Test Profile

During temperature shock testing, the polarizers showed slight delamination at corners or edges of some displays. These delaminations are believed to be attributable to a need for a thicker, more pliant adhesive layer. The dissimilar thermal coefficient of the sapphire cannot be ruled out, but the delaminations were not consistent, and were not characteristic of this type of failure.

2.8 Conclusions

This program did not address any possible visual performance differences that typically exist between commercial and custom military LCDs. Consequently, there remain tradeoffs in this domain which must be considered in choosing the best display for a given application.

In our particular investigation into the thermal dimension of the application of commercial displays to the military setting, we found that solar loading dominated the thermal problem. Though backlight heating is always a concern, in this particular application, its heat contribution to the problem was less significant than the solar loading.

Additional mounting and LCD stack improvements allow commercial displays as large as 5x5-inch to function in the F-16 environment. The basic enabler is a good thermal connection to the relatively cool display housing. In the larger sizes, the incorporation into the stack of one or more transparent layers of relatively high thermal conductivity material is necessary to facilitate lateral heat flow.

We used sapphire material to achieve this high lateral thermal conductivity. It is a relatively expensive material, but not prohibitively so. The approximate cost for two layers in a 3.6x4.6-inch display was $125. Its use, or that of a component yielding a similar result, depends on the overall tradeoffs for a given application. Another consideration for this material is the potential impact of thermal coefficient of expansion differentials which are of increasing significance as display size increases

LCD stack sizes greater than 5x5-inch require more aggressive active cooling (e.g., heat-pipes) in order to prevent undesirable temperature buildup and gradients in the LCD. Even these measures failed for sizes larger than 7x7-inch or 6x8-inch, under the F-16

environment. For these sizes, moving air must be available to facilitate heat removal from the face of the display, or the solar load must be reduced.

With no solar loading, no active cooling would be required for the displays modeled, as long as a good heat flow path is maintained from the LCD stack to the cooler display housing. No heat pipes or thermo-electric coolers are needed. In some larger sizes, lateral heat flow should be improved by incorporating a transparent heat-conducting layer similar to the sapphire layer(s) modeled.

Additional observations for specific display sizes and configurations follow.

3.6x4.6-inch display (Configuration 1) – Under the specified solar load, the structure is unable to conduct sufficient heat from the glass to the frame due to a high thermal contact resistance across the frame/glass contact area. The glass temperature exceeds the 80°C goal. The resulting thermal gradient across the glass is significant due to the low thermal conductivity of the Corning 7059™ glass.

3.6x4.6-inch display (Configuration 2) – The addition of the thermally-conductive RTV reduced the edge temperature of the glass from 81.1 to 73.4°C with solar load, but the center temperature stayed relatively unchanged. It is apparent that the RTV works well to increase the joint coefficient between the LCD and the frame. However, the in-plane thermal resistance of the glass layers precludes sufficient heat flow to the edges of the glass assembly.

3.6x4.6-inch display (Configuration 3) – The replacement of the heater glass with sapphire material improves the in-plane conductivity. As a result, the center temperature under solar load drops by 9°C, and the gradient across the display drops from 21.6°C to 4.9°C . However, the edge temperature increases from 73.4°C to 81.1°C, indicating that the thermal connection to the cooler frame is inadequate.

3.6x4.6-inch display (Configuration 4) – The use of the thermally-conducting RTV to complete the thermal path between the sapphire layer and the aluminum frame takes full advantage of the improved lateral heat flow, achieving the desired cooling of the LCD stack. The center temperature drops nearly 15°C to 71.1°C with the solar load present.

Accordingly, this display can be adapted to meet the F-16 requirements with the following modifications:

- Laminate a sapphire (or other suitable transparent heat-conducting) cover layer to the LCD stack to improve lateral heat flow out of the stack.
- Apply thermal RTV to bond the LCD and sapphire layer to the aluminum chassis to improve heat flow out of the LCD stack.

In the absence of a solar load, there is no concern with the maximum specified operating temperatures.

4x4-inch Display (Configuration 4) – The cross sectional area of the 4x4-inch LCD stack, and the length of the conduction path from the center of the display to the frame are very similar to the 3.6x4.6-inch display. Accordingly, the behavior is essentially the same, and the same adaptations are required.

5x5-inch Display (Configuration 5) – For the 5x5 display, a single layer of sapphire was not sufficient to reduce the LCD glass temperature below the 80°C goal. The goal was reached by replacing the rear heater glass with a second sapphire layer.

5x5-inch Display (Configuration 6) – In addition to the second layer of sapphire, the model for this display was also adapted to incorporate heat pipes, used to extract heat from the frame near the display face. It was assumed that the heat pipes were in turn connected to TECs that extract heat from the pipes.

Although the heat pipes were not necessary at this display size, their addition lowers the temperature another 5°C. The TECs were assumed to remove 2 watts from each heat pipe, 8 watts total, while requiring 13.3 watts to operate (assuming a 60% efficiency, an industry norm). The heat pipe operating efficiency was 0.45°C/W.

6x6-inch Display (Configuration 6) – The 6x6-inch display was modeled in both Configuration 5 and Configuration 6. As shown in Figure 2-5, the heat pipes (Configuration 6) were clearly required for this display for compliance. The TECs were

operated at 13.3 watts to remove 2 watts from each heat pipe, 8 watts total. The heat pipe operating efficiency at this temperature was 0.48°C/W.

6x8- and 7x7-inch Display (Configuration 6) – These two displays are nearly equivalent in active area, consequently they behave similarly. When operating under the same conditions, the 6x8-inch display is a little cooler, attributable to the shorter thermal path along the narrow axis of the panel. For the analysis the TECs operate at 20 watts and 33 watts to remove 12 watts and 20 watts respectively from the display. With the increased thermal load, the heat pipes operate at an efficiency of 0.25 °C/W.

8x10-inch Display – With the longer thermal paths in the glass, the effectiveness of edge-cooling the glass falls off significantly, with the center temperatures well above the 80°C mark. The heat pipe efficiency drops to 0.15 °C/W. At this efficiency the TECs consume approximately 100 watts to reduce the center of the display to 80°C, an unacceptable net increase in power dissipation. At the same time, the temperature gradient across the glass approaches 20°C, an unacceptable gradient. Consequently, this size display cannot operate in the F-16 environment unless cooling air is available.

Interestingly enough, even this large display operates well within specifications without TECs or heat pipes, in the absence of the F-16 solar loading.

Sharp (Commercial Automotive) Display – Finally, while the particular Sharp display we used should not be taken as representative of all industrial/automotive-grade displays,

it may be said that the temperature limits for this particular unmodified device appear to be only operational limits. No unrecoverable loss of functionality occurred as a result of several excursions outside its specified operating temperature range, over the full mil temperature range, and as high as 130°C in one series of stress tests. We also found that the measured LCD clearing temperature exceeded the manufacturer's recommended maximum operating temperature by as much as 9°C.

3. Chip-on-Glass Driver Bonding

3.1 Introduction and Background

Most of the LCD glass used in avionics applications is connected to its driving electronics using a flexible interconnecting element called a TAB, an acronym for tape automated bonding. Tape automated bonding specifically refers to the process by which the driver chips are accurately positioned and bonded to a repeated sequence of circuit patterns on a 70mm wide polyimide film base containing etched copper interconnect circuitry. While it is something of a misnomer in this application, the term "TAB" is widely used to apply to the individual flex circuit parts, which are excised from the tape prior to attachment to the glass panels. The laminated copper-polyimide flexible circuit component may contain one or more driver chips, depending on the particular application. Several TABs are required to drive the LCD glass. At one end of the TAB is an etched fine-pitch connecting pattern for bonding directly to the fine-pitch conductors on the edge of the LCD glass. Figure 3-1 demonstrates TAB processing. The TAB is inner lead bonded to the driver chip, then laser excised to separate the finished TAB driver from the packaging. It is now ready for bonding to the AMLCD and PWB.

The TAB not only provides a flexible connection from glass to circuit board, but also reduces the number of interconnections to the circuit board through use of addressing logic in the driver chip(s). Consequently, at the other end of the TAB, a somewhat coarser connecting pattern provides connections to a circuit board.

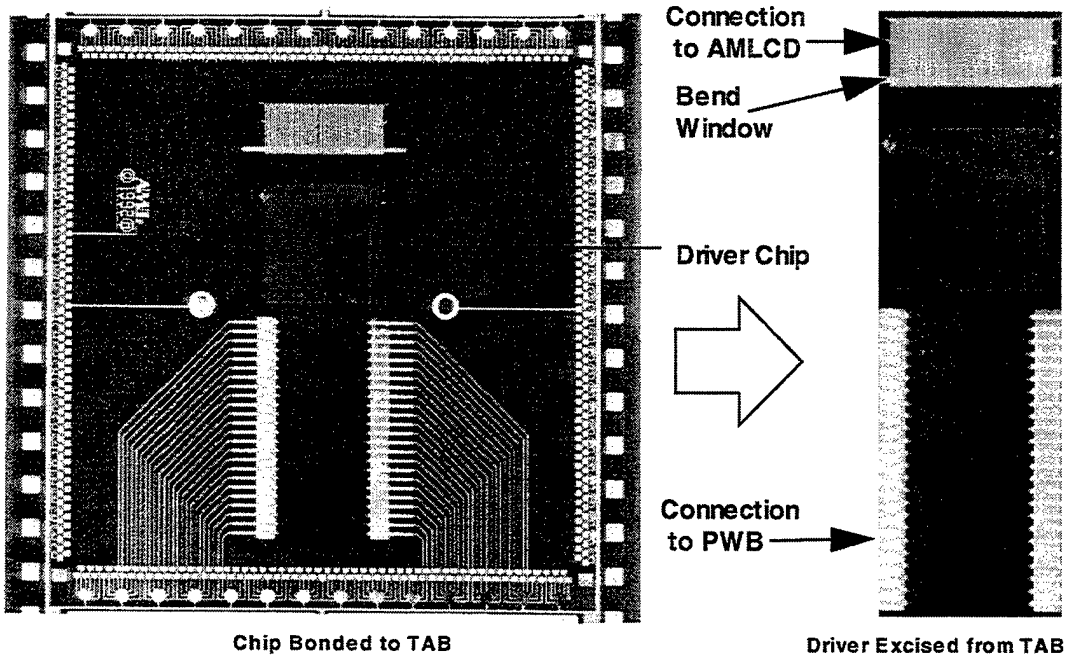

Figure 3-1 F-16 AMLCD TAB Column Driver

There is an opportunity here because this is something of a compromise solution. For example, if the driver chips were small enough, and sufficient real estate were available on the glass substrate of the display, then the chips could be reasonably moved onto the glass, bonding directly to the conductors on the glass. This would provide another significant reduction in the number of connections from the glass to external circuitry, providing benefits in reliability, yield, and assembly.

Presently, the bonding of the TAB to the transparent conductive patterns of the LCD glass involves the precise alignment of two fine-pitch conductor patterns. If this delicate alignment and bonding process fails, it is common to discard the assembly which contains both expensive glass and expensive drivers.

The TAB must physically connect between the glass and its circuit board with very little lateral stress in the TAB. As installed, the TAB is connected in-plane with the LCD (Figure 3-2), then is bent backward, away from the face of the display, in order to make connection with the corresponding circuit board. This makes both the physical design of the mounting features, and the process of assembly a high-precision process. If the TAB is stressed or distorted, it is extremely susceptible to failure under vibration. In addition, there is a trade-off between using anisotropic conductive films or adhesives which are brittle, but provide a good electrical connection because they do not relax over time versus one that has some elasticity built-in to allow for vibration.

On the other hand, if the driver chips can be mounted on the glass (flip-chip-on-glass, or FCOG), then the conductive pattern on the flexible interconnect element is much simpler (Figure 3-2). There are no driver chips mounted on the flex, and there are fewer and more robust conductor traces on the flexible substrate. Flip-chip is a chip style which permits direct connection between the bare, unpackaged chip and the glass substrate through tiny conductive bumps on the chip. The chip is inverted, or "flipped," with the bumps facing the substrate, and the bumps bonded electrically to the traces on the substrate. This fabrication simplicity favors lower fabrication cost, and lower assembly cost with less precision required, leading to lower risk of misalignment.

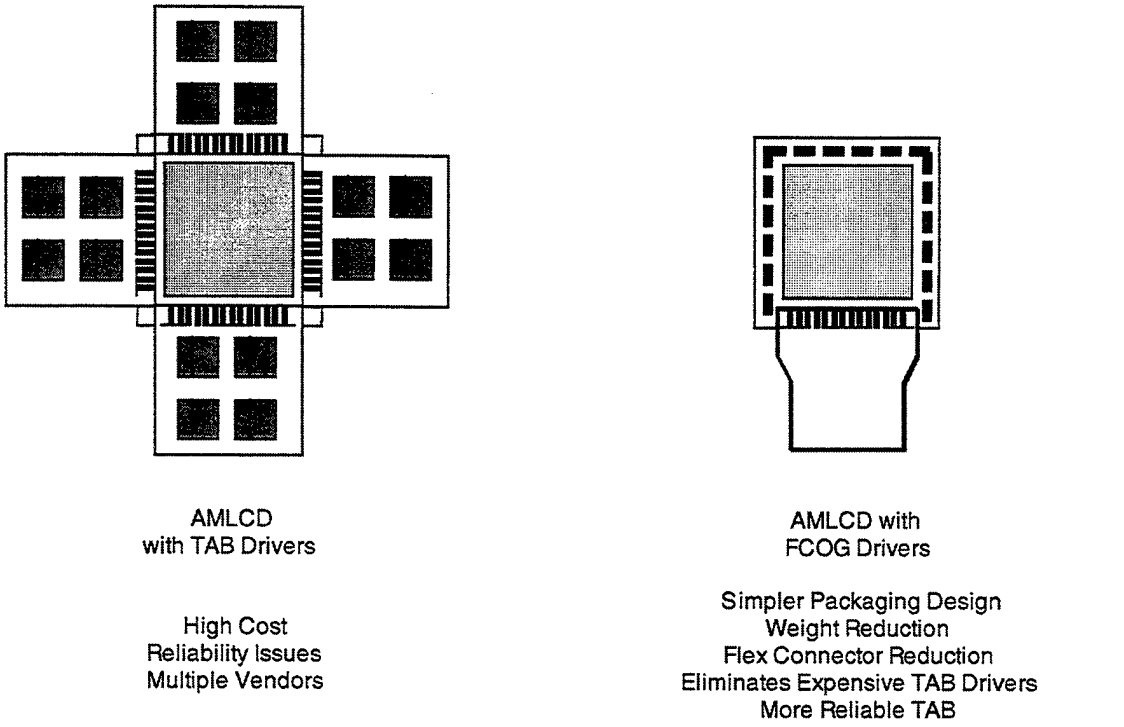

Figure 3-2 Benefits of Flip Chip Over TAB

Overall cost is another factor with today's TAB. The drivers for a fully militarized display may cost as much as the LCD glass stack itself. This is not only because of the higher cost of the custom drivers, but also because there is a three tier manufacturing process for the TAB. One supplier manufactures the driver chips, another the etched flexible TAB substrate, and still a third performs the assembly of the chip(s) to the flexible substrate and testing of the assembly. Consequently, there is significant cost added by three other suppliers by the time the panel manufacturer takes delivery of the TAB driver assemblies. In addition, the panel manufacturer must still bond the TAB to the LCD glass stack. The ability to bond the driver chip directly to the display glass would eliminate some of these subcontractor costs.

For FCOG, one supplier manufactures the driver chips, the same or another manufacturer bumps the driver chip contacts, and the LCD supplier bonds the chips to the display glass. Figure 3-3 illustrates this process compared to the FCOG process.

An additional way to improve yielded manufacturing cost is to provide the ability to remove and replace a malfunctioning driver chip during the manufacturing process. While it is generally possible to remove and replace the entire TAB during manufacturing, this requires the replacement of the entire TAB assembly, as contrasted with just the cost of the bumped chip for FCOG. The removal of the TAB from the somewhat delicate high density interconnects on the glass can often damage the interconnects, leading to a new row or column failure. During chip to TAB inner lead bonding, there is no rework capability. If the chip does not bond properly to the inner leads, the TAB is discarded. During FCOG bonding, if rework is necessary, the glass is cleaned and a new driver chip bonded in its place.

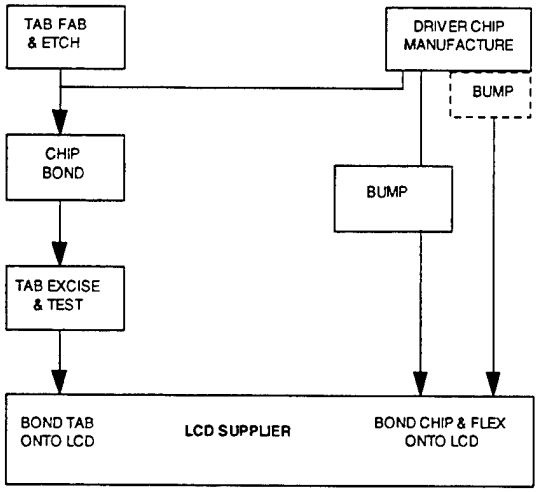

Figure 3-3 TAB vs FCOG Process Flow

To summarize, FCOG technology increases system reliability, and reduces system cost:

1. FCOG incorporates reworkability into the driver attachment process, with manufacturing yield improvements.

2. Drivers used in FCOG cost less than TAB drivers. For example, for a given commercially available driver at low volume:
   - Bare driver chips (no associated packaging) cost $6.84 each.
   - Au-bumped driver chips (no associated packaging) cost $8.64 each.
   - The cost for the same driver mounted in a TAB package must include non-recurring engineering (NRE) and tooling charges to accommodate the interconnect layouts of both the LCD glass and the PWB onto the TAB. After NRE and tooling charges in the order of ≅ $15,000.00, low volume TAB costs are ~$27.00 each for a simple, one chip TAB LCD driver. [Costs were based on Test Vehicle 1 LCD driver costs].
3. Simplified flex layout with no fine-pitch traces reduces costs.
4. Fewer suppliers are involved in FCOG, typically two. (TAB involves three suppliers).
5. Smaller numbers of interconnects improve reliability, and cost of ownership over the display's lifetime.

There are three prerequisites to achieving these benefits.

1. There must be sufficient room in the host display unit for the slightly wider glass required to provide a footprint on the periphery for the added driver chips.
2. In order to minimize that extra real estate (typically critical in avionic displays), narrow aspect ratio flip-chip drivers must be available. (This is the case for some smaller commercial displays that use flip-chip techniques to bond the drivers on

the glass substrate, as is the case with the Sharp display baselined in the thermal modeling activity.

3. A chip bonding material and process must be identified which is robust in the presence of the worst of anticipated temperature, humidity, vibration, and shock environments, and hopefully also enables repairability, at least during the manufacturing process.

The first prerequisite is design-related, specific to a given application. In the case of the second prerequisite, so-called "slim-jim" flip-chip packages are available for at least some commercial drivers. They may reasonably be expected to be made available for military applications if sufficient market is apparent, or if sufficient non-recurring expense can be borne by the using manufacturer or ultimate customer. Non-recurring expense (NRE) for driver redesign is estimated to be ≥ $15,000.00, including tooling. NRE would only be incurred if no suitable COTS drivers were available. As FCOG bond techniques are proven reliable and cost-effective, it is predicted that more AMLCD manufacturers will design in the FCOG layout onto the glass, like the Sharp display. Bonding material advances were needed to make a reliable, lasting connection between the chip and the glass.

We addressed the third prerequisite in this program. In the early stages of the program, it was not known whether commercial FCOG materials and practices were capable of functioning under military conditions or not. In the course of the program, we temperature-tested a specimen of the Sharp product and found that this specific display

operated after exposure to the full military temperature extremes, and in fact remained functional after cooling down from a two-hour exposure to 130°C! However, we were unable to ascertain the identity of the IC bonding materials and process used in the device.

Accordingly, this portion of the program set out to identify and test several commercially available prospective materials and fabrication processes. This was not an exhaustive evaluation of all available materials, but instead looked at a subset of candidates which appeared to be most likely candidates. The parameters used for selecting anisotropic conductive materials to investigate included humidity resistance, thermal stability, mechanical bond strength, electrical contact resistance, curing method, and availability.[7] We sought at least one candidate. Among the materials and processes investigated, we found one successful candidate, a Sony CP84301 ACF (anisotropic conducting film), capable of surviving the F-16 environment. Some of the other candidates may have performed satisfactorily with additional dialogue with the material supplier and some adjustments of our processes. The remainder of this section describes FCOG interconnect materials investigated, FCOG test vehicles used to test the materials, and the FCOG technology interconnect testing used to determine the reliability of each material.

3.2 Selection of Flip-Chip-on-Glass Interconnect Method

A gold-bump and anisotropic conductive material process was selected for this portion of the program. A fused solder-bump connection process was not considered because the

higher-temperature process presents a thermal shock problem with the glass substrate. In addition, flux and solders are prone to destructively etch or corrode the very thin display connector runs.

Anisotropic conductive adhesives (ACA) and an anisotropic conductive film (ACF) were evaluated as the means for making electrical connections from the chips to the on-glass conductors. These materials suspend a large quantity of gold microspheres in an insulating material that also serves as an adhesive. In its pristine form, the ACA and ACF are insulating because there are insufficient spheres to form a continuous sphere-to-sphere electrical path through the material.[8] However, when a gold-bumped chip is pressed into the material, in the Z-direction the bumps trap gold spheres against the conductors on the display glass, making a low-resistance connection (Figure 3-1). The materials are called anisotropic or Z-axis materials because this conductivity is created only in the z-axis.[9] Insulating properties are maintained in the horizontal plane.

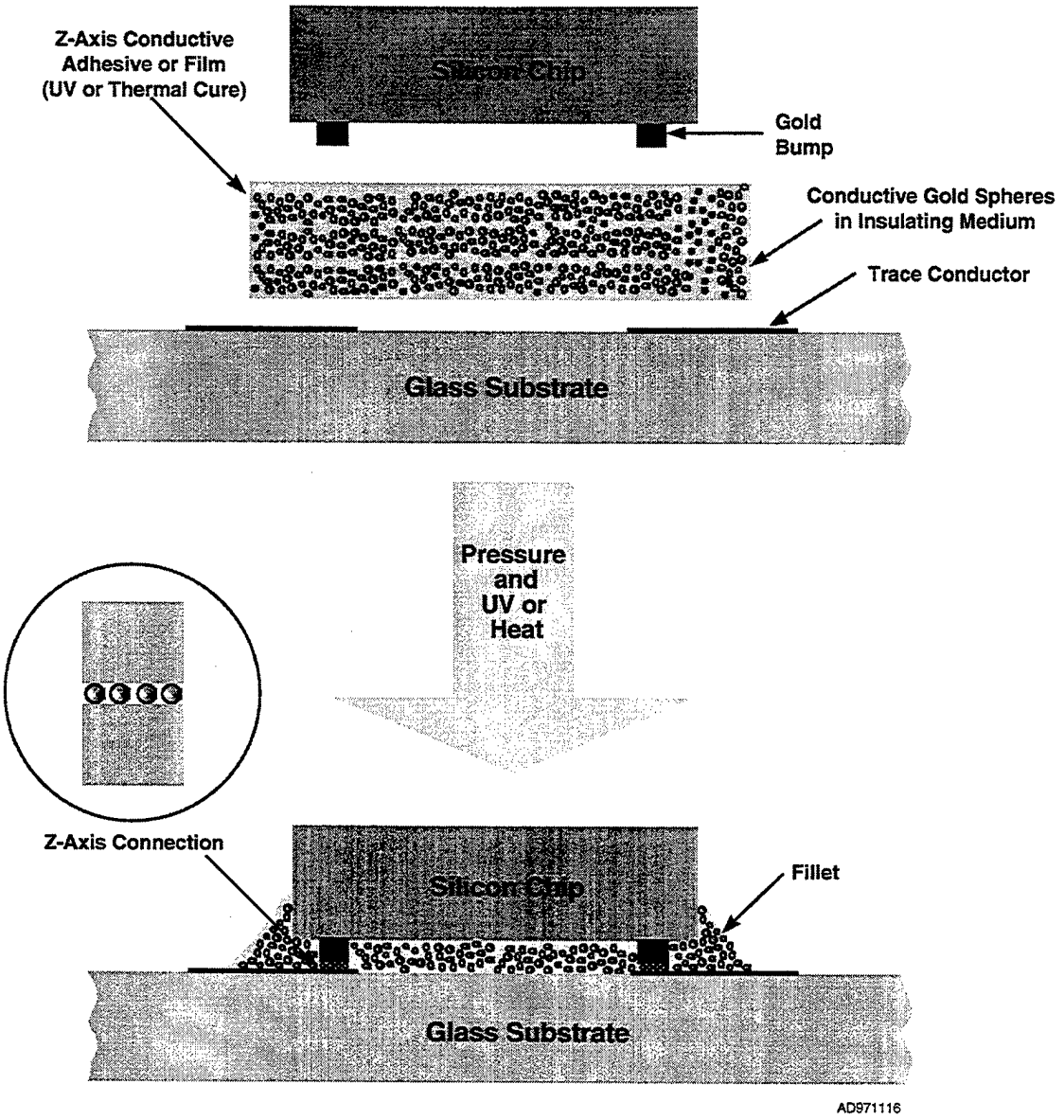

Figure 3-4 Flip-Chip Bonding Process

3.3 Definition of Test Articles

The essence of the testing is to create a representative chip connection scenario, then test the performance of the connection both electrically and environmentally. To accomplish

this, five test chip layouts were created on silicon. These were used in conjunction with two glass substrates.

Because the Z-axis adhesives and films are insulating in the plane of the film, there is an automatic insulating adhesive underfill of the chip. The tasks at hand were to find a material which, after bonding, yielded low electrical interconnect resistance, with high stability and reliability over a range of demanding environmental conditions.

The following materials were used for FCOG bonding experiments:

- Uniax UV-183 ACA ⇒ UV curable ACA with Au microspheres.
- Uniax ET-232 ACA ⇒ Two part, UV initiated, heat curable (thermoset) ACA with Au microspheres.
- Elatech R001 ACA ⇒ Two part, UV initiated, heat curable (thermoset) ACA with Au microspheres.
- Sony CP84301Q ACF ⇒ Thermoset ACF with thin dielectric coated Au microspheres, which allows denser loading of Au while maintaining Z-axis only contact.

The UV curable Uniax UV-183 ACA was attractive because the UV curable driver attach process allowed the easiest processing and reworkability. The bonding process consists of dispensing the ACA directly onto the glass, aligning the flipped LSI driver Au-bumped pads with the LCD traces, applying pressure to the chip, tacking the material with UV light, and electrically testing the panel to assure a good chip connection.

The alignment of the chip to the LCD traces is accomplished by looking through the display glass with optics which have the depth of focus needed to see the Au bumps through the ACA or ACF. The Au bumps are easily seen through the material, but alignment to the ITO traces is critical to achieve maximum contact area. If defective, chips are easily removed and another chip bonded in its place. This allows pre-selection of known good driver die, reducing costs associated with driver yield issues.

Upon acceptance through test, the conductive adhesive cure is run to completion. The UV-curable Z-axis adhesive process requires no thermal bonding. The bonding process is done at room temperature, is fast, and minimizes damage to the display or drivers due to heat. Unfortunately, as will be shown, the material did not withstand humidity testing.

The UV-initiated, heat curable Elatech R001 ACA was considered for use because the UV-curable driver attach process allowed easy processing and rework, while the thermoset properties promised to be more robust against the F-16 environment. The bonding process consists of dispensing the ACA directly onto the glass, aligning the flipped LSI driver Au-bumped pads with the LCD traces, applying pressure to the chip, tacking the material with UV light, and electrically testing the panel to assure a good chip connection. If defective, chips are easily removed and another chip bonded in its place. This allows pre-selection of known-good driver die, reducing costs associated with driver yield. Upon acceptance through test, the conductive adhesive is heated for a thermal cure. This bonding process is initiated at room temperature, but thermal curing is

necessary to complete the thermosetting process. It will be shown that this material did not hold up to the F-16 vibration environment.

The thermoset Sony CP84301Q ACF ultimately survived every test we imposed. A higher density of dielectric-coated Au microspheres allows better electrical contact. When pressure is applied, the dielectric film fractures, exposing the conductive particles in the bond region. To create the bond, a strip of the ACF is placed directly onto the glass, and the gold pads of the flipped LSI driver chip are aligned with the panel electrodes. Pressure is then applied to the chip, at the same time tacking the material with a pre-bond platen temperature of 80°C at 5 kgf/cm^2 for 5 seconds. The panel is then electrically tested to verify the chip connection. If defective, chips are removed and replaced. This allows pre-selection of known-good driver die, reducing costs associated with driver yield. Upon acceptance through test, the conductive adhesive is fully cured at 200°C at 400 kgf/cm^2 for 30 seconds. The resulting FCOG bond, as will be shown, is highly reliable in the F-16 environment.

3.4 Flip-Chip-on-Glass Test Vehicles

To evaluate the FCOG bonding material performance in the F-16 environment, test vehicles were needed. To operate efficiently, two types of glass test vehicles were used. The first, Test Vehicle 1, consisted of a simple commercial off-the-shelf TN-STN dot-matrix passive LCD (3 line, 12 characters per line), with the layout for bonding a Philips PCU2116CU/12 LCD driver, and the necessary electronics for testing the LCDs both

during and after the driver chip attach process. Honeywell provided the LCDs, Philips drivers, and electronics.

Four hundred LCDs and drivers were used. These LCDs and drivers provided a relatively inexpensive functional device for preliminary screening of FCOG bonding materials. This allowed HTC to get a head start on testing the materials while Test Vehicle 2 was being designed and fabricated. Figure 3-5 shows the dot matrix LCD with driver chip bonded and working. Figure 3-6 shows the Au-bumped Philips LCD driver.

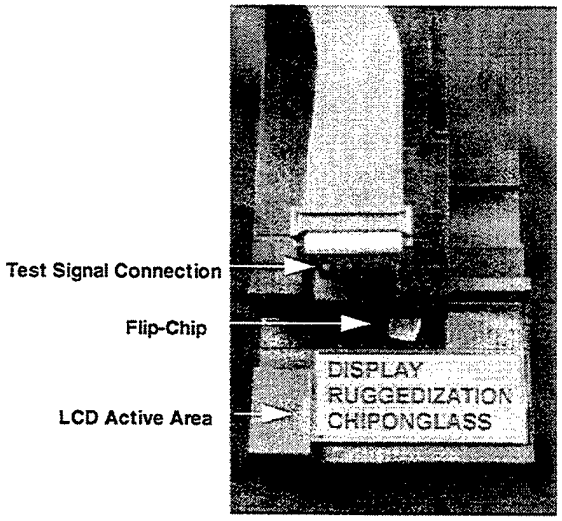

Figure 3-5 Test Vehicle 1

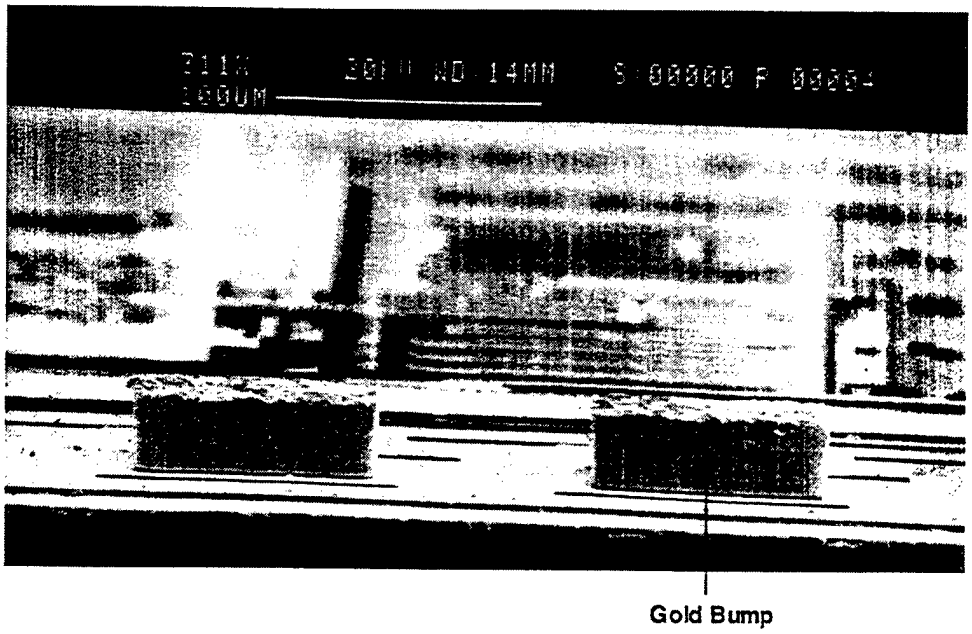

Figure 3-6 Au-Bumped Philips LCD Driver

Table 3-1 shows the detailed features of the Test Vehicles.

Table 3-1 Test Vehicle Characteristics

"Driver IC"	Test Vehicle 1	Test Vehicle 2		
	Philips PCU2116CU/12 LCD Drivers	Test Chip 1	Test Chip 2	Test Chip 3
Die Size, mm	5.6x7.1	3x12	3x12	3x12
Number of I/O Pads	128	154	228	300
Bump Material	Gold	Gold	Gold	Gold
Bump Pitch, microns	130 - 160	150	100	75
Bump Size, microns	100x100	100x100	100x100	50x50
Bump Height, microns	25	25	25	15
"LCD" Substrate				
Glass Size, mm	32x45.9x1.1	100x100x1.1	100x100x1.1	100x100x1.1
Conductor Traces	ITO	ITO, NiCr or Au	ITO, NiCr or Au	ITO, NiCr or Au
Test Vehicle 2 Dielectric Studies	**Test Chip 4**	**Test Chip 5**		
	100 gaps, 100 µm gap, 20 µm ITO, NiCr or Au lines on glass	150 gaps, 50 µm gap, 20 µm ITO, NiCr or Au lines on glass		

The purpose of Test Vehicle 2 was to allow characterization of all critical parameters of a large number of interconnects. This included test structures for analyzing electrical, mechanical, and environmental performance of the FCOG bond materials. Due to high failure rates of the Uniax UV-183 ACA and ET-232 ACA, only the Sony ACF and the Elatech R001 ACA were used on Test Vehicle 2.

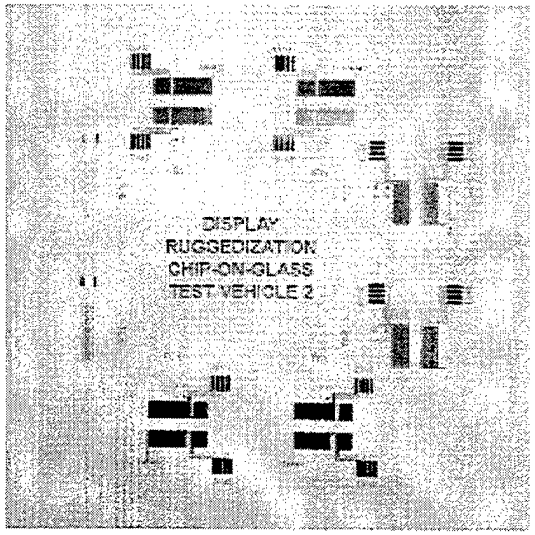

Figure 3-7 Patterned Test Vehicle 2 Glass Before FCOG Bonding

Test Vehicle 2 (Figure 3-7) consisted of a 4x4x0.043-inch glass substrate with patterned ITO, NiCr, or Au traces designed for probe testing electrical characteristics both before and after vibration and environmental testing. The layout included daisy chains (Figure 3-8) for transit string resistance, four-point probes for contact resistance, individual pad pairs for failure point source isolation measurements, and an interdigitated structure for dielectrics studies. The interdigitated dielectric structures allowed testing for shorting between pads and confirmation of a z-axis only interconnect; i.e., no conduction in the x or y planes. Figure 3-7 shows the patterned test glass before chips are bonded.

The 3x12-mm thermally-oxidized silicon test chips were laid out with a large number of simple straight Au conductors terminated in connection pads. The chips were passivated over the Au busses, except in the vias over the bond pad area. For electrical analysis, two

chips each of three interconnect densities were bonded to corresponding electrode patterns on glass substrates. Three bond pad pitches (Test Chip 1 = 150 μm; Test Chip 2 = 100 μm; and Test Chip 3 = 75 μm) were employed to represent what would be used on real commercial LCDs. Test Chip 4 and Test Chip 5 were used for dielectric studies, which consisted of thermal SiO_2 on silicon and were bonded to their corresponding locations. Test Chip 4 consisted of 20 μm interdigitated lines with 100 gaps spaced 100 μm apart. Test Chip 5 consisted of 20 μm interdigitated lines with 150 gaps spaced 50 μm apart. These structures allowed verification of Z-axis only electrical connections. See Table 3-1 for a summary of details on Test Vehicle 2 characteristics.

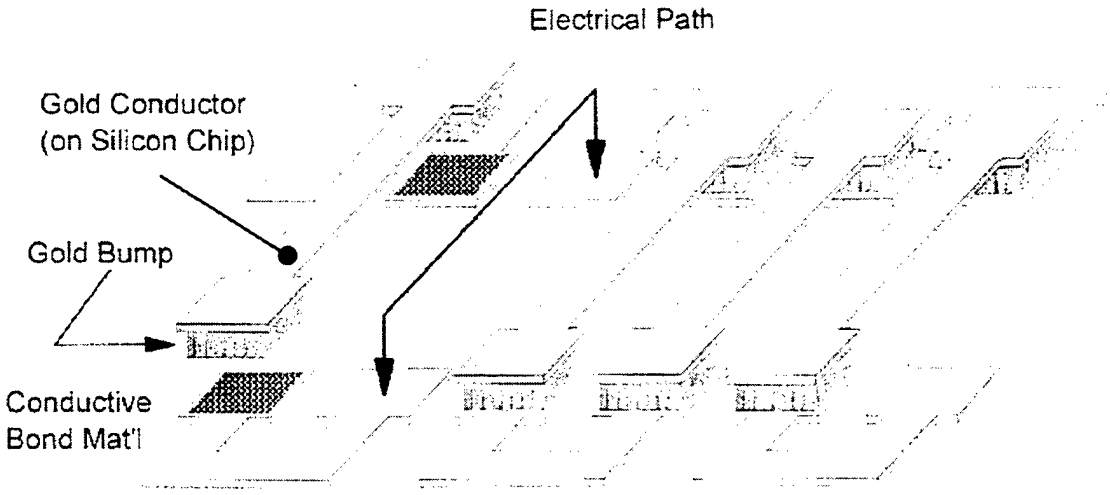

Figure 3-8 Conductive Pad and Jumper Pattern (on Glass Substrate)

Test Chip 1 (TC1) consists of 77 lines (154 I/O pads), 150 μm pitch, 125 μm pads with 100 μm vias through SiNx passivation. Figure 3-9 shows the detailed layout of TC1. Figure 3-10 shows the finished Au-bumped Test Chip 1.

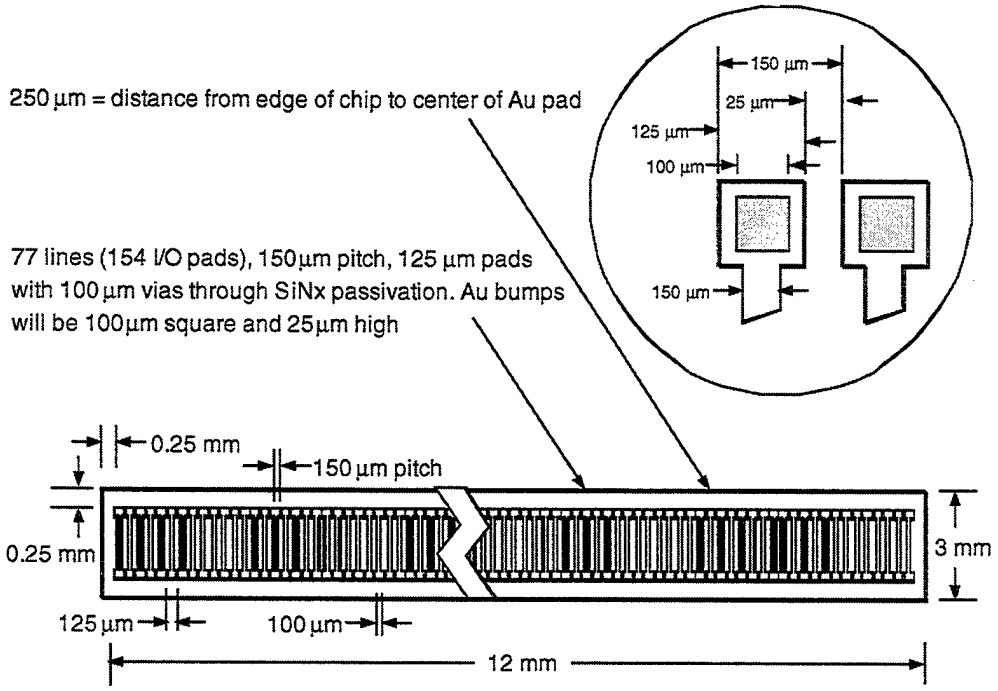

Figure 3-9 Test Chip 1 Layout

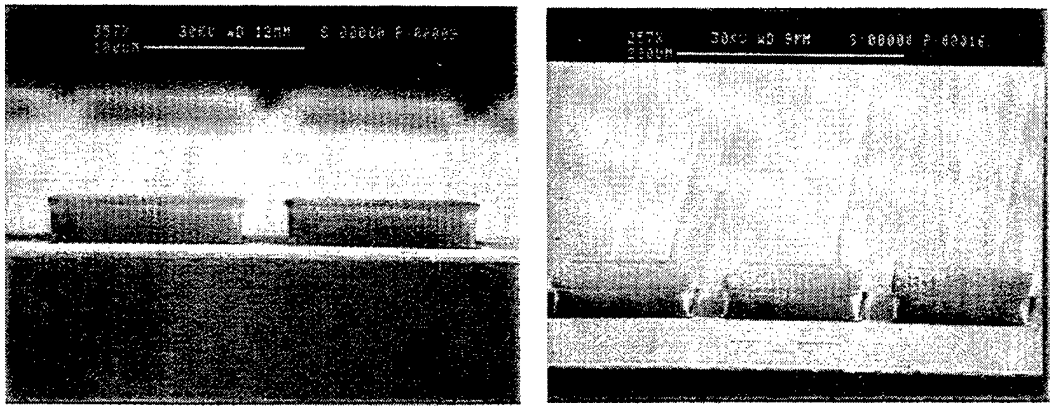

Figure 3-10 Au-Bumped Test Chip 1

Test Chip 2 (TC2) consists of 114 lines (228 I/O pads), 100 µm pitch, staggered 125 µm pads with 100 µm vias through SiNx passivation. Offsetting the pads allows a denser interconnect with the same pad size as TC1. Figure 3-11 shows the detailed layout of TC2. Figure 3-12 shows the finished Au-bumped Test Chip 2.

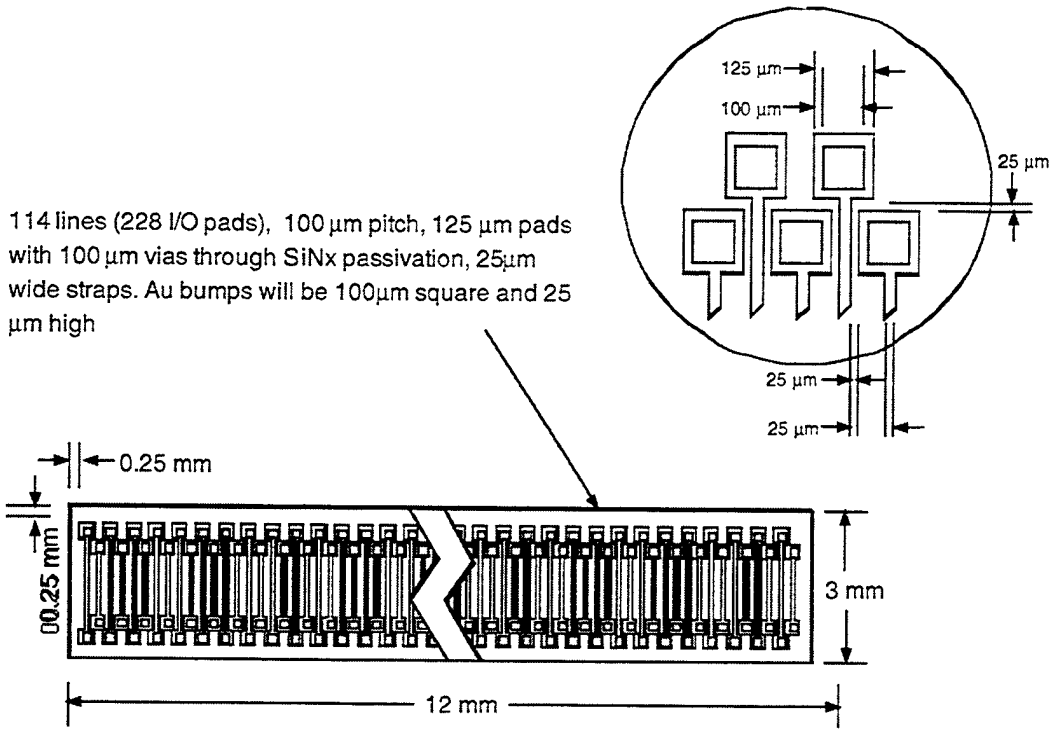

Figure 3-11 Test Chip 2 Layout

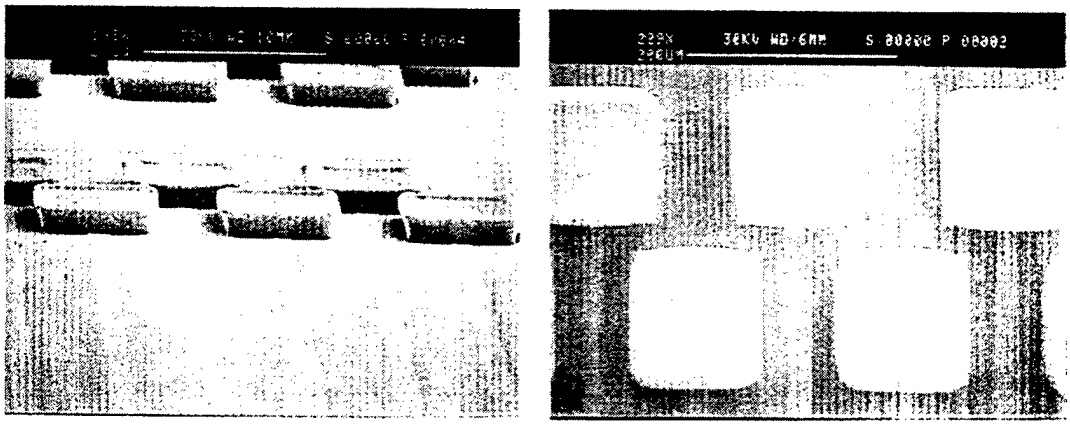

Figure 3-12 Au-Bumped Test Chip 2

Test Chip 3 (TC3) consists of 150 lines (300 I/O pads), 75 µm pitch, 60 µm pads with 50 µm vias through SiNx passivation. This test chip allowed a study of the effects of reducing the contact area in half to increase I/O pad density. Figure 3-13 shows the detailed layout of TC3. Figure 3-14 shows the finished Au-bumped Test Chip 3.

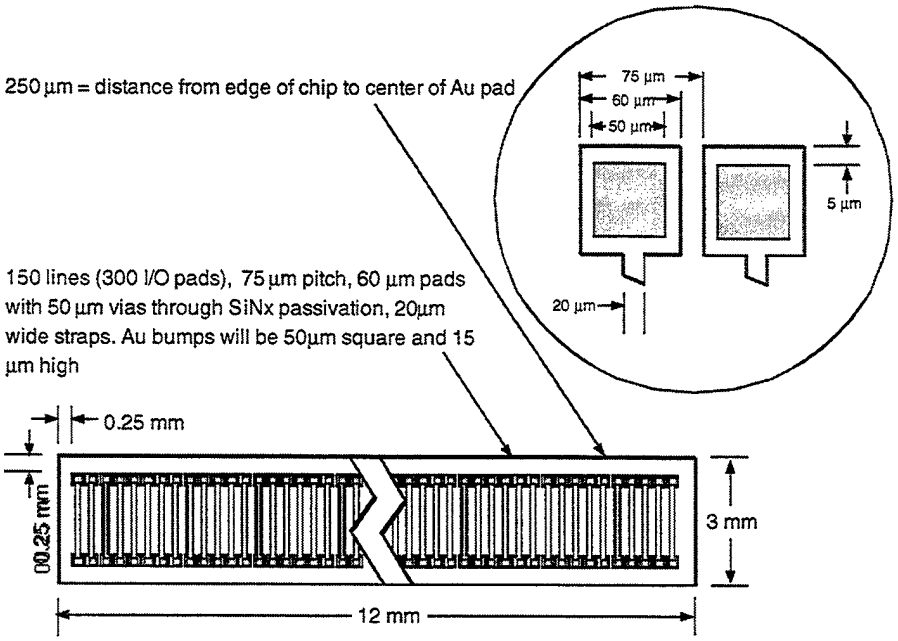

Figure 3-13 Test Chip 3 Layout

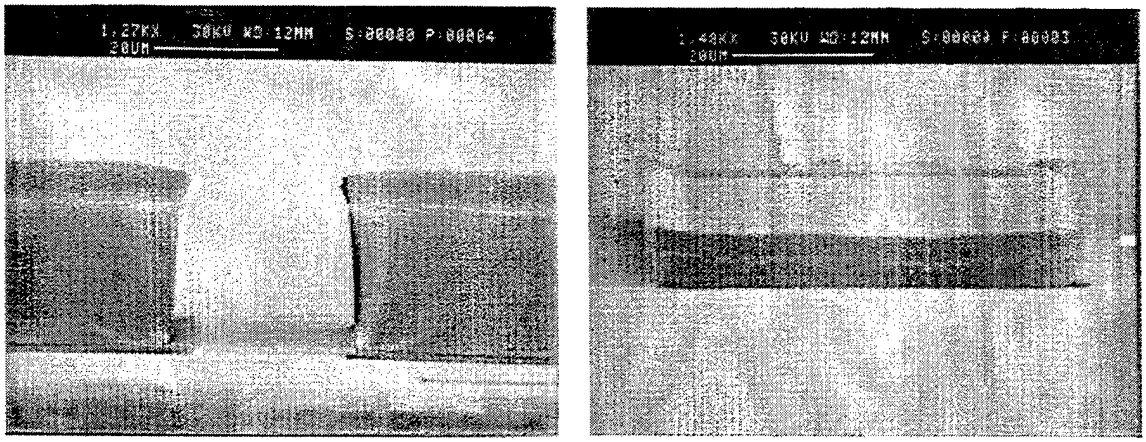

Figure 3-14 Au-Bumped Test Chip 3

Test Chip 4 (TC4) consists of thermal SiO_2 on silicon for the chip and electrodes on the glass, consisting of 100 interdigitated 20-μm lines with 100 μm gaps for insulation resistance (dielectric) measurements. Figure 3-15 shows the detailed layout of TC4.

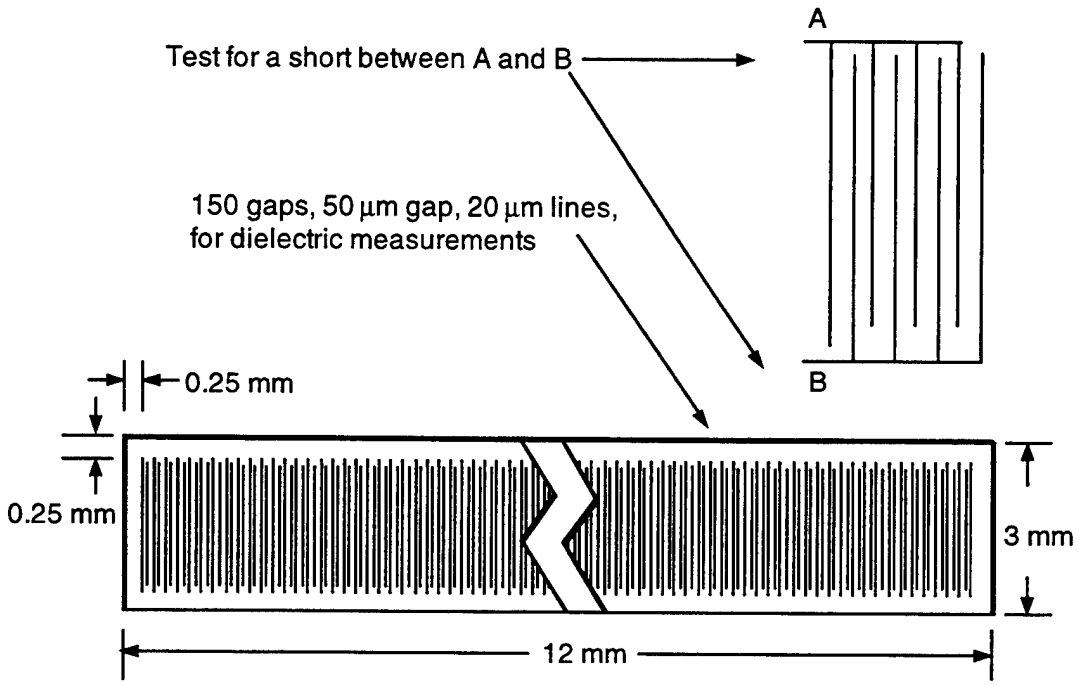

Figure 3-15 Test Chip 4 Layout

Test Chip 5 (TC5) consists of thermal SiO_2 on silicon for the chip and electrodes on the glass, consisting of 150 interdigitated 20-μm lines with 50-μm gaps for insulation resistance (dielectric) measurements, shows the detailed layout of TC5.

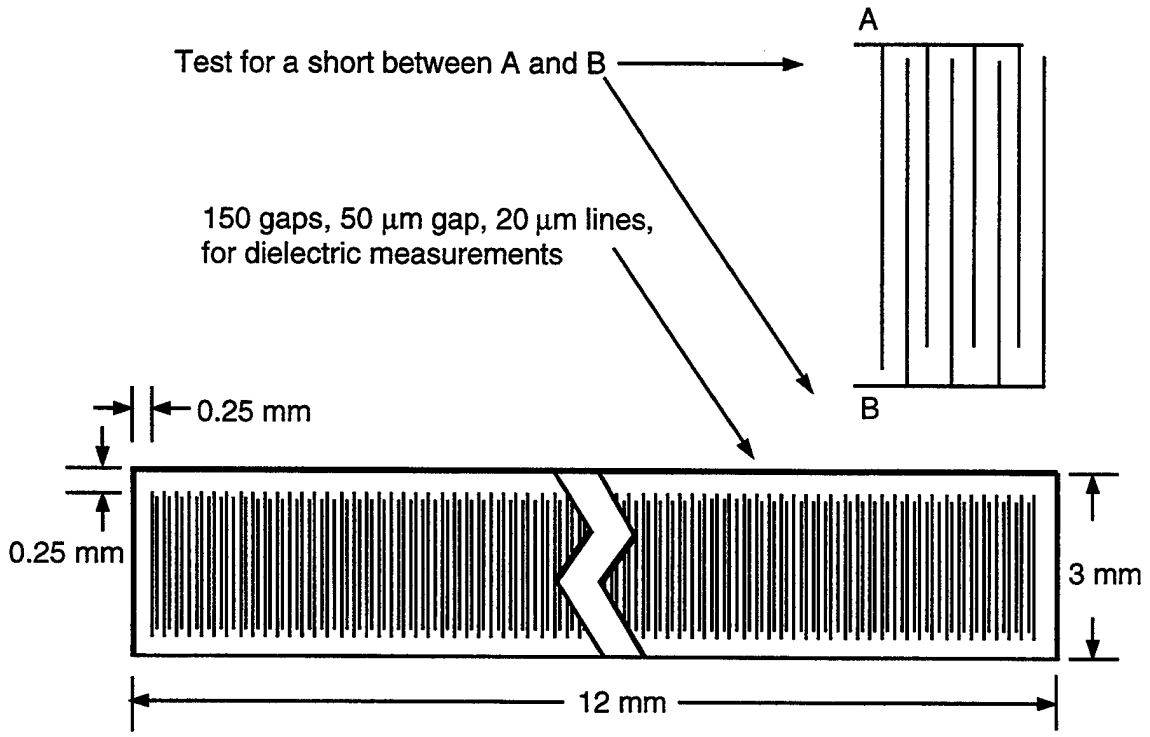

Figure 3-16 Test Chip 5 Layout

FCOG bonding and Au bumping were done at International Micro Industries, Inc. (IMI), in Mount Laurel, NJ. The flip-chip bonder used for bonding test chips on Test Vehicle 2 as well as Philips drivers on Test Vehicle 1, is shown in Figure 3-17. This bonder allowed bonding of both UV and/or thermoset based ACA and ACF FCOG materials.

3.5 Flip-Chip-on-Glass Interconnect Testing

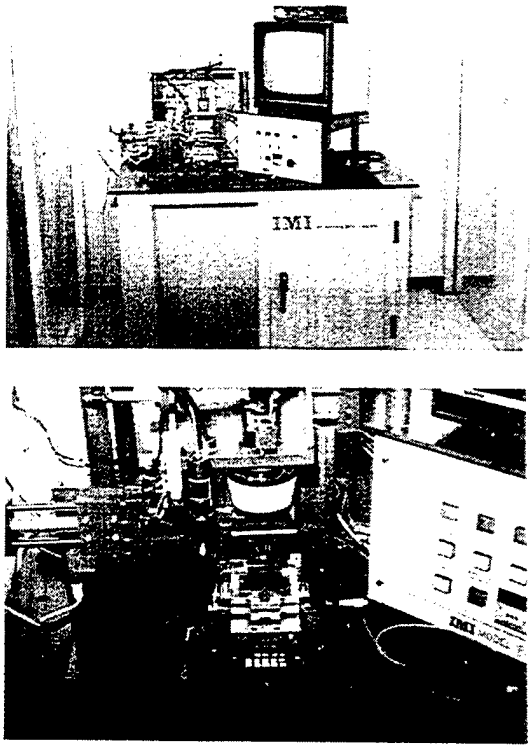

Figure 3-17 Flip-Chip Bonder for ACA/ACF

FCOG reliability tests conducted included:

- Electrical ⇒ Contact Resistance vs.

  Temperature (25°C - 120°C)

  Insulation Resistance (Dielectric Studies)
- Mechanical ⇒ Bond Strength
  - Random and Gunfire Vibration
  - C-mode Scanning Acoustic Microscopy
  - Die Shear
  - SEM Analysis of Au Bumps
- Environmental (per F-16 Specifications)
  - Temperature cycling
  - Temperature Shock
  - Humidity

It should be noted that the primary reason for using a 4x4x0.043-inch base glass for the probe electrodes is to allow the deflections such as a 4x4-inch AMLCD would experience during random and gunfire vibration. Vibration tests were not performed on Test Vehicle 1 due to its small size. The primary reason for making the test chips for Test Vehicle 2 the size of 3x12-mm is to simulate "slim chip" drivers, which would most likely be used on an AMLCD in the future.

An overview of electrical, mechanical, and environmental tests performed is shown in Table 3-1. Electrical performance of the adhesive bonds were studied by evaluating

initial contact resistance sensitivity to changes in temperature, and stability of the contact resistance over time at elevated temperatures. Insulation resistance was measured using TC4 and TC5 to detect any conduction in the x-y plane. These tests were performed on Test Vehicle 2 only. Au busses on the glass allowed true measurements of the resistance characteristics of the FCOG bond materials.

Table 3-2 Electrical, Environmental and Mechanical Test

COG Bond Media Test - Vehicle 1 (IMI LCD with Philips Driver)						
	Electrical	Thermal Cycling	Temperature Shock	Humidity	Electrical	C-SAM
UV-183	10 LCDs w/Drivers	10 LCDs w/Drivers	10 LCDs w/Drivers	10 LCDs w/Drivers	10 LCDs w/Drivers	2 LCDs w/Drivers
UV-183 w/enc.	10 Samples	10 Samples	10 Samples	10 Samples	10 Samples	2 Samples
Elatech	10 Samples	10 Samples	10 Samples	10 Samples	10 Samples	2 Samples
Elatech w/enc.	10 Samples	10 Samples	10 Samples	10 Samples	10 Samples	2 Samples
Sony	10 Samples	10 Samples	10 Samples	10 Samples	10 Samples	2 Samples
Sony w/enc.	10 Samples	10 Samples	10 Samples	10 Samples	10 Samples	2 Samples

COG Bond Media Test - Vehicle 2 (4 " x 4 ") 8 Test Chips per Substrate = 112 Test Chips Bonded								
	Electrical	Random Vibration	Gunfire Vibration	Temperature Shock	Humidity	Electrical	C-SAM	Die Shear
3 Sony TV2 4 Elatech TV2								
3 Sony TV2 4 Elatech TV2								

Mechanical integrity of the FCOG bonds was evaluated using several techniques. A vibration fixture was designed and built at Honeywell's Defense Avionic Systems Division to hold the 4x4-inch substrates with bonded test chips during vibration testing. Random vibration was performed per F-16 PIDS at 7.1 Grms for 1 hour along each axis (3 hours total). See Figure 3-18 for profile. Gunfire vibration was performed per F-16 specifications for both combined and random sinusoidal vibrations for 1 hour along each axis (3 hours total). See Figure 3-19 for profile.

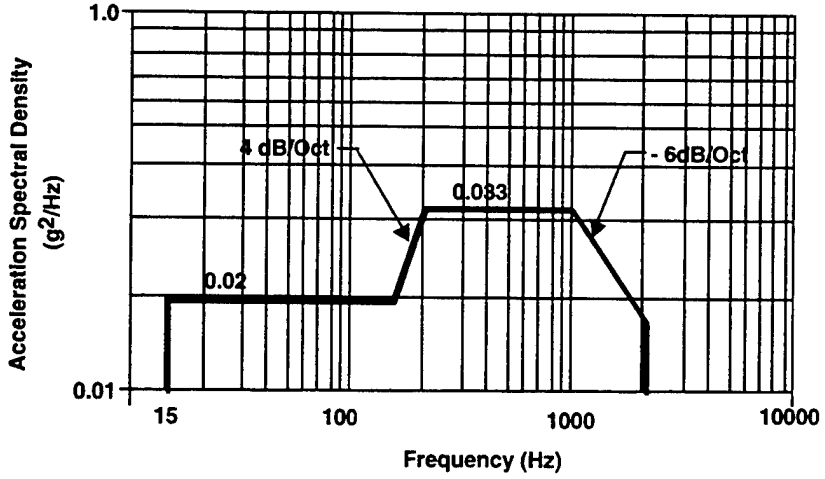

Figure 3-18 Random Vibration Profile.

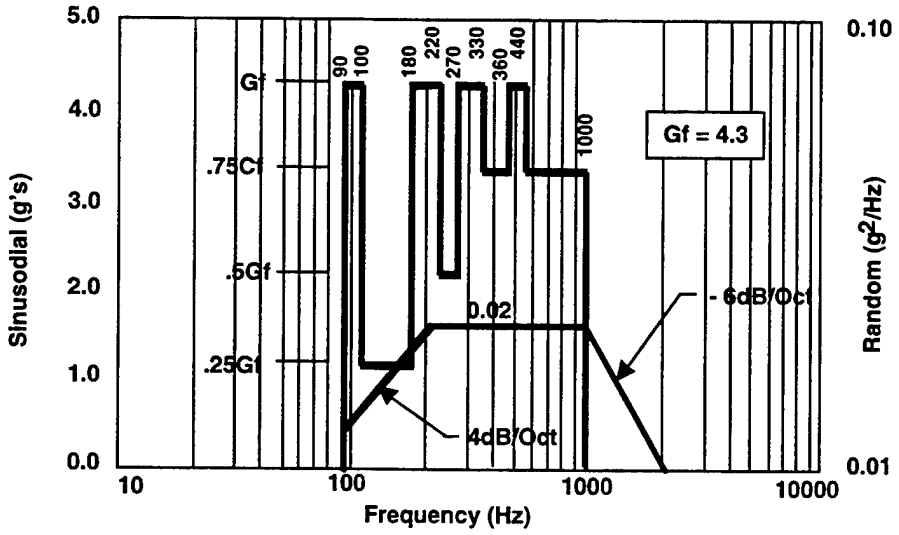

Figure 3-19 Gunfire Vibration Profile.

C-mode scanning acoustical microscopy (C-SAM) of the chip-to-glass interconnect was performed on both Test Vehicle 1 and Test Vehicle 2 at Sonoscan, Inc. (Bensenville, Illinois). The C-SAM is a reflection-mode acoustic microscope. The C-SAM method

involves pulse-echo ultrasound over a range from 5 to 180 MHz to produce images of samples at various depth levels.

A focused ultrasonic transducer alternately sends pulses into and receives echoes from discontinuities within the sample. The echoes are separated in time based on the depths of the reflecting features in the sample. An electronic gate is used to select a specific depth or interface. A very high speed mechanical scanner is used to index the transducer across the sample and produce images. The resulting acoustic image is made from the amplitude of the returned echo and the phase (polarity) of the returned echo. Both of these attributes of the echo are governed by the acoustic impedance mismatch between the two materials at an interface. The acoustic impedance of a material is the density times the longitudinal velocity. Dissimilar materials will show higher amplitude reflections at the boundary than material with similar material properties. C-SAM is a non-destructive test. Figure 3-20 schematically illustrates C-mode scanning acoustic microscopy.

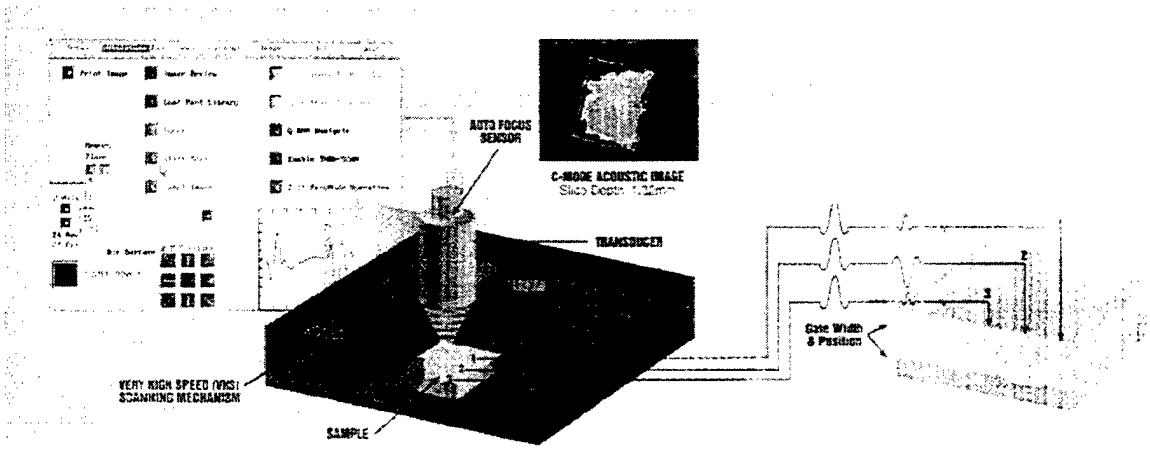

Figure 3-20 C-mode Scanning Acoustic Microscopy

See Appendix D for color version.

The flip chips were imaged from both the top through the silicon and from the bottom through the display glass. Because of the very small size of the Au bumps, a high acoustic frequency of 100 MHz was used on Test Vehicle 1 to achieve high resolution. On Test Vehicle 2, an even higher acoustic frequency of 180 MHz was used to achieve higher resolution needed for the Au bump densities on the 3x12-mm test chips. The images produced correlate well with electrical test results.

Die shear strength testing was performed on both Test Vehicle 1 and Test Vehicle 2 per Honeywell Quality Control Directive using a Dage MCT22 shear tester in the Honeywell Microelectronics area in Phoenix. The purpose of the test is to determine the integrity of the materials and procedures used to attach semiconductor die to substrates. This determination is based on a measure of force applied to the die, the type of failure

resulting from this application of force (if failure occurs), and the visual appearance of the residual die attach media (ACA or ACF) and substrate metallization. The direction of the applied force is parallel with the plane of the substrate and perpendicular to the die being tested. All parts that underwent C-SAM analysis were put through die shear.

SEM analysis was used to examine the Au-bumping process used on Test Chips 1, 2, and 3 (Test Vehicle 2). This technique was very helpful in tuning the Au bump processing to achieve the best quality contact needed for FCOG bonding.

Thermal cycling testing per F-16 PIDS were performed on both Test Vehicle 1 and Test Vehicle 2. The tests consisted of 10 cycles from -54°C to +55°C (stabilization required) at a rate of no less than 5°C/minute. See Figure 3-25 for profile. The purpose of this test is to reveal potential flaws such as congealing of liquid, cracking or rupture of materials, deformation of components, and fatigue of adhesives (ACA or ACF) in equipment that will experience these conditions.

Temperature shock testing per F-16 PIDS were performed on both Test Vehicle 1 and Test Vehicle 2. The tests consisted of 25 cycles from -54°C to +85°C (stabilization required) at a rate of no less than 30°C/minute. See Figure 2-27 for profile. The purpose of this test is to reveal potential flaws such as congealing of liquid, cracking or rupture of materials, deformation of components, and fatigue of adhesives (ACA or ACF) in equipment that will experience these conditions.

Humidity testing per F-16 PIDS Mil-Std-810E, Method 507.3 was performed on both Test Vehicle 1 and Test Vehicle 2. The tests consisted of 10 cycles of 24-hour duration from 30°C to 60°C and relative humidity between 85% and 95%. See Figure 3-21 for profile. The purpose of this test is to reveal potential flaws associated with swelling, condensation, corrosion, coating and adhesive (ACA or ACF) breakdown, and degradation of components.

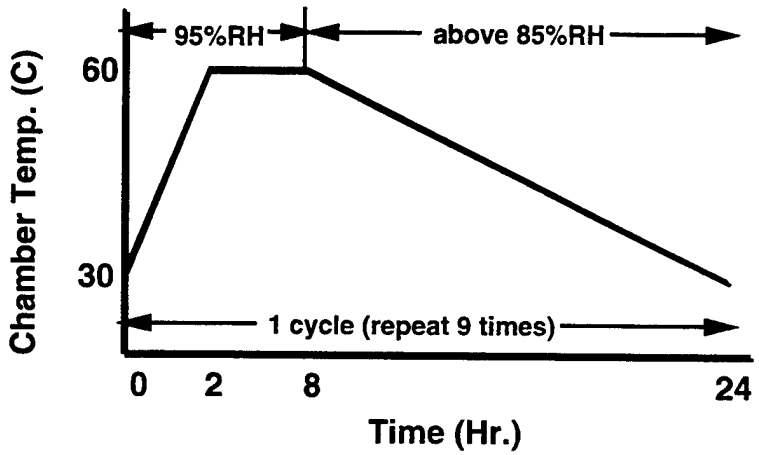

Figure 3-21 Humidity Profile

3.6 Flip-Chip-on-Glass Interconnect - Test Results

The test results for Test Vehicle 1 are as follows:

- Uniax UV-183 ACA (UV curable with Au microspheres).
  - 60 LCDs with driver chips put through electrical (functional) and environmental tests.
  - Survived temperature shock & cycling, but 50% failure rate through humidity.
- Elatech R001 ACA (UV initiated, thermal cure with Au microspheres).

- 60 LCDs with driver chips put through electrical (functional) and environmental tests.
- 98% Yield after temperature cycling, shock, and humidity.

• Sony CP84301Q ACF (Thermoset film with Au microspheres).

- 60 LCDs with driver chips put through electrical (functional) and environmental tests.
- 98% Yield after temperature cycling, shock, and humidity.

Lot #1 (bonded with UV-183 ACA) had the highest incidence of electrical failure after humidity cycling. C-SAM photography was used to generate Figure 3-22 through Figure 3-27 shows the bonded driver chip before humidity testing. Figure 3-22 shows the bonded driver chip before humidity testing. This untested sample shows good bond integrity and an underfill with very few voids.

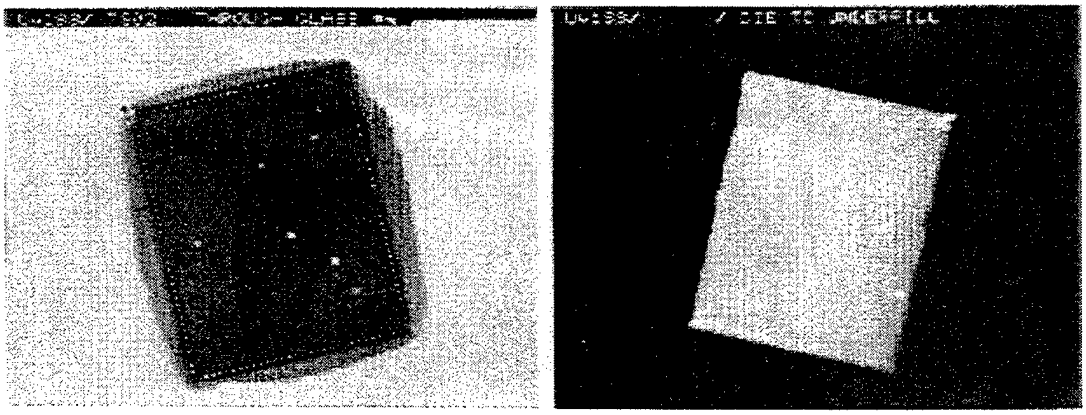

Die to Underfill Interface

Glass/ITO to Underfill Interface

Before humidity testing

Figure 3-22 Driver Chip Bonded with UV-183 ACA (C-SAM)

Figure 3-23 shows the bonded driver chip after humidity testing. This sample shows delamination of the epoxy underfill from the edges, as well as some discontinuities at the bond sites. The delaminations are clearly humidity induced. Figure 3-24 shows the delamination in a more clear, magnified state. This material was eliminated for consideration for use for military avionics applications at this point based on its demonstrated environmental instability.

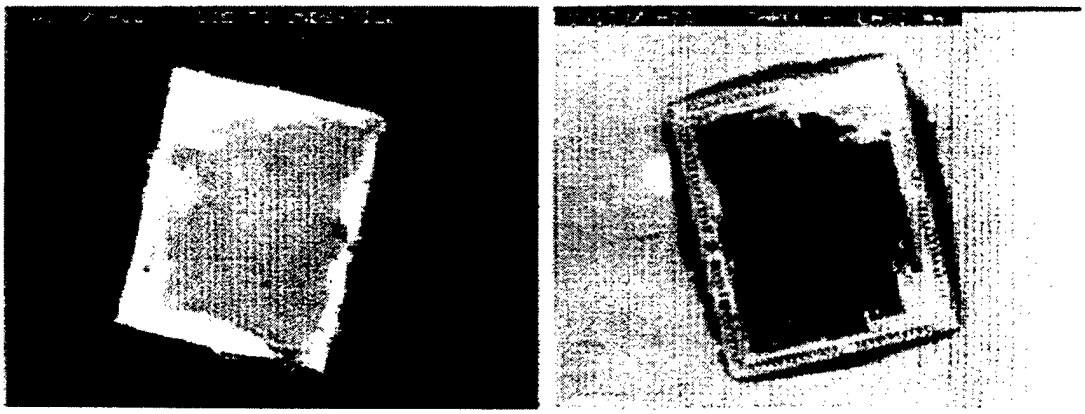

Die to Underfill Interface

Glass/ITO to Underfill Interface

Light gray areas indicate delamination after humidity testing

Figure 3-23 Driver Chip Bonded with UV-183 ACA (C-SAM).

Lot #2 (bonded with Sony CP84301Q ACF) had the best combined electrical and C-SAM test results. Figure 3-25 shows bond sites with very good chip-to-glass continuity. All samples had < 4% small round voids in the underfill (Sony says this is normal). This material was used for FCOG bonding on Test Vehicle 2 to further investigate its potential to survive the military avionics environment.

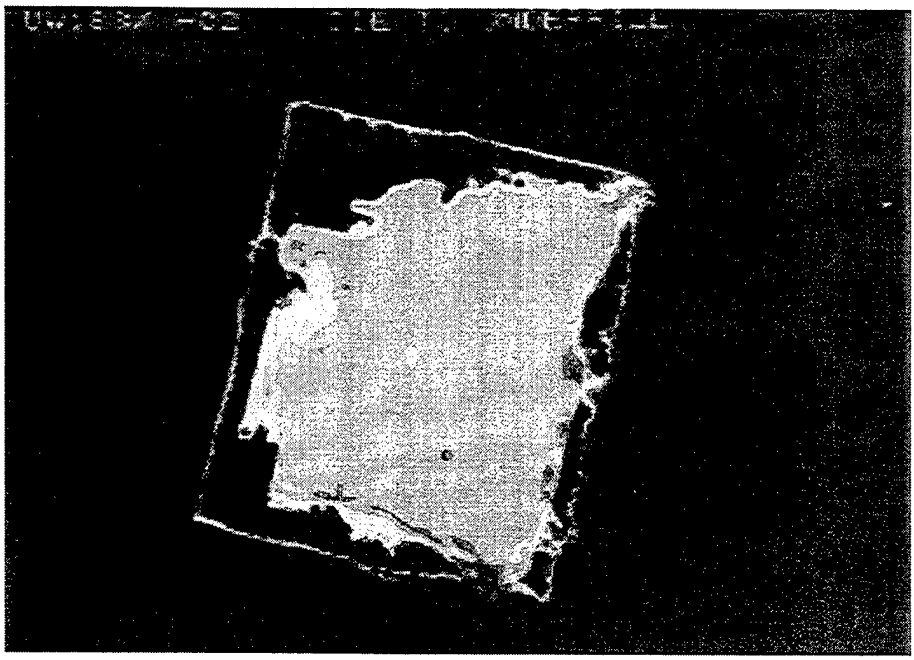

Delamination (red) of die to underfill, UV-183 ACA, after humidity cycling.
Failed electrical and die shear.

Figure 3-24 Driver Chip Bonded with UV-183 ACA (C-SAM)

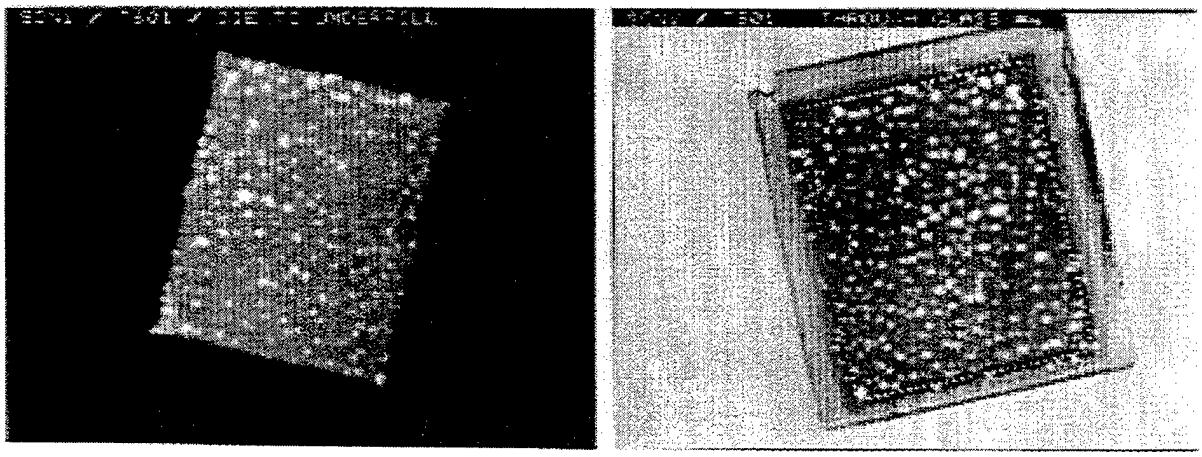

Die to Underfill Interface

Glass/ITO to Underfill Interface

Small gray areas indicate small voids.

Figure 3-25 Driver Chip Bonded with UV-183 ACA (C-SAM)

See Appendix D for color version.

Lot #3 (bonded with Elatech R001 thermoset ACA) had very good electrical results and interesting C-SAM results. Figure 3-26 shows good bonding of the die to the ACA when seen through the top of the chip (die to underfill interface), but a different result at the glass/ITO to underfill interface. At the glass/ ITO to underfill interface, there is clear evidence of ACA shrinkage in the fluid state, resulting in many finger-like channels of air extending in from the edge of the chip. The cause is believed to be insufficient cure time (inadequate time for the heat to flow through the entire ACA material layer). All of the parts tested showed this void-creation behavior to varying degrees. Even with the development of the voids, the electrical contact remained sound. Figure 3-27 shows the delamination in a more clear, magnified state. Since this material had such high electrical test yield, it was decided to further examine this material on Test Vehicle 2 to see if it could withstand the military avionics environment.

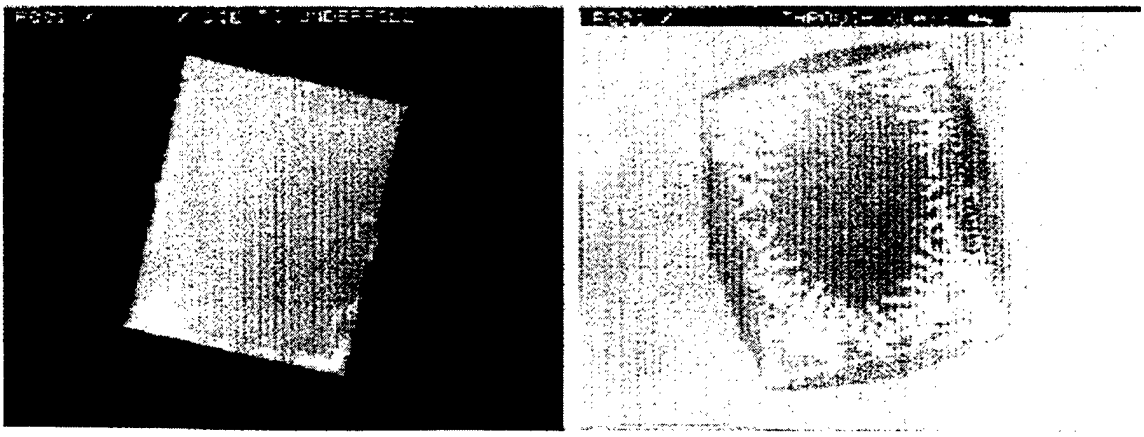

Light gray areas indicate delamination

Figure 3-26 Driver Chip Bonded with Elatech R001 ACA (C-SAM).

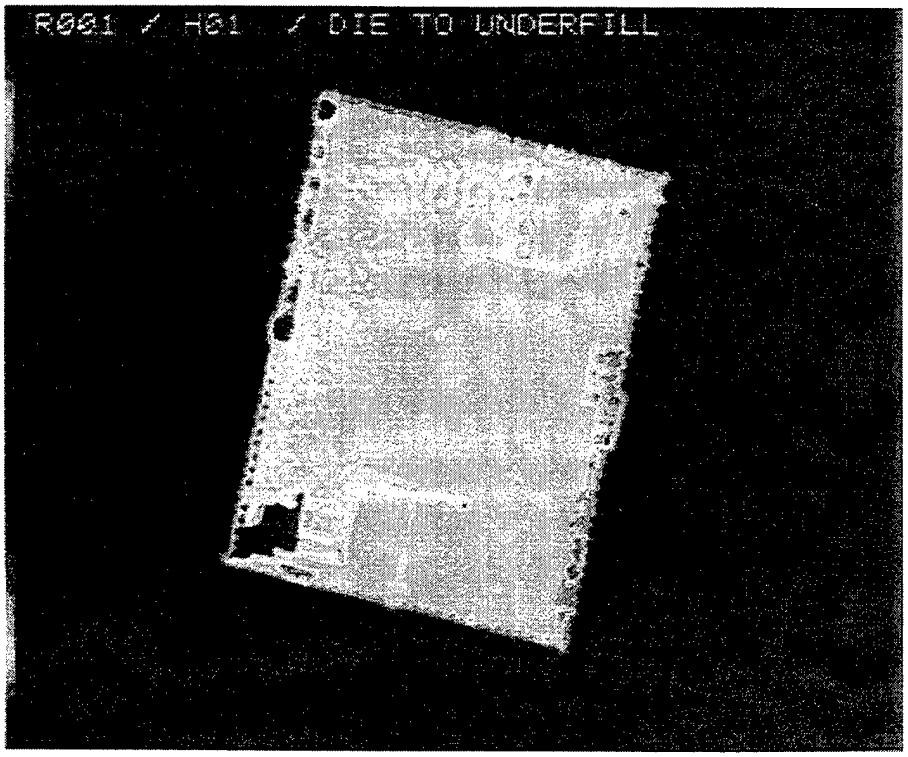

Slight delamination (red) of die to underfill, Elatech R001 ACA, after humidity cycling. Passed electrical and die shear.

Figure 3-27 Driver Chip Bonded with Elatech R001 ACA (C-SAM)

See Appendix D for color version.

All parts that underwent C-SAM analysis were also put through die shear. All three types of FCOG bond materials exceeded Honeywell's die shear strategic criteria, as shown in Figure 3-28. It turns out that these materials are quite strong. Normally, 5 kilograms of force is the maximum amount applied during shear testing; however, we applied 9 kilograms of force and the die still did not come off, they were still electrically functional.

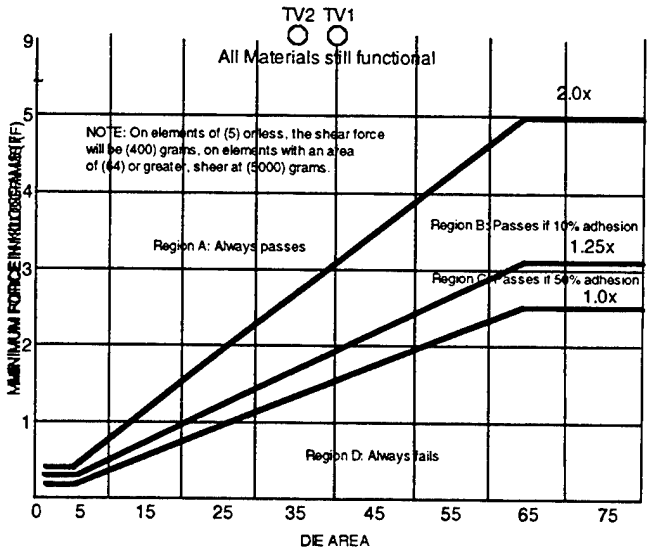

Test Vehicle #1 Driver Chip Area = 39.765 mm^2

Test Vehicle #2 Test Chip Area = 36 mm^2

Figure 3-28 Device Shear Strength Test Criteria, Honeywell Quality Control Directive F84-15

The test results for Test Vehicle 2 are as follows:

- Elatech R001 ACA (UV initiated, thermal cure w/ Au microspheres).
  - Eight TV2 substrates with bonded chips (64 test chips) were put through testing.
  - Exhibited electrical and mechanical failures after random vibration, gunfire vibration, and thermal shock.
- Sony CP84301Q ACF (Thermoset film with Au microspheres).
  - Six TV2 substrates with bonded chips (48 test chips) were put through testing.
  - 100% Yield after random vibration, gunfire vibration, thermal shock, and humidity.

Figure 3-29 is a C-SAM of Test Chip 3, which is the highest density of interconnect with the smallest (50 μm) contact area. Figure 3-29 shows bond sites with very good chip-to-glass continuity, very good die to underfill interface. This material also has a very good glass/electrode to underfill interface.

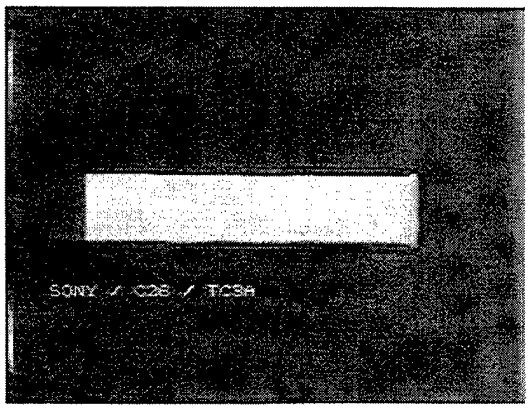

After random and gunfire vibration testing. 50 m bond sites at 75 m pitch yielded excellent electrical and mechanical reliability, with Sony ACF.

Figure 3-29 Au-Bumped HTC Test Chip

Electrical results are also very good for the Sony ACF material. Figure 3-30 shows the string resistance vs. temperature through 100 contacts (Au bump on Au contact). The initial contact resistance at 20°C was 2 ohms/0.1 mm^2, and at 120°C $\approx$ 2.5 ohms/0.1 mm^2. This is very acceptable. These measurements were taken after all environmental and vibration tests were performed. See Appendix D for color version.

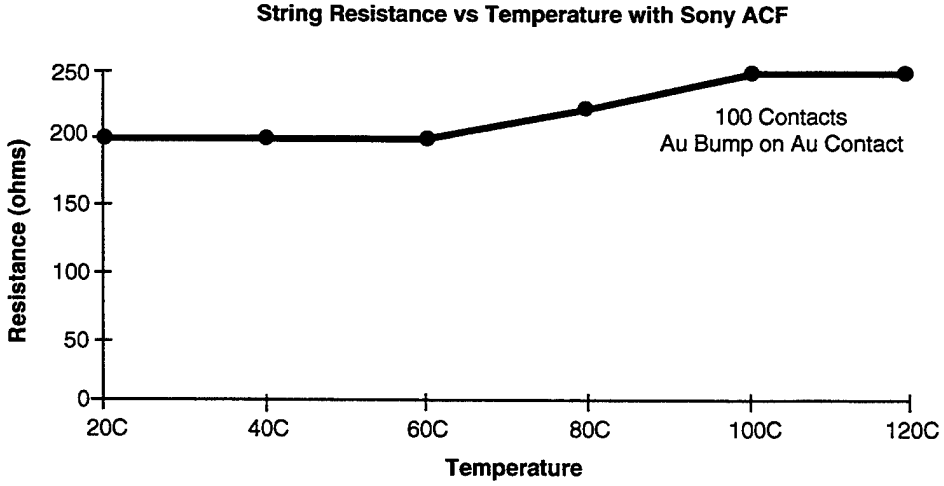

Figure 3-30 String Resistance vs. Temperature with Sony ACF

Figure 3-31 shows the FCOG bond resistance vs. temperature through 2 contacts (Au bump on ITO contact). The initial contact resistance at 20°C = 6.25 ohms/0.1 mm^2, and at 120°C ≈ 7.0 ohms/0.1 mm^2. This is very acceptable. Since ITO has a higher sheet resistance that Au, a higher contact resistance was expected. These measurements were taken after all environmental and vibration tests were performed.

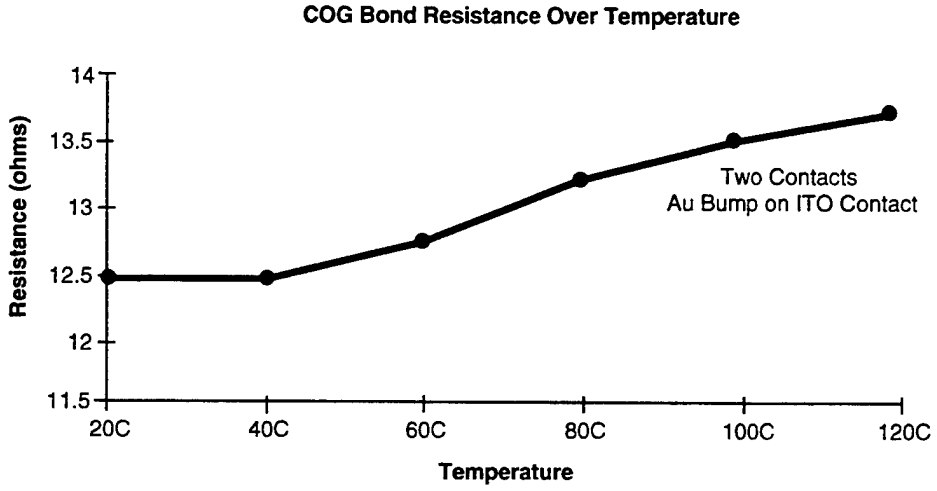

Figure 3-31 FCOG Bond Resistance Over Temperature

Dielectric isolation studies of all materials indicated a true z-axis only interconnect, with insulation resistance ~10^9 ohms. This is also very acceptable.

3.7 Conclusion

In conclusion, we have shown that at least one flip chip interconnecting material has been demonstrated reliable in the F-16 environment. The Sony CP84301 ACF bond material performs and holds up well under the environmental conditions of the F-16 aircraft. It

may also be suitable for use in other fine-pitch interconnect applications, such as flex to printed wiring board.

Now that a reliable FCOG bonding material/process has been found, a next step would be to reduce the technique to practice. A study needs to be performed in conjunction with an LCD supplier to examine how this FCOG technology can be implemented on commercial AMLCDs, most of which are designed for TAB drivers. One open question is whether there is a way to adapt FCOG drivers onto existing glass. In this program, we did not address the question of pad redistribution and/or driver re-layout. This program addressed the reliability of the materials in F-16 environment, a step considered crucial before addressing the driver itself.

Honeywell is continuing to examine the potential of flip-chip technology. Most commercial displays come with pre-defined contact pads and limited contact area. Two possible ways to use FCOG drivers with commercial glass are to redistribute the contact pads and re-layout the driver chip.

1. Driver chips would require pad redistribution and layout to fit the LCD conductor pattern.
2. Provide an intermediate connecting means to make the connection between the flip chip and the traces on the glass.

There is a growing trend in Japan for implementation of FCOG into the displays.[10] Some products using FCOG technology already exist on the market, such as the automotive

quality Sharp AMLCD with FCOG drivers we used on this program. As interconnection bonding materials are improved and made to meet the demanding military environmental reliability conditions, it is expected the use of FCOG drivers will become more widespread. The potential of reducing an entire level of interconnection, increasing reliability, and reducing system costs, is a very attractive benefit.

Appendix A – Component Temperature Spread - Two Conditions

The accompanying figures show temperature extremes for the three major display components under two sets of boundary conditions.

The worst-case thermal environment for the F-16 is the one central to the study, the 50°C ambient and 883 W/m^2 solar loading condition. The minimum and maximum temperature data for the principal components is shown in Figure A-1.

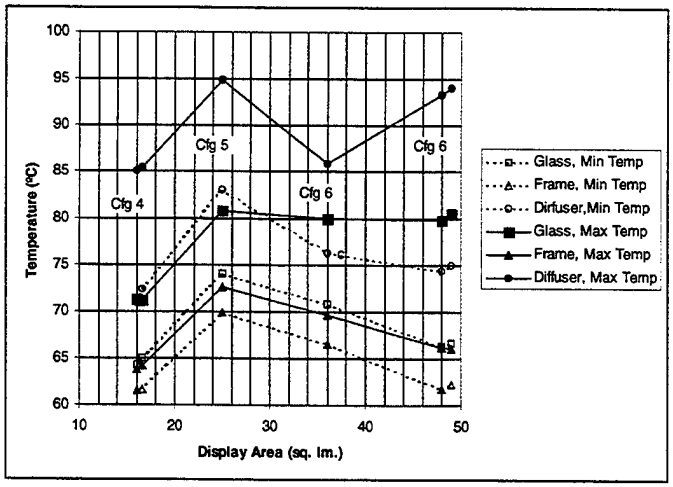

Figure A-1 Boundary Condition 1 - 50°C Ambient; 883 W/m^2 Solar Load

Figure A-2 shows the same parameters for second set of boundary conditions, corresponding to the typical upper mil-temperature limit, 55°C. For this case, the solar loading needed to be reduced to 677 W/m^2 to allow the glass to operate satisfactorily in this higher temperature environment.

A comparison of the data in the two figures reveals a substantial similarity. The delicate balance of the thermal equation is clear from this comparison. A 20% reduction in the solar loading was required to offset the 5°C increase in ambient temperature. Further, without the solar load reduction, it is evident that the glass temperatures would have risen above the target 80°C objective by approximately the same 5°C

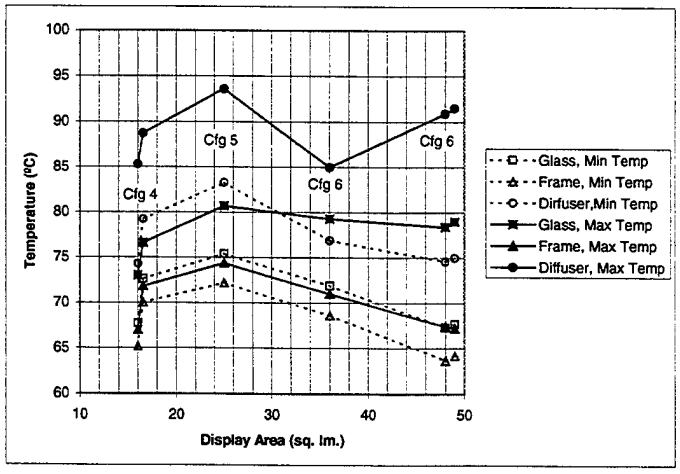

Figure A-2 Boundary Condition 2 - 55°C Ambient: 667 W/m^2 Solar Load

Appendix B – Tabular Temperature Data for Section 2

LCD Temperature Extremes for 3.6x4.6-inch Display, with and without Solar Load

Thermal Design	LCD Temperature With Solar Load (°C)		LCD Temperature Without Solar Load (°C)	
	Max	Min	Max	Min
Configuration 1	96.4	81.1	60.0	57.7
Configuration 2	95.0	73.4	59.8	56.9
Configuration 3	86.0	81.1	58.5	57.9
Configuration 4	71.1	65.0	57.0	56.2

LCD Temperature Extremes for 4x4-inch Display, with and Without Solar Load

Thermal Design	LCD Temperature With Solar Load (°C)		LCD Temperature Without Solar Load (°C)	
	Max	Min	Max	Min
Configuration 3	84.3	79.6	58.4	57.7
Configuration 4	71.3	64.3	56.9	56.1

LCD Temperature Extremes for 5x5-inch Display, with and without Solar Load (Configurations 5 and 6)

Thermal Design	LCD Temperature With Solar Load (°C)		LCD Temperature Without Solar Load (°C)	
	Max	Min	Max	Min
Configuration 5	80.8	74.0	61.3	60.6
Configuration 6*	74.9	67.3	55.0	53.5

*With heat pipes removing 8 watts (13.3 watts at TEC)

LCD Temperature Extremes for 6x6-inch Display, with and without Solar Load (Configurations 5 and 6)

Thermal Design	LCD Temperature With Solar Load (°C)		LCD Temperature Without Solar Load (°C)	
	Max	Min	Max	Min
Configuration 5	86.2	78.3	63.3	63.0
Configuration 6*	80.0	70.8	57.5	56.0

*With heat pipes removing 8 watts (13.3 watts at TEC)

LCD Temperature Extremes for 6x8-inch Display, With and Without Solar Load (Configurations 5 and 6)

Thermal Design	LCD Temperature With Solar Load (°C)		LCD Temperature Without Solar Load (°C)	
	Max	Min	Max	Min
Configuration 5	88.2	77.2	63.4	62.5
Configuration 6*	79.8	66.3	—	—

*With heat pipes removing 8 watts (33 watts at TEC)

LCD Temperature Extremes for 7x7-inch Display, With and without Solar Load (Configurations 5 and 6)

Thermal Design	LCD Temperature With Solar Load (°C)		LCD Temperature Without Solar Load (°C)	
	Max	Min	Max	Min
Configuration 5	88.7	77.3	63.5	62.6
Configuration 6*	83.8	71.0	—	—
*With heat pipes removing 12 watts (20 watts at TEC)				
Configuration 6†	80.5	66.6	—	—
†With heat pipes removing 20 watts (33 watts at TEC)				

LCD Temperature Extremes for 8x10-inch Display, with and without Solar Load

Thermal Design	LCD Temperature With Solar Load (°C)		LCD Temperature Without Solar Load (°C)	
	Max	Min	Max	Min
Configuration 5	94.9	80.1	64.9	64.0
Configuration 6*	89.0	71.2	—	—

*With heat pipes removing 24 watts (40 watts at TEC)

Appendix C – Parameter Sensitivity to Display Size

Sensitivity studies were carried out to evaluate the effect of display size on a number of parameters:

- LCD temperature rise above ambient, with and without solar loading.
- LCD temperature gradient, with and without solar loading.

In addition, we assessed LCD temperature dependence on backlight power. The results are given in the graphs following.

Figure C-1 summarizes the behavior or LCD center temperature as a function of display size. The data is for displays operated at 200 fL luminance. The upper curve shows a steady elevation of center temperature with increasing display area. This was the behavior that created a practical upper limit on commercial display size under the environmental conditions and design guidelines of the F-16, and using the cooling techniques described herein. At some point, the high 883 W/m^2 solar loading can overwhelm most practical cooling techniques in the absence of moving air.

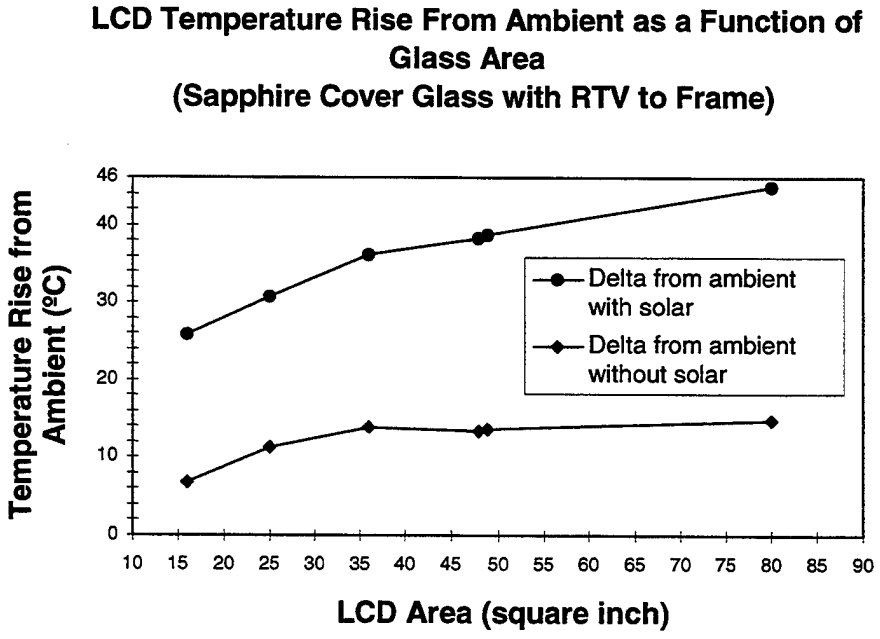

Figure C-1 LCD Temperature Sensitivity to Display Area

The lower plot separates out the behavior of the display with only the backlight power to contend with. In this case, as the display size increases, the curve flattens out at about 35°C. This indicates that above 35°C the larger surface area of the display provides enough cooling to stabilize the LCD center temperature.

LCD temperature gradient is essentially only affected by solar loading (Figure C-2). Again, the steady upward movement of the upper curve indicates that there is an upper limit based on the glass tolerance for temperature gradient. In the absence of solar loading (lower curve), there is a small but almost constant temperature difference, showing negligible sensitivity to display size.

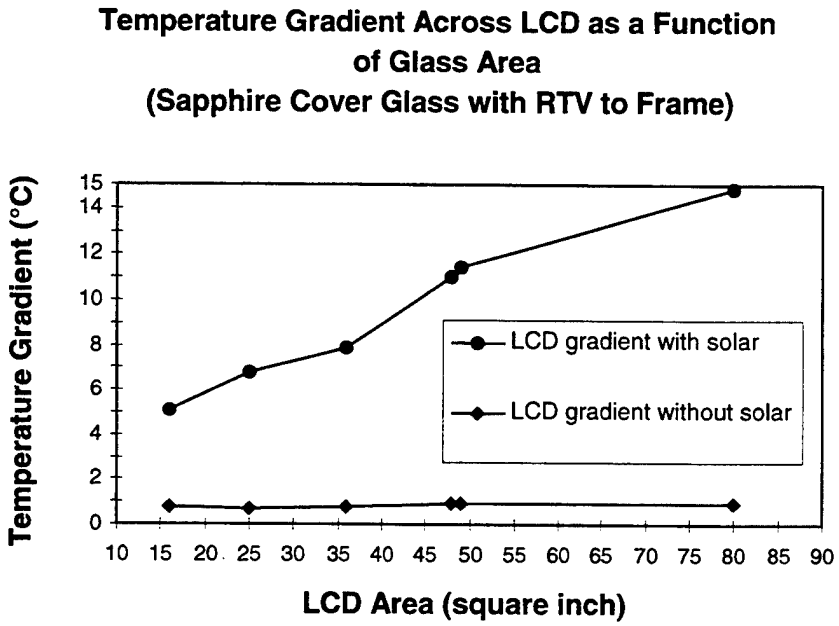

Figure C-2 LCD Temperature Differential Sensitivity to Display Area

The data were also examined for dependence of LCD temperature on backlight power. The case shown in Figure C-3 is a 3.6x4.6-inch display under no solar load. The temperature rose above ambient rises steadily in reaction to increasing display luminance, rising from 10°C to nearly 20°C over the luminance range. On the other hand, the center-to-edge temperature differential is only slightly affected, with the temperature rising only about 2°C as the backlight luminance is increased from 200 fL to 400 fL. This is an indication that, in the absence of solar loading, heat flow in a stack of this configuration is sufficient to keep the glass temperature differentials and stress in the glass low.

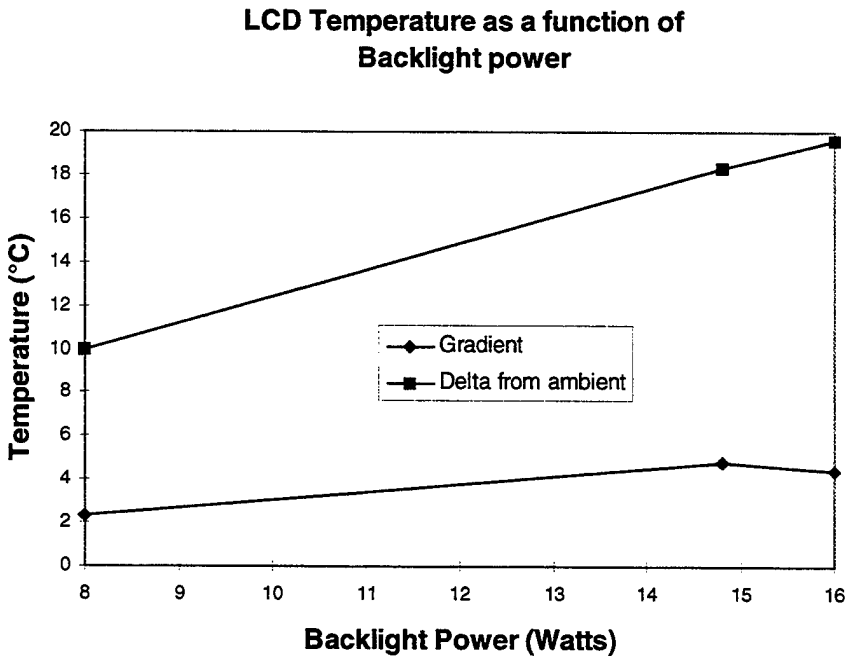

Figure C-3 LCD Center Temperature Sensitivity to Backlight Power

Appendix D – Thermal Model Validation

In the course of the research, several configurations of the Sharp display were fabricated and tested under different ambient conditions. The purpose of the physical display test structures was two-fold, (1) validation of the thermal model, and (2) confirmation of the thermal management concepts developed during the research.

Thermal models constructed from basic principles, known material properties, and estimates of unknowns are virtually always incomplete until a correlation is established between predictions and measured values for equivalent structures. We used the measured data as a basis for adjusting the ESC™ model parameters to produce more accurate predictions. This was necessary in order to obtain credible predictions for larger displays for which we had no physical equivalents to measure. Our objective was to obtain a prediction error less than 5°C. This potential for prediction error is acknowledged in our design goal of 80°C, compared with the Sharp operating temperature limit of 85°C.

During the process of adjusting the thermal model parameters, were also able to observe the sensitivity to those adjustments. That information helped us understand the behavior of the various components in the flat panel display assembly, and improve the prediction of thermal behavior of other display configurations and sizes.
The temperature measurements were performed using a Fluke 2286A Data Logging System. Type T Copper-Constantan thermocouples were used. The accuracy of the system was ±0.3°C. The same system measured the ambient temperature and provided temperature feedback to the environmental chamber's temperature controller to eliminate any inter-system temperature differential error.

The temperature prediction and measured values for these runs are compared and the errors computed in Table C-1. With a single exception, the errors were confined within the desired ±5°C error band, and the average magnitude of the errors was less than 3°C. FOR the purposes of this program, this was an acceptable level of correlation between predicted and measured values.

In general, the predictions were most accurate or the edges of the cover glass, and least accurate for the center of the cover glass. However, the center temperature for the glass was consistently cooler than the estimate, a favorable direction for the error. Overall, the prediction error was judged unlikely to compromise the program's design objectives.

Table D-1 Temperature Prediction Error

Verif. Run	POLARIZER CENTER			COVER GLASS EDGE		
	Predicted	**Measured**	**Delta**	**Predicted**	**Measured**	**Delta**
1	60.0	61.3	1.3	57.4	58.6	1.2
2	67.3	65.7	-1.6	61.0	62.2	1.2
3	68.5	69.6	1.1	64.5	64.9	1.4
4	81.5	76.4	-5.1	70.3	70.6	0.3
	Avg. Error		-1.1	Avg. Error		1.0
	Avg. Absolute Error		2.3	Avg. Absolute Error		1.0
Verif. Run	**COVER GLASS CENTER**			**DIFFUSER EDGE**		
1	73.9	67.2	-6.7	60.0	57.4	-2.6
2	82.8	79.4	-3.4	60.9	62.3	1.4
3	59.5	55.6	-3.9	51.4	55.2	3.8
4	73.1	68.1	-5.0	60.2	64.2	4.0
	Avg. Error		-4.8	Avg. Error		1.7
	Avg. Absolute Error		4.8	Avg. Absolute Error		3.0

The pages following contain the results for four separate verification analyses.

Verification Run 1 – Configuration: display glass configuration as received from Sharp, without cover glass or heater glass; LCD stack mounted in the same aluminum chassis used for all configurations; 200 fL (8 Watt bulb power) backlight; 50°C Ambient.

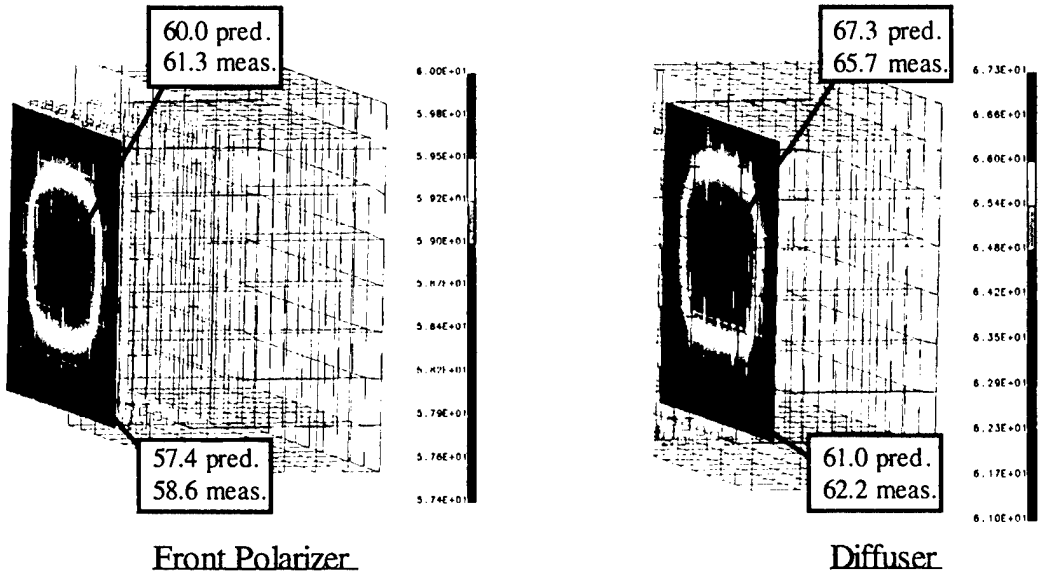

Figure D-1 Verification Run 1

Verification Run 2 – Configuration: display glass as received from Sharp, without cover glass or heater glass; LCD stack mounted in aluminum chassis; 448 fL (14.8 Watt bulb power) backlight; 50°C Ambient.

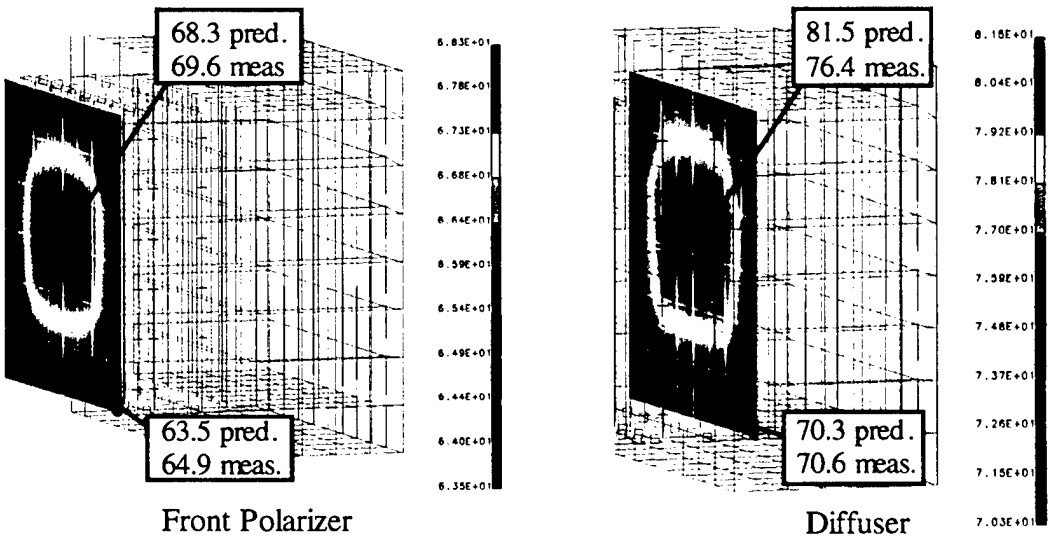

Figure D-2 Verification Run 2

Verification Run 3 – Configuration: display glass as received from Sharp, but with Corning 7059™ cover glass and heater glass added; LCD stack mounted in aluminum chassis; 200 fL (8 Watt bulb power) backlight; 25°C ambient; 883 W/m^2 solar load. [Corresponds to "Configuration 1" of the 3.6x4.6 as detailed in the body of the report].

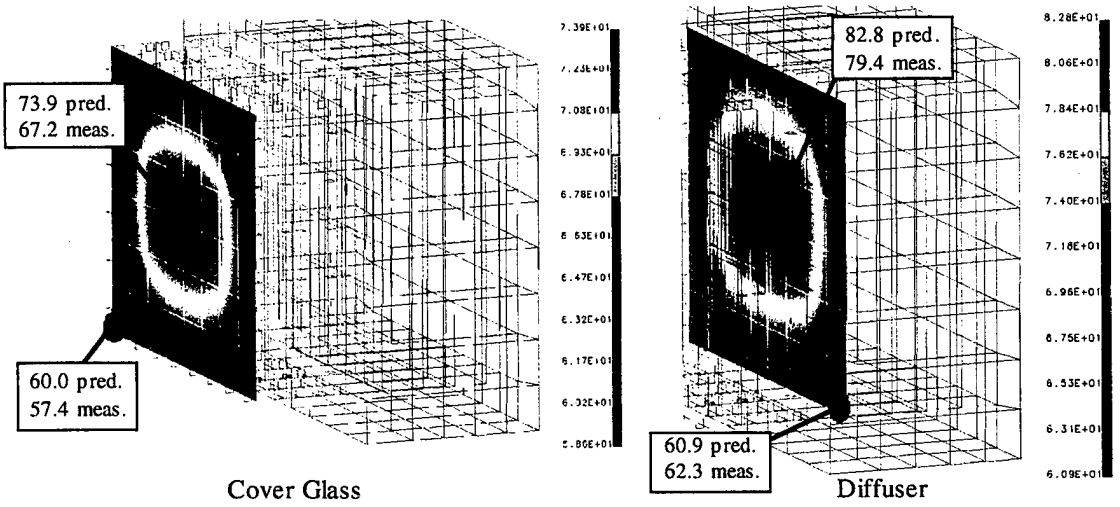

Figure D-3 Verification Run 3

Verification Run 4 – Configuration: display glass as received from Sharp, but with sapphire cover glass and heater glass added; LCD and sapphire cover glass have a T642 RTV bond to the housing (Configuration 4); LCD stack mounted in aluminum chassis; 200 fL (8 Watt bulb power) backlight; 30°C ambient; 883 W/m^2 solar load. [Corresponds to "Configuration 4" of the 3.6x4.6 as detailed in the body of the report].

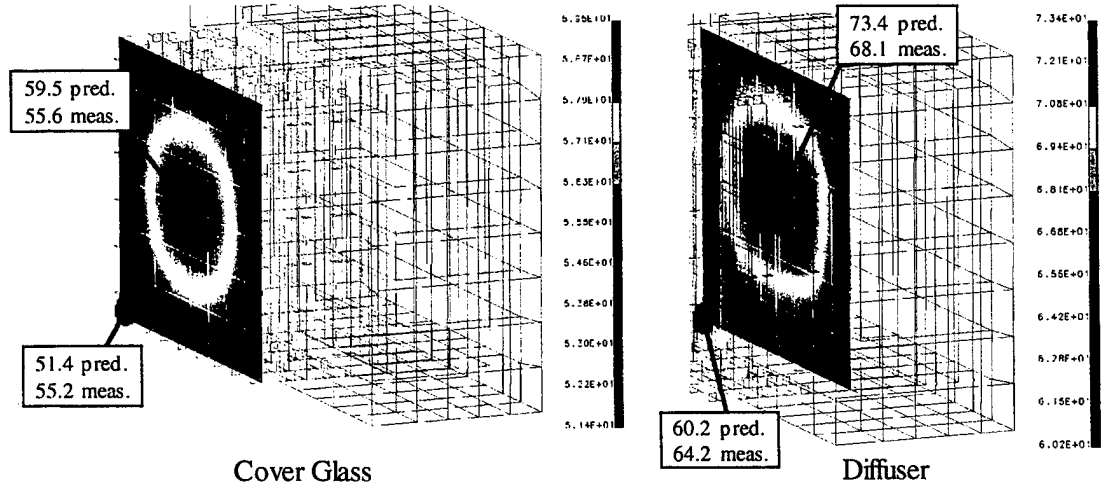

Figure D-4 Verification Run 4

Appendix E – Additional Color Photos

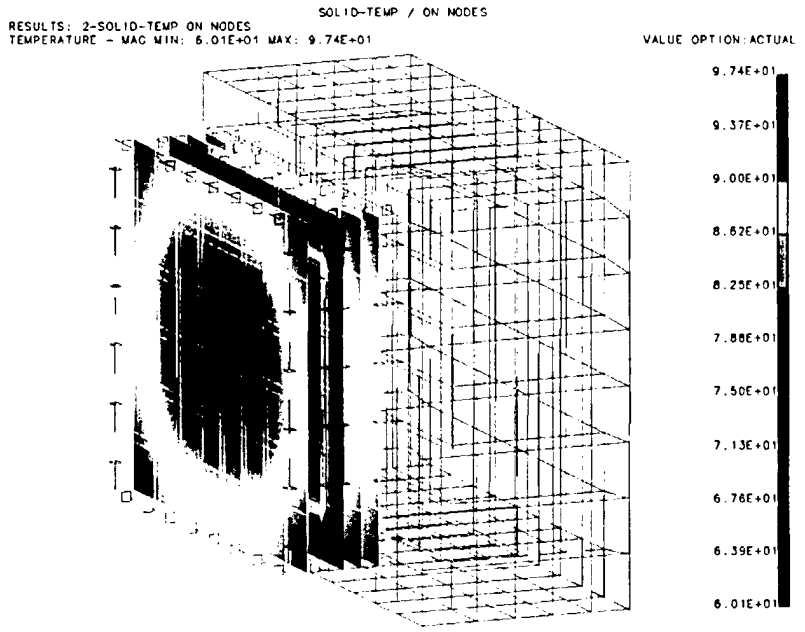

Figure E-1 Sample Results - LCD Stack Temperature (°C)

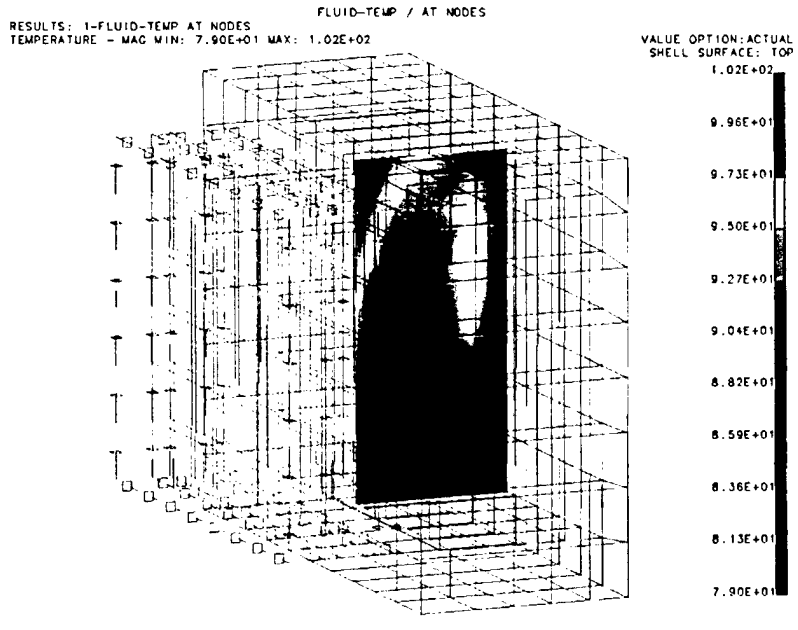

Figure E-2 Sample Results - Air Slice Temperature (°C)

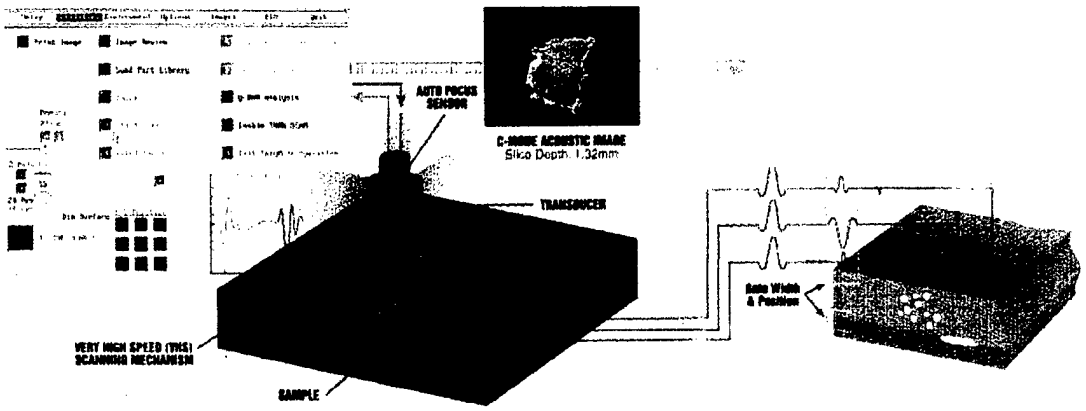

Figure E-3 C-mode Scanning Acoustic Microscopy

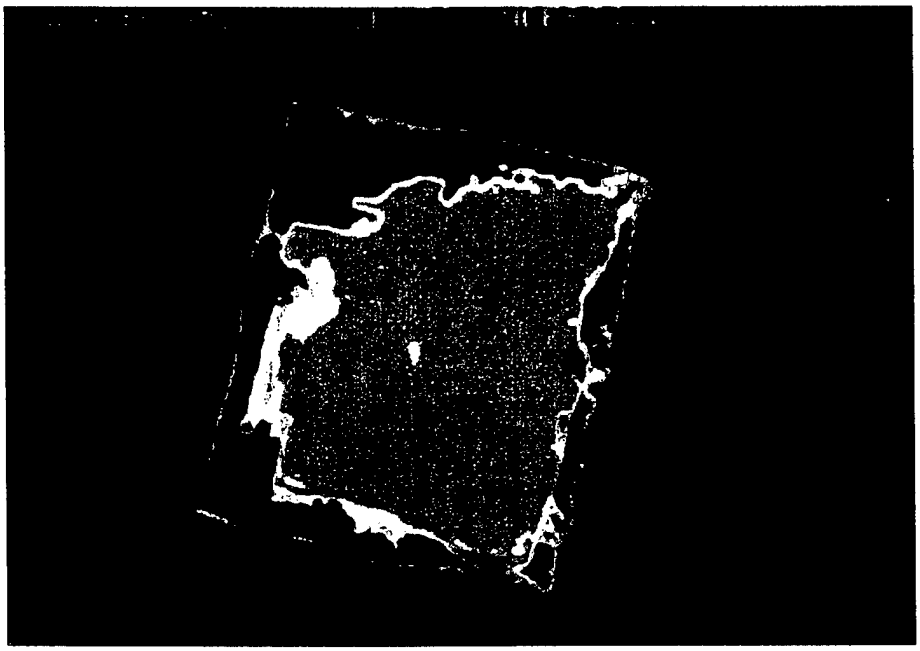

Delamination (red) of die to underfill, UV-183 ACA, after humidity cycling. Failed electrical and die shear.

Figure E-4 Driver Chip Bonded with UV-183 ACA (C-SAM)

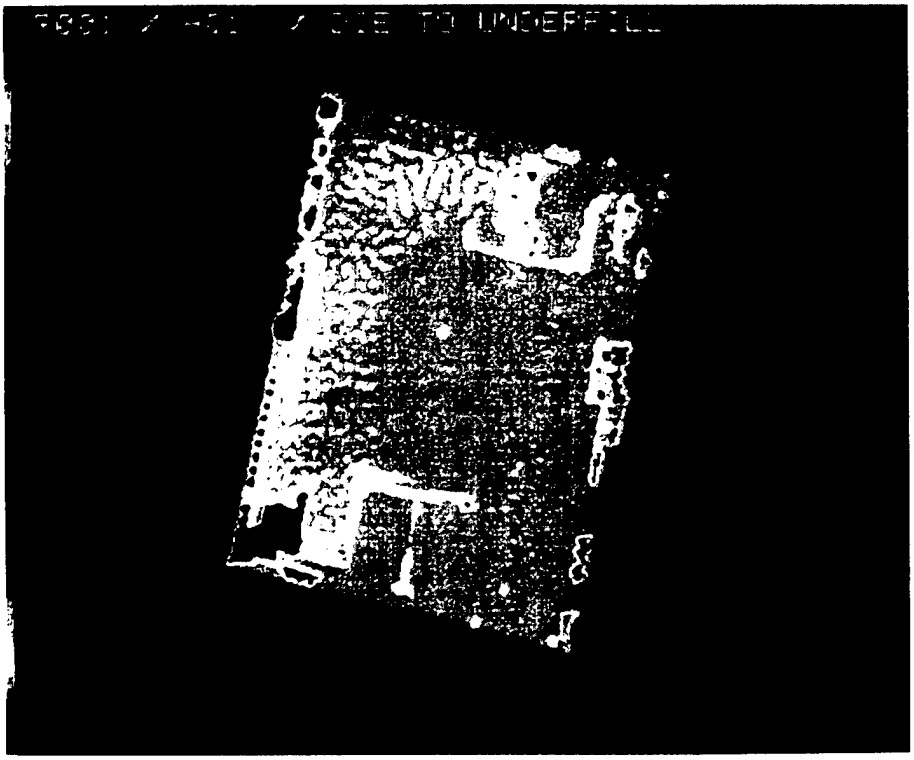

Slight delamination (red) of die to underfill, Elatech R001 ACA, after humidity cycling. Passed electrical and die shear.

Figure E-5 Driver Chip Bonded with Elatech R001 ACA (C-SAM)

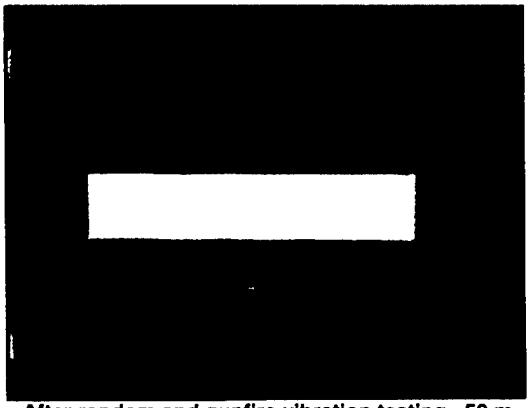

After random and gunfire vibration testing. 50 m bond sites at 75 m pitch yielded excellent electrical and mechanical reliability, with Sony ACF.

Figure E-6 Au-Bumped HTC Test Chip

References

[1] Prime Item Development Specification for the Color Multifunction Display; Specification No. 16ZE532; Appendix B, Environmental Criteria for F-16 A/B and C/D.

[2] R.E. Orkis, 'An Improved Full Color F-16 A/B and F-16 C/D Multi-Funtion Display Using a Ruggedized COTS Active matrix Color Liquid Crystal Display," Battelle Memorial Institute, Columbus, OH 1995, SPIE Proceedings, Vol. 2462, p. 198-210.

[3] Joseph B. Murdoch, Illumination Engineering - From Edison's Lamp to the Laser, Macmillan Publishing Company, New York, New York, 1985, pp. 218-219.

[4] The Infrared Handbook, Office of Naval Research, Department of the Navy, Arlington, VA, 1978, pp. 3-35 to 38.

[5] The Cool Times, Noren Products Incorporated, Menlo Park, CA, Vol. 2, No.1, p. 3.

[6] P. Hogerton, J. Hall, J. M. Pujol, and R. Reylek, "Investigations Into The Use of Adhesives for Level-1 Microelectronic Interconnections," 1989 Materials Research Society Symposium Proceedings, Vol. 154, pp. 415-424.

[7] C. H. Lee, K. I. Loh, and F. Wu, "Flip Chip-on-Glass With Anisotropically Conductive Adhesives," Electronic Packaging & Production, 1995 Vol. 35, No. 9, pp. 74-76.

[8] S. F. Tead, G. L. Bluem, F. B. McCormick, "Z-Axis Adhesive Use in Electronic Interconnection Applications," 1995 Society of Plastics Engineering Regional Technical Symposium Proceedings, p. 114.

[9] J. C. Hwang, C. Wilson, "Advanced Bare-Die Packaging Technology for Liquid Crystal Displays," 1994 International Electronics Packaging Conference Proceedings, pp. 357-363.

[10] J. E. Semmens, L. W. Kessler, "Characterization of Flip Chip Interconnect Failure Mode Using High Frequency Acoustic Micro Imaging With Correlative Analysis," 1997 IEEE International Reliability Physics Symposium Proceedings, pp. 1-8.